



Giuseppe Mancuso

Enhancement of wastewater and sludge treatment processes by hydrodynamic cavitation



**Enhancement of wastewater and sludge treatment processes by
hydrodynamic cavitation**

Giuseppe Mancuso



UNIVERSITY OF TRENTO - Italy

Department of Civil, Environmental
and Mechanical Engineering

Doctoral thesis in *Civil, Environmental and Mechanical Engineering, XXIX cycle*

Faculty of Engineering, *University of Trento, Italy*

Academic year *2016 / 2017*

Supervisor

Prof. Dr. eng. Gianni Andreottola, University of Trento, Italy

Co-Supervisor

Dr. eng. Michela Langone, University of Trento, Italy

Manuscript committee

Prof. Dr. eng. Francesco Pirozzi, University of Naples “Federico II”, Italy

Prof. RNDr. Milada Kozubková, VŠB- Technical University of Ostrava, Czech Republic

Panel members

Prof. Dr. eng. Marco Ragazzi, University of Trento, Italy

Prof. Dr. eng. Vincenzo Torretta, University of Insubria, Italy

Prof. Dr. eng. Marco Baratieri, University of Bolzano, Italy

Dr. Alessandro Paletto, CRA-MPF, CREA, University of Trento, Italy

University of Trento

Trento, Italy

(2017)

To my family: papà, mamma, Martina e Floriana

Contents

Contents

Outline of the thesis.....	1
Chapter 1	5
A critical review of the current technologies in wastewater treatments plants by using hydrodynamic cavitation process: Basic principles	5
Abstract.....	7
1. Introduction	7
2. Brief background of cavitation process	9
3. HC generation and mechanisms	12
3.1. HC flow regimes.....	14
3.2. HC types.....	15
3.2.1. Attached cavitation	16
3.2.2. Convected cavitation.....	18
3.2.3. Vortex cavitation.....	18
4. Mechanisms of pollutants degradation.....	19
5. The effect of various parameters on HC effectiveness	20
5.1. Device construction parameters size.....	20
5.1.1. Influence of cavitating device geometry.....	21
5.2. Technological process parameters.....	22
5.2.1. Influence of liquid flow velocity	22
5.2.2. Influence of liquid inlet pressure.....	23
5.2.3. Influence of cavitation number	24
5.2.4. Influence of liquid temperature	25
5.2.5. Influence of liquid pH.....	26
5.3. Properties of the liquid medium.....	27
5.3.1. Influence of pollutant concentration	27
5.3.2. Influence of liquid viscosity	28
5.3.3. Influence of surface tension	29
5.3.4. Influence of dissolved gas content.....	30
6. Methods to evaluate cavitation efficiency.....	30
6.1. Pollutants degradation in wastewaters	30
6.2. Biological wastewater treatments	31
7. Conventional scheme of a HC experimental system.....	32

8. Reactor used for generation of cavitation in wastewater treatment field.....	35
9. Main fields of application of cavitation in a wastewater treatment plant.....	36
10. Modelling	37
11. Concluding comments	38

Chapter 2 39

Decolourization of Rhodamine B: A swirling jet-induced cavitation combined with NaOCl..... 39

Abstract.....	41
1. Introduction	41
2. Materials and Methods	44
2.1. Reagents.....	44
2.2. HC system.....	44
2.3. Procedures	46
2.4. Calculations.....	48
3. Results and discussion	49
3.1. Degradation using HC alone.....	49
3.2. Synergetic effect between HC and NaOCl	50
3.3. Effect of NaOCl concentration	53
3.4. Effect of the pressure	54
3.5. Effect of geometry	56
3.5.1. Effect of the orifice plate thickness.....	56
3.5.2. Effect of the double cone.....	57
3.6. Effect of operative pH.....	58
3.7. Effect of initial dye concentration.....	59
3.8. Energy consumption analysis.....	61
4. Conclusions	63

Chapter 3 65

A swirling jet-induced cavitation to increase activated sludge solubilisation and aerobic sludge biodegradability 65

Abstract.....	67
1. Introduction	67
2. Materials and Methods	69
2.1. Sludge characterization	69
2.2. HC system.....	69
2.3. Methods.....	71
2.3.1. HC tests.....	71

2.3.2.	Respirometric technique.....	71
2.3.2.1.	Aerobic biodegradability	73
2.3.2.2.	Microbial activity	74
2.4.	Calculations.....	74
2.5.	Analytical methods.....	75
3.	Results and discussion	75
3.1.	Effect of temperature	76
3.2.	Effect of inlet pressure: flow velocity and pressure drop	77
3.3.	Effect of solid concentration	79
3.4.	Effect of geometry	80
3.4.1.	Number and diameter of injection slots of Ecowirl reactor.....	80
3.4.2.	Number of Ecowirl heads	82
3.5.	Comparison of energy efficiency	83
3.6.	Effect of supplied energy.....	84
3.7.	Effect of HC on biodegradability of treated sludge.....	87
3.8.	Effect of HC on microbial activity.....	88
4.	Conclusions	90

Chapter 4 93

Experimental and numerical investigation on performance of a swirling jet-induced reactor.....93

Abstract.....	95
1. Introduction	95
2. Materials and Methods	97
2.1. Experimental setup.....	97
2.2. Experimental tests.....	98
2.3. Reactor geometrical configurations	99
2.4. Cavitation noise measurements	99
2.5. Numerical simulations.....	100
2.5.1. Reactor model and boundary conditions.....	101
3. Results	102
3.1. Non-cavitating model.....	103
3.1.1. Fluid dynamics.....	103
3.1.2. Flow velocity and flow pressure distributions	104
3.2. Cavitating model.....	106
3.2.1. Fluid dynamics.....	106
3.2.2. Flow velocity and flow pressure distributions	107

3.2.3. Cavitation noise measurements	109
4. Conclusions	111
Summary and outlook	115
List of Figures	119
List of Tables.....	125
References	129
Appendix A.....	143
Appendix B.....	147
Acknowledgements.....	151
Publications & relevant works	155

Outline of the thesis

Outline of the thesis

In the past decades, hydrodynamic cavitation (HC) process was the subject of study by many researchers worldwide. This phenomenon was widely studied in order to understand the reason of its negative effects on hydraulic machinery such as pumps, turbines, valves, etc. Many efforts were made in order to better understand mechanisms of HC process with the main aim of preventing its generation and trying to avoid severe physical damage such as erosions, vibrations and noises.

In recent years, in order to cope with a decrease in available water resources worldwide, an increasing demand of water by population in developing/developed countries and more restrictive environmental legislations on water quality, HC was increasingly used as a novel energy-efficient technique in the field of wastewaters treatment.

The main purpose of this thesis is to investigate on the effectiveness of a modified swirling-jet device called Ecowirl reactor, patented by Econovation GmbH, Germany and produced and commercialized by Officine Parisi s.r.l., Italy. Experimental studies were carried out in order to evaluate the effects of different operative conditions and parameters such as reactor geometry, flow rate, flow velocity, pressure, medium pH, medium concentration and medium temperature on (i) the degradation of a toxic and carcinogenic pollutant dye (Rhodamine B, RhB) in waste dye aqueous solutions and on (ii) the improvement of activated sludge solubilisation and aerobic sludge biodegradability in the field of biological wastewater treatments.

In order to better understand the fluid dynamics into Ecowirl reactor, it was modelled. The model based on previous experimental data was implemented in a Computational Fluid Dynamics software (ANSYS, 16.2).

The research described in this thesis was conducted at the Department of Civil, Environmental and Mechanical Engineering of the University of Trento, Italy, and a two month – period was spent at the Department of Hydrodynamics and Hydraulic Equipment of VŠB- Technical University of Ostrava, Czech Republic.

This study was financially supported by the Autonomous Province of Trento, Italy (Program for the development of Small Medium Enterprise, L6/99, Project n.S155/2013/693264/12.1), and Officine Parisi s.r.l., Italy.

Chapter 1 of this thesis concerns the application of HC process as novel and effective technology in the field of wastewater treatment. It describes basic principles of both HC generation and organic pollutants degradation. Furthermore, an overview of different types of HC and of existing methods to evaluate the efficiency of cavitation process is provided.

Chapter 2 describes the use of a swirling-jet induced reactor to degrade Rhodamine B dye from a waste aqueous solution. With this purpose, the effect of different parameters and operative conditions on the extent of degradation of Rhodamine B was studied.

In *Chapter 3*, the swirling-jet induced reactor was used to increase activated sludge solubilisation and aerobic sludge biodegradability in a wastewater treatment plant.

In *Chapter 4*, a three-dimensional Computational Fluid Dynamic (CFD) analysis of the swirling jet-induced reactor was implemented in order to gain a better understanding of the fluid dynamics into the swirling-jet induced reactor and to investigate the effect of reactor geometry on basic physical quantities such as flow velocity and flow pressure into the swirling jet-induced reactor.

Chapter 1

A critical review of the current technologies in wastewater treatments plants by using hydrodynamic cavitation process: Basic principles

Chapter 1

A critical review of the current technologies in wastewater treatments plants by using hydrodynamic cavitation process: Basic principles

Giuseppe Mancuso, Michela Langone, Gianni Andreottola

Department of Civil, Environmental and Mechanical Engineering, University of Trento, via Mesiano 77, 38123, Italy

Abstract

In the last years, hydrodynamic cavitation (HC) was increasingly used for a variety of applications in wastewater treatments, ranging from biological applications such as cell disruption to chemical reactions such as oxidation of organic pollutants in aqueous effluents, including bio-refractory toxic chemicals. HC is induced in a water solution by subjecting the liquid to velocity variations by introducing constrictions, such as orifice plate, Venturi or throttling valve, in the flow. It involves the formation, growth, implosion and subsequent collapse of microbubbles or cavities, occurring in extremely small intervals of time and releasing large magnitudes of energy over a very small location. In this paper, the vast literature on HC is critically reviewed, focusing on basic principles behind it, in terms of process definition and analysis of governing mechanisms of both HC generation and pollutants degradation. Available literature on the effects of various parameters on HC effectiveness was assessed, focusing on construction parameters, technological process parameters, and properties of the liquid medium. An overview of the different methods of evaluating the efficiency of cavitation process was provided. Knowledge build-up and optimization for such complex systems from mathematical modelling was highlighted. Mathematical models can be useful tools in order to gain a better understanding of how HC devices work in cavitating conditions and further to optimize HC devices performances in terms of cavitation effects.

Keywords: Hydrodynamic cavitation, Pollutant degradation, Wastewater treatment, Computational Fluid Dynamics, Modelling

1. Introduction

In the past decades, HC process was the subject of study by many researchers worldwide. This phenomenon was widely studied in order to understand the reason of its negative effects on hydraulic machinery such as pumps, turbines, valves, etc. [1–6]. Many efforts were made in order to better understand mechanisms of HC process with the main aim of preventing its generation and trying to avoid severe physical damages such as erosions, vibrations and noises [1,5]. With this purpose, many studies were carried out in order to define parameters and methods trying to predict the cavitation inception [7].

Instead, in recent years, in order to cope with a decrease in available water resources worldwide and

an increasing demand of water by population in developing countries and moreover, higher restrictive environmental legislations on water quality, HC was increasingly applied as innovative technique in the field of wastewaters treatment. *Fig. 1* shows the robust increase in the number of peer- reviewed publications in the databases of Web of Science on innovative wastewater treatment and, further, on HC as innovative application in wastewater treatment field listed.

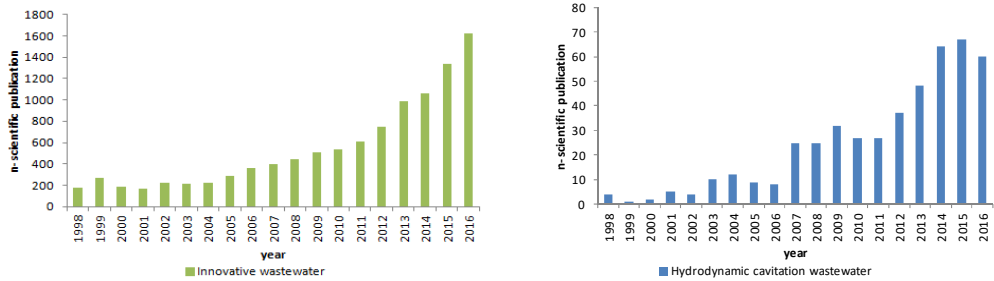


Fig. 1- Increase in the number of peer-reviewed publications listed in the databases of Web of Science with “innovative wastewater” and “hydrodynamic cavitation wastewater” as keys words.

Due to its elevated oxidative capability, HC, as a sole technique or in combination with other techniques, was used for a variety of applications, ranging from biological applications such as cell disruption to chemical reactions such as oxidation of organic pollutants in aqueous effluents, including bio-refractory toxic chemicals [8,9].

Generally, the effectiveness of cavitation process in wastewater treatment was widely demonstrated by using acoustic cavitation (AC) [10,11], which showed to overcome some limitations of advanced oxidation processes (AOPs) that are commonly not capable of completely degrading complex compounds. In the last decade, the restrictions due to the high costs related to the AC application were overcome by the development of HC technologies [12]. HC techniques are proving to be characterized by higher removal efficiencies compared to other conventional treatment techniques and by higher energy efficiencies [13,14] and lower issues of secondary contaminations.

While many works were carried out on the application of the AC in wastewater treatment, HC was studied to a lesser, but published researches showed promising outcomes, in the field of sludge [15–18] and biomass pre-treatment before anaerobic digestion [19] and denitrification process [9], activated sludge reduction [14], carcinogen and toxic dyes [8], pharmaceuticals, toxic cyanobacteria, bacteria and viruses removal [20].

2. Brief background of cavitation process

Cavitation can be defined as the phenomenon of generation (inception), growth, coalescence, fission, travelling, and implosive collapse of bubbles or cavities (*Fig. 3*) within a liquid in less than a few microseconds. It results in very high local temperature (500 - 15,000 K) and pressure (100 - 5,000 atm) [21,22], inducing physical and chemical effects, in addition to the mechanical ones.

Depending on the mode of its generation, cavitation can be classified in acoustic cavitation (AC), hydrodynamic cavitation (HC), optic cavitation (OC) and particle cavitation (PC). OC and PC occur when a liquid is irradiated with light of high intensity or a laser. In OC, photons are used to rupture the liquid, while in PC other types of elementary particles such as protons and neutrinos accomplish a breakdown in the liquid [23]. On the contrary, AC and HC are based on local pressure drops, which allow breaking down the liquid. By using AC, the acoustic waves cause the local pressure fluctuations generating local pressure drops, while by using HC, the geometry of particular cavitating devices imply velocity fluctuations in a liquid flow causing local pressure drops. Although all four types of cavitation generate bubbles, it was found that only AC and HC are able to make the desired chemical changes in treated matters in environmental field [24,25].

In order to gain a better understanding of the physical meaning of the cavitation process based on local pressure drop, it can be taken into account the well-known concept in thermodynamics of vapour pressure. As shown in *Fig. 2*, in the phase diagram of water the curve from the triple point to the critical point separates the liquid and vapour domains. Crossing that curve is representative of a reversible transformation under static or equilibrium conditions. Phase transformations from the liquid phase to the vapour phase (evaporation) or, vice versa, from the vapour phase to the liquid phase (condensation) occur at a specific value of pressure known as the vapour pressure, p_v , for each temperature value. Cavitation is very similar to boiling, except that the main driving mechanism is not a temperature change but a pressure change. Cavitation bubbles in a liquid typically grow in a low pressure region; bubbles are transported by convection into a higher pressure region; whereupon they collapse [26].

When cavitation occurs, first it is possible to observe a breakdown or a void creation into the fluid. Afterwards, this void is filled by vapour with the eventual saturation. Actually, all those phases are simultaneous and the instantaneous saturation of the void with vapour can be justifiably assumed [26].

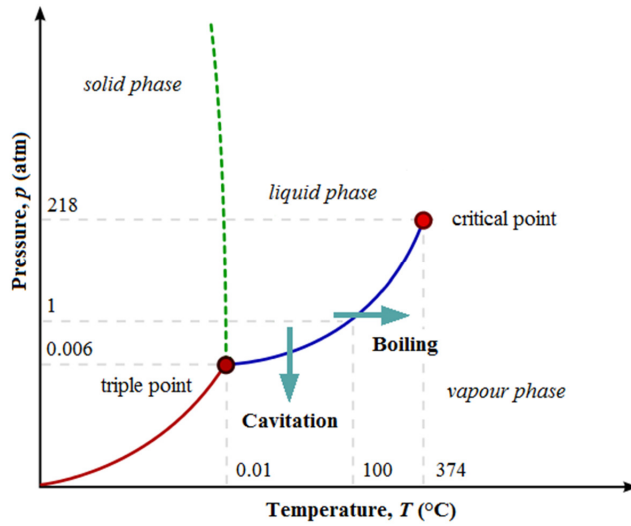


Fig. 2- Phase diagram of water (adapted from Brennen [27]).

It is widely accepted that cavitation inception strongly depends on the water quality, especially nuclei concentration in water. Occurrence of cavitation bubbles initiates from weak points in water, namely bubble nuclei, which break the bond between the water molecules. These nuclei are generally tiny gas bubbles or solid nuclei.

Despite some differences in cavitation bubbles generation by using AC and HC, on a small scale, the principles that governs the hydrodynamic bubble and the acoustic bubble growth are the same. In AC, when the ultrasound wave propagates into the liquid, it generates compressions and rarefactions. The compression cycles exert a positive pressure on the liquid by pushing the molecules together, whereas the rarefaction cycle exerts a negative pressure by pulling the molecules from one another. Due to the low pressure, cavitation bubbles are formed in the rarefaction regions. These bubbles grow in successive cycles and reaches to an unstable diameter collapsing violently [28]. In HC, due to the presence of a constriction into the fluid, low flow pressure are achieved, resulting in cavitation bubbles generation. At the downstream of the constriction, as the liquid expands, the flow pressure recovers and this results in growth of bubbles achieving an unstable diameter whereby the cavities collapse violently [29]. Bubbles that occur in a cavitating flow are often far from spherical. However, it is often argued that the spherical analysis exhibits satisfactory higher-level bubbles dynamic modelling. Moreover, it is often assumed that an isothermal bubble growth up to the maximum radius occurs, in which the bubble is mainly filled by vapour at equilibrium at the ambient temperature [30].

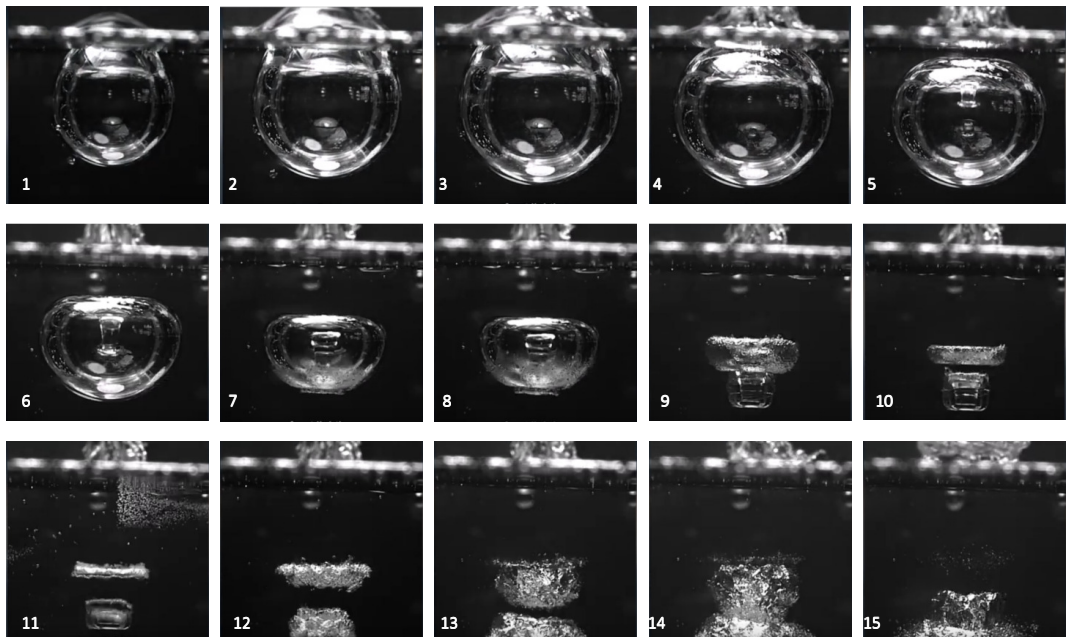


Fig. 3- Growth, implosion and collapse of bubbles in cavitation process. 1-3: static pressure < vapour pressure → vapour bubble grows at low pressure; 4: static pressure = vapour pressure → no further growth of bubble; 5-15: static pressure > vapour pressure → implosion and collapse; 9-15: → micro-jets (adapted from Cavitation - Easily explained!, IET Institute for Energy Technology, <https://www.youtube.com/watch?v=U-uUYCFDTrc>).

Many studies were carried out on dynamics of bubbles collapse [31], showing the presence of several peculiar phenomena that can take place in a very short period, while the overall environment remains at the ambient atmospheric conditions. After the growth phase, bubbles can collapse, generating new rebound bubbles of smaller size that can grow and collapse several times again. This phenomenon, known as *rebound*, is due to the presence of gas trapped in bubbles during the collapse [27,32]. Rebound bubbles can also sometimes break into several bubbles (*fission* of bubbles). The shape of rebound bubbles depends on the symmetry or asymmetry of the dynamics of the collapse. A perfectly spherical collapse produces a spherical rebound bubble, while an asymmetry leads to the deformation of the bubble and to the generation of a *micro-jet* emerging from the rebound bubble [27]. Micro-jet can reach velocities in the order of 100 m s^{-1} [33], increasing the turbulence and the mass transport coefficient. Because of its high velocity, micro-jet can contribute to promote changes in water clusters, agglomerations of fibres and molecules. During the collapse phase, the high velocity of the bubble interface and the compressibility of the liquid lead to the generation of shock waves into the liquid. At this stage, very high temperatures of several thousand Kelvin occur [21], but these last for very

short time (in 1 sec the temperature drops to the temperature of the surrounding fluid). Such extreme conditions are sufficient to dissociate vapours trapped in the cavitating bubbles, resulting in the generation of free radicals, such as $\cdot\text{H}$ and $\cdot\text{OH}$, which are very strong and not specific oxidizing species [34,35]. At the very last stage of the collapse, the pressure and temperature of the gas inside bubbles are so high that light is emitted. This phenomenon of light emission is known as *luminescence* [36].

Based on the degree of intensity, in terms of the magnitude of pressure or temperature, cavitation can be classified as either *transient* or *stable* [28]. In transient cavitation, bubbles radius expands to at least twice the initial size. During the collapse phase, bubbles can collapse to a minute size of its original size in a limited time frame, resulting in a no mass flow of permanent gas through the bubble-liquid interface [25] and causing a very violent implosion. This allows the realise of a significant amount of energy in the form of an acoustic shock-wave and as visible light. At this stage, temperature of the vapour within the bubble and pressure can achieve several thousand Kelvin and several hundred atmospheres, respectively. In stable cavitation, on the other hand, bubbles contain more gas and thus have a less violent collapse compared to transient bubbles. The shock-waves and micro-jets caused by stable bubble implosions thus generate a lower pressure compared to transient ones [37–39].

In HC, it was demonstrated that if the intensity of turbulence is quite low, the pressure recovery downstream the constriction can be approximated by a linear expression with respect to a distance downstream the constriction stable cavitation occurs. When the intensity of turbulence increases and pressure recovery is no more linear the cavitation bubble behaviour can be defined as transient [40].

3. HC generation and mechanisms

HC is produced by pressure variations in a flowing liquid caused by flow velocity variations in the system by introducing constrictions, such as orifice plate, Venturi or throttling valve, in the flow. According to the Bernoulli principle (*Eq. 1*), when the liquid passes through the constriction, the flow velocity (*Fig. 4 a*) and, then, the flow kinetic energy increase at the expenses of the flow pressure (*Fig. 4 b*).

$$\frac{V^2}{2g} + \frac{p}{\rho g} + z_1 = \text{constant} \quad \text{Eq. 1}$$

where V is the fluid flow velocity at a point on a streamline, g is the acceleration due to gravity, z is

the elevation of the point above a reference plane, p is the pressure at the chosen point, and ρ is the density of the fluid at all points in the fluid.

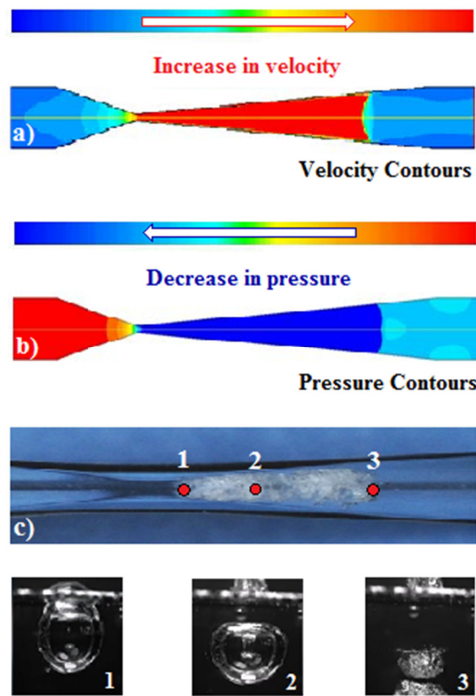


Fig. 4- Effect of a constriction on flow velocity and pressure in a Venturi system: a) contours of flow velocity magnitude; b) contours of flow pressure magnitude; c) high-speed camera frames.

The total energy of cavitation process is constant, but some of the energy is converted into turbulence and heat during the process; therefore, the downstream flow pressure will always be less than the upstream flow pressure. If the throttling of the constriction is sufficient, the flow pressure at the throat of the constriction equals or falls below the vapor pressure of the liquid at the given temperature, and the vaporous cavities are formed.

This condition can be formulated as:

$$P_{\min} = P_v \quad \text{Eq. 2}$$

where p_{\min} is the minimum static flow pressure and p_v is the vapor pressure at a given temperature of the liquid. Depending on the geometry of the constriction, with further lowering of the pressure, the cavities continue to grow reaching their maximum size at the lowest flow pressure and

subsequently when the liquid flow expands, resulting in a decrease in flow velocity, the flow pressure recovers and this results in the implosion and the collapse of these earlier formed cavities [29,41], (Fig. 4 c).

3.1. HC flow regimes

In characterizing cavitating flows, the most used parameter is the cavitation number C_v , Eq. 3. It is a dimensionless number that can be expressed as reported in the following equation:

$$C_v = \frac{p_r - p_{v(T)}}{\Delta p} = \frac{p_r - p_{v(T)}}{\frac{1}{2} \cdot \rho \cdot v^2} \quad \text{Eq. 3}$$

where p_r is the measured downstream recover pressure in the undisturbed flow [Pa] (a conventional reference point close to the point where cavitation inception is expected and where flow pressure is easily measurable), p_v the vapour pressure of the liquid at the operative temperature T (i.e. 2.35 kPa at 25°C) [Pa], Δp the pressure difference that characterizes the system, and ρ , v are the liquid density [kg m^{-3}] and the measured liquid velocity [m s^{-1}] at the cavitating constriction, respectively.

This parameter indicates the probability of cavitation occurring in a flow regime. As shown in Eq. 3, C_v is can be defined as the ratio between the forces collapsing cavities respect to those initiating their formation. Therefore, high values of C_v involve more collapsing forces and lower initiating forces indicating lower cavitation activity. Cavitation may occur because of either a decrease in flow pressure at the reference point or an increase in the Δp -value.

Cavitation begins to occur at values below cavitation inception number, C_v^* . In most of studies, it was observed that cavities formation starts at C_v equal to 1 [29]. However, due to the presence of dissolved gases in the liquid and other solid particles, cavitation can start for C_v greater than 1. Typical values of C_v^* are in the range 1- 2.5 for orifices flow in the pipe [42].

Many reports indicate that with a decrease in C_v below 1, more cavities are formed, resulting in an increase of cavitation effects. It was also observed that a further decrease in C_v implies the achievement of a condition for which cavities start coalescing with each other due to large number and volumetric concentration of cavities and forms vaporous cloud (*choked cavitation/supercavitation*), resulting in a decrease in cavitation intensity [43].

The threshold C_v^* depends on all the usual factors considered in fluid mechanics such as flow geometry, viscosity, gravity, surface tension, turbulence levels, thermal parameters, wall roughness and gas content of liquid in terms of dissolved and free gases [33].

In HC, five different flow regimes can be identified depending on cavitation number value, compared to the threshold value C_v^* , [33]:

- *Non-cavitating flow*: when the pressure of the liquid is higher than the saturated vapour pressure, cavitation does not occur ($C_v > C_v^*$). In this stage, known as non-cavitating flow phase, there is no evidence of cavitation bubbles into the liquid.
- *Cavitation inception or limited cavitation*: in this phase, the pressure of the liquid equals or falls below the vapor pressure of the liquid. Cavitation number is equal or slightly lower than the threshold value ($C_v \leq C_v^*$). Cavitation is just barely detectable, resulting in the appearance of scattered cavitation bubbles into the fluid. This phase is always characterized by strong noise of collapsing bubbles due to an instability of the generated cavities.
- *Developed cavitation*: even lower values of cavitation number ($C_v \ll C_v^*$) allow the complete development of the cavitation bubbles.
- *Supercavitation*: This stage represents the final state of cavitation ($C_v \lll C_v^*$). In this regime, the pressure in cavitating area is low and a big fixed cavity is formed. Compared with other types of cavitation, the interface of a supercavitation cavity is stable. The cavity stays attached to the constriction and the cavity closure is downstream. The cavity acts as if it is an extension of the constriction. The length of the cavity does not vary significantly even though considerable oscillations can occur at its closure.
- *Desinent cavitation*: in this phase, cavitation bubbles completely disappear as a result of raising the downstream flow pressure. Desinent cavitation is often used as a threshold between cavitating and non-cavitating flows.

Recently, it was proved that C_v cannot be used as a single parameter in providing cavitation conditions and that large inconsistencies regarding its determination in the previous reports exist [44]. Moreover, C_v is not always determinable in HC devices due to some operative difficulties in flow velocity or pressure measurements in cavitating zone (turbulent flow), especially when the complexity of the geometry of the cavitating device is increased [8].

3.2. HC types

Cavitating flows can exhibit a number of different kinds of cavitation depending on the flow configurations. Three main classification families are the *attached cavitation*, the *convected cavitation* and the *vortex cavitation* [27].

3.2.1. Attached cavitation

In the attached cavitation, a wake or a region of separated flow filled with vapour can be observed. The cavity interface is partly attached to the solid surface. The liquid-vapour interface can be smooth and transparent or has the shape of a highly turbulent boiling surface. Attached cavitation can be partial or appears as supercavitation when the cavity grows in such a way to envelop completely the solid body. This type of cavitation on a hydrofoil (*Fig. 5 a*) or propeller blade is usually termed “sheet cavitation”, whereas in the context of pumps it is known as “blade cavitation”. Moreover, in the context of bluff bodies (*Fig. 5 b*), a vapour-filled wake is often called a “fully developed” or “attached” cavity. Clearly sheet, blade, fully developed and attached cavities are terms for the same large-scale cavitation structure.

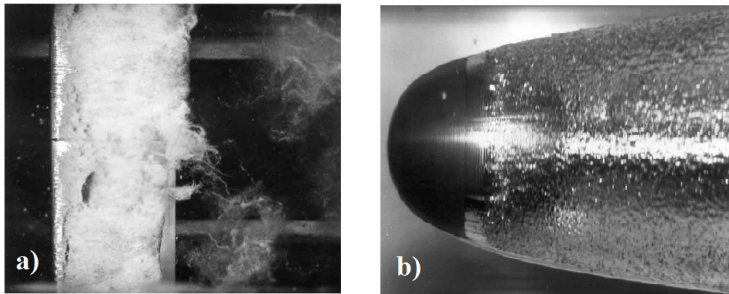


Fig. 5- Attached cavitation on: a) hydrofoil and b) bluff body. The flow is from left to right (reproduced from Brennen [27]).

When generated transient cavities are of the same order as the main attached cavity, attached cavitation is also called “cloud cavitation”, where a periodic formation and collapse of a “cloud” of cavitation bubbles can be observed. *Fig. 6* shows the formation (*Fig. 6 a*), separation (*Fig. 6 b*) and collapse (*Fig. 6 c*) of a cavitation cloud on a hydrofoil oscillating in pitch. The temporal periodicity may occur naturally or it may be the response to a periodic disturbance imposed on the flow. A very common example of imposed fluctuations can be provided by the interaction between rotor and stator blades in a pump or turbine. Recently, in a shear induced HC reactor, where two facing rotors with special radial grooves are spinning in opposite directions, the developed cavitation was studied by Petkovšek et al. [45]: attached cavitation and bubbles shed from the attached cavitation were observed on the solid surface of the teeth rotors, in the gap between the rotor and the housing. A cavitation cloud between the aligned grooves was also detected.

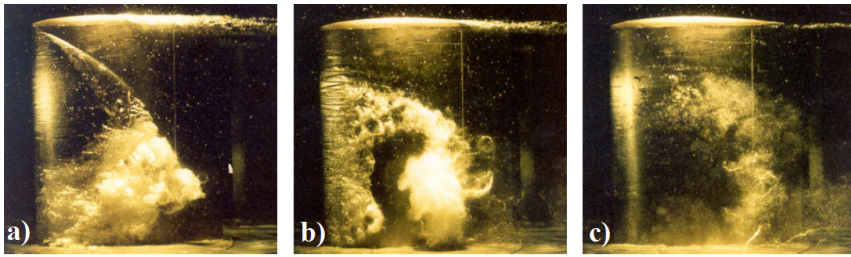


Fig. 6 - a) Formation, b) separation and c) collapse of a cavitation cloud on the suction surface of a hydrofoil. The flow is from left to right (reproduced from Brennen [27]).

To effectively exploit the positive effect of HC, the developed cavitation should be studied and controlled in HC reactors. For instance, recently Dular et al. [20] studying a Venturi device where attached cavitation occurred [46], showed the progress of the developed cavitation, Fig. 7.

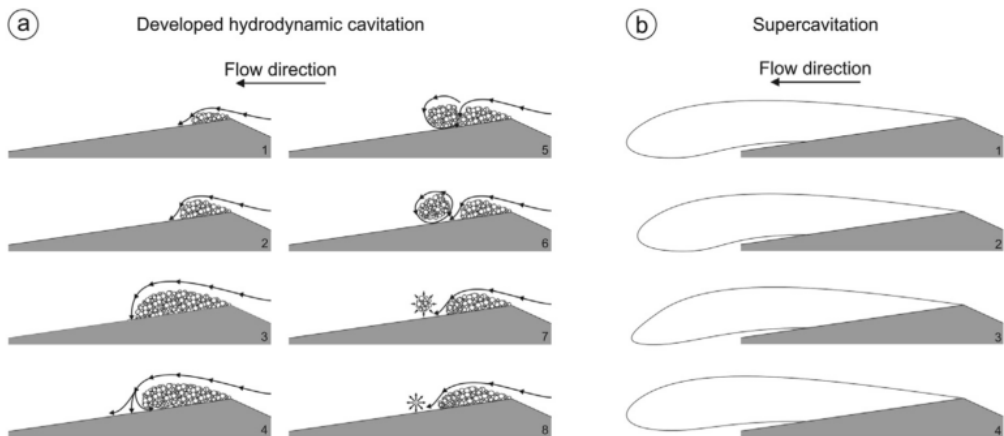


Fig. 7- Schematic representation of “developed HC” (a) where highly dynamical vapour cloud shedding associated with high pressure pulsations is expected and “supercavitation” (b), which is characterised by a single quasi steady large cavitation pocket (reproduced from Dular et al. [20]).

It was observed that the flow followed a distinctive pattern where cavitation structures of different shapes and sizes were shed from the attached cavity. Due to the pressure difference between the outer flow and the inside of the attached cavity, the streamlines curve towards the cavity and the surface beneath it. This caused the attached cavity to close and the formation of a stagnation point at which the flow was split into outer flow, which reattached to the wall, and the re-entrant jet, which travelled upstream, carrying a small quantity of the liquid to the inside the cavity. As the re-entrant jet travelled upstream, it lost momentum, turn upwards and “cut” the attached cavity, causing cavitation cloud separation (shedding). The cloud was then entrained downstream by the main flow

and can violently collapse in a region of pressure recovery. During the separation, circulation around the structure can appear, causing it to reshape, break up etc. Meanwhile the attached cavity began to grow and the process was periodically repeated (*Fig. 7 a*). As the system pressure is decreased, and consequently the flow velocity is increased, a small cavity will extend and grow more and more. It becomes a supercavity as soon as it stops to close on the cavitator wall but inside the liquid, downstream of the cavitator (*Fig. 7 b*). Supercavitating flow is not characterized by noise, vibration and erosion.

3.2.2. Convected cavitation

While in the attached cavitation the cavity interface is partly attached to the solid surface, in the convected cavitation the entire cavity interface is moving with the flow. Cavitation bubbles are generated in the liquid for low-pressure gradients and move with it as they expand and collapse during their life cycles (*Fig. 8*).

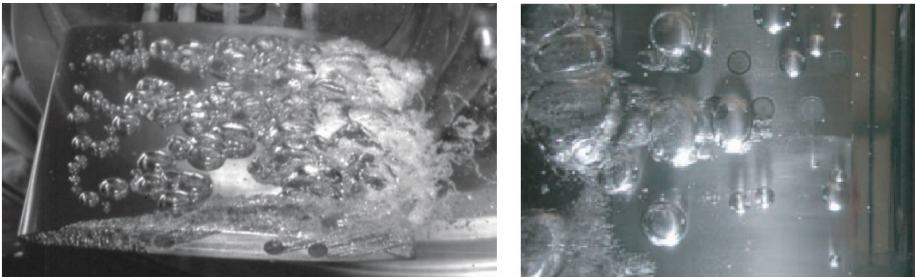


Fig. 8- Travelling bubble cavitation in convected cavitation (reproduced from Brennen [27]).

3.2.3. Vortex cavitation

Many flows with high Reynolds numbers contain a region of concentrated vorticity where the pressure in the vortex core is often significantly smaller than in the rest of the flow and thus cavitation inception can occur. With further reduction of the cavitation number, the entire core of the vortex may become filled with vapour. *Fig. 9* shows some examples of cavitation vortex in a hydrofoil (*Fig. 9 a*), in a propeller (*Fig. 9 b*) and in a turbine (*Fig. 9 c*). It may happen that vortex cavitation bubbles remain smaller compared to the vortex core radius, with nearly spherical rapidly growing and collapsing bubbles entirely within the confines of the vortex core. However, at lower flow pressures the initially near-spherical bubble can expand and elongate to fill the core of the vortex and continue to grow along the vortex axis, becoming highly elongated [47].

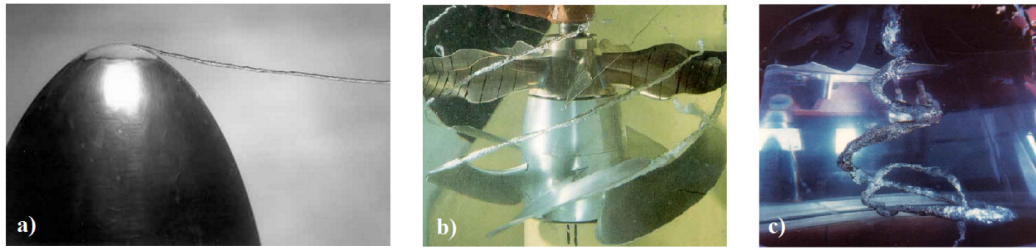


Fig. 9- Vortex cavitation in a) hydrofoil, b) propeller and c) turbine (reproduced from Brennen [27]).

4. Mechanisms of pollutants degradation

The violent collapse of the cavities in cavitating systems results in the formation of reactive hydrogen atoms and hydroxyl radicals as well as gives rise to thermal hot spots, which can yield pyrolytic cleavage of chemicals [48]. Thus, HC results in number of effects (both chemical and mechanical) in the system, Fig. 10.

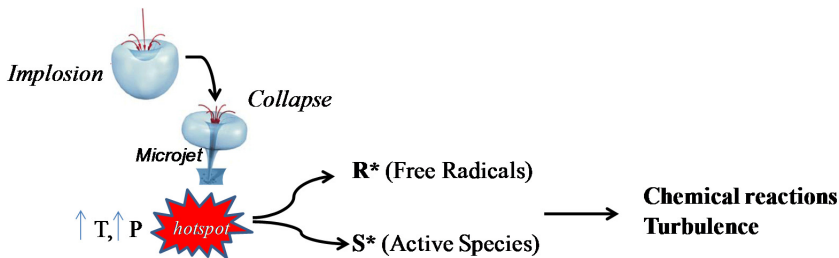


Fig. 10- Mechanisms of bubble collapse and formation of radicals and reactive species used for the degradation of contaminants.

The two main chemical mechanisms for the degradation of pollutants using HC are the thermal decomposition of the volatile pollutant molecules entrapped inside the cavity during the collapse of the cavity and secondly, and the reaction of $\cdot\text{H}$ and $\cdot\text{OH}$ radicals with the pollutant occurring at the cavity-water interface. In the case of non-volatile pollutants, the main mechanism for the degradation of pollutants will be the attack of hydroxyl radicals on the pollutant molecules at the cavity-water interface and in the bulk fluid medium.

Mechanical effects are also significant: (i) generation of shock waves by the collapsing cavity, (ii) liquid micro-jet formation, and (iii) creation of interfacial turbulence and powerful hydraulic shear stress due to the high flow velocity. Mechanical effects can directly rupture molecular bonds on the macromolecular main chain, especially the complex large molecular weight compounds, thus

degrading the refractory organic matters. The broken down intermediates are more amenable to $\bullet\text{OH}$ attack as well as biological oxidation, which can further enhance the rate of oxidation/mineralization of the pollutants [43]. Furthermore, the micro-jet of high velocity ($>100 \text{ m s}^{-1}$ [33]) disturbs the boundary layer at the solid surface, leading to the breakdown of the liquid film responsible for the resistance to the mass transfer. Furthermore, chemical and mechanical effects are also responsible for the enhancement of the heat transfer. The heat transfer rate almost doubles in the presence of cavitation in a conduit [49].

5. The effect of various parameters on HC effectiveness

Overall, a significant number of parameters exists that affect HC effectiveness, which influence the numbers of generated (reactive) bubbles and the collapse conditions. An overview of the effective parameters in HC was suggested by Braeutigam et al. [50] and showed in Fig. 11.

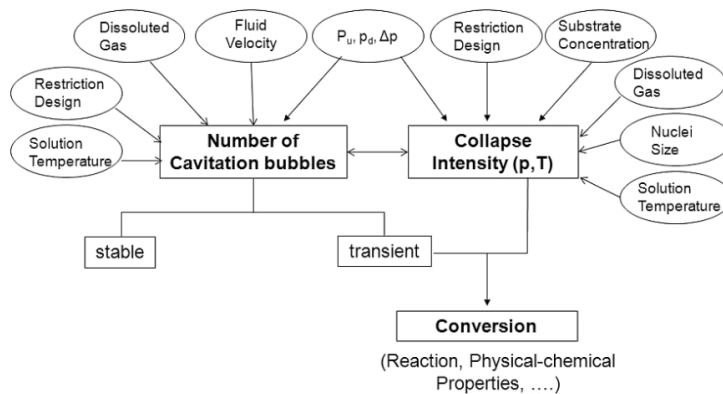


Fig. 11- Overview of the effective parameters in HC (reproduced from Braeutigam et al. [50]).

Thus, the main factors, which determine the HC field and its effectiveness, are (i) device construction parameters; (ii) technological process parameters; (iii) properties of the liquid medium [51]. The influence of all these aspects on HC effectiveness are separately analysed in following paragraphs.

5.1. Device construction parameters size

A first group of factors that influence the HC effectiveness includes parameters that determine the structural characteristics of the HC reactor, which consists of a cavitation inducer and a flow chamber.

5.1.1. Influence of cavitating device geometry

HC effectiveness depends on the size and shape of the cavitation inducer and flow chamber, which both affect the number of cavitation bubbles and the collapse intensity. Recently, many researchers are focusing on the optimization of cavitating device geometries in order to obtain maximum cavitation effects, in terms of both number of cavitation events and significant pressure drops, thus decreasing the energy consumption. With this purpose, different HC devices were developed (Fig. 12), among them static orifice plates [8,50], nozzles [16], Venturi [43,44,52], swirling jet [8,9] and rotor-stator systems [18].

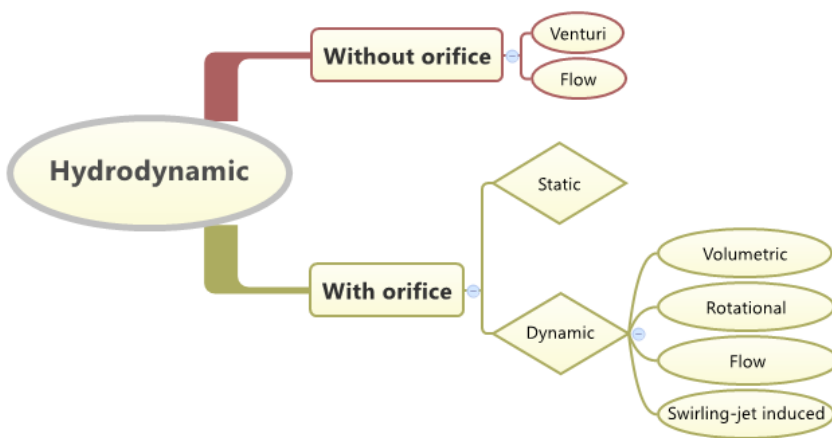


Fig. 12- HC Cavitation reactor classification (adapted from Ozonek [51]).

Furthermore, different geometric configurations of each device were investigated. Some example of different HC reactors present in the literature are following reported.

Šarc et al. [44] considered four very similar Venturi shapes and exposed them to the same operative conditions (constant flow pressure, constant flow velocity, constant temperature). Significant differences in typology, dynamics and aggressiveness of cavitation were found. By using a high-speed camera, they observed how cavitation size and appearance could vary significantly when the divergence angle of the Venturi system was changed. Similarly, Kim et al. [15] investigated the effect of different Venturi outlet inclination angles on the performance of their HC system that was used to increase sludge solubilisation.

Several researchers investigated the influence of the geometry of orifice plate systems on HC intensity [13,53], studying the effects of the number and diameter of holes [13,53,54], the plate thickness [8,53], the hole shape [54]. The highest cavitation intensity is generated by using the lowest free area.

However, for the same free area, plates with higher diameter of the hole and lower number of holes generate relatively lower intensities [11,13].

A swirling jet cavitation device was investigated by Wang et al. [55]. Then, an innovative swirling jet-induced cavitation device was proposed by Mancuso et al. [8,9] and Langone et al. [56], studying the influence of the injection slots number, the geometry of the double cone, and the number of HC devices in series on the HC effectiveness.

Patil et al. [57] developed an efficient stator and rotor assembly. Afterwards, a novel stator and rotor configuration was developed by Petkovšek et al. [58] that studied the effect of different shapes of the teeth of one rotor on the cavitation process [45].

5.2. Technological process parameters

This second group includes parameters that are associated with the characteristics of the technological process, such as the liquid flow velocity/kinetic energy, the pressure at the inlet to the HC system, the liquid temperature, the liquid pH, the HC “processing” time (the number of times the liquid passes through the cavitation region).

5.2.1. Influence of liquid flow velocity

In a HC device, the number of cavitation bubbles is mainly related to an increase of the velocity/kinetic energy of the liquid. Increasing flow velocity, higher local pressure oscillations are expected, and pressure may fall below vapour pressure of the liquid at the operative temperature, causing partial vaporization of the liquid and generating cavities. As can be deduced from *Eq. 3*, an increase in flow velocity implies a decrease in cavitation number, resulting in an increase of cavitation effects. Higher flow velocities further imply higher turbulence levels.

The flow velocity can be varied either by adjusting the pump flow rate (and thus the pump discharge pressure) or by changing the geometry of the cavitating device (i.e. reducing the constriction area).

Šarc et al. [44] observed different cavitation conditions by changing the flow velocity at the throat of a Venturi system, by varying the inlet pressure, while keeping constant the cavitation number and the geometry of their HC system. They observed a slightly increase in cavity growth when the flow velocity was increased. Using Venturi systems, Saharan et al. [43] studied the effect of the flow velocity on the degradation of RR120 by increasing the inlet pressure from 3 to 10 bar. It was observed that the degradation rate increased with an increase in the inlet pressure reaching a maximum (5 bar) and then dropped, due to the onset of supercavitation. Similar results using Venturi system were reported

by Prajapat and Gogate [59] and Gore et al. [60].

In the same way, Joshi and Gogate [61] investigated the influence of flow velocity at the throat of a single orifice plate by varying the inlet pressure. In their experiments, the inlet pressures were varied in the range from 3 to 6 bar, by varying the flow rate. They observed that the extent of degradation of dichlorvos increased as the inlet pressure was increased from 3 bar to an optimum value of 5 bar. In this range, higher inlet pressures, and thus higher flow velocities, promoted an increasingly violent collapse of cavities, and thus an increasingly hydroxyl ions generation, resulting in an enhancement in the extent of degradation. However, at a pressure of 6 bar, the extent of degradation decreased indicating the onset of supercavitation, resulting in an extremely rapid growth of bubbles downstream of the orifice leading to splashing and vaporization of the flow.

Wang and Zhang [62] reported a continuous increase in the degradation rate of alachlor with increasing flow velocity using a swirling jet-induced reactor. The authors increased the flow velocity by increasing the inlet pressures from 2.0 to 6.0 bars, while keeping constant the geometry of their HC system. These results are in agreement with the study of Mancuso et al. [9] that, studying a novel swirling jet-induced cavitation reactor to improve the sludge disintegration, observed an increase in sludge disintegration degree by increasing the inlet pressure from 2.0 to 4.0, due to an increase of flow velocities. However, using the same HC device and degrading a waste dye aqueous solution (Rhodamine B), supercavitation occurred at 3.0 bars [16].

In a rotor-stator system, Badve et al. [63] varied the velocity of liquid on the surface of the rotor by changing the speed of rotation of the rotor. Their results showed that as the rotation speed increased, the liquid surface velocities increased as well, and the cavitation number decreased.

Nevertheless, also the geometry is essential to increase the flow velocity and thus to maximize cavitation effects. Sivakumar and Pandit [13], using multiple hole orifice plates operating at the same inlet pressure, showed an increase of the cavitation process efficiency with the increase of the flow velocity due to geometry variations. In an innovative swirling jet-induced reactor, Mancuso et al. [9] obtained an increasing effectiveness of the HC process, in terms of activated sludge solubilisation, by increasing the flow velocity due to the decrease of the injection slots number while keeping constant the inlet pressure.

5.2.2. Influence of liquid inlet pressure

Fluid inlet pressure influences both number of cavitation bubbles and collapse intensity. In HC systems, an increase in the inlet pressure always implies an increase in flow rate, and viceversa. As seen in

section 5.1.1, higher inlet pressures involved higher flow rate and thus higher flow velocity, increasing turbulence levels and local pressure oscillations. Therefore, increasing the inlet pressure an acceleration in HC process is expected. Furthermore, higher inlet pressures involves higher pressure drops through the HC device, resulting in both higher shear forces that break down bacterial cell walls and in a higher release of organic matter [9]. Treating wastewaters containing RhB by using both a multi hole orifice plate system and a swirling jet reactor, a higher extent of degradation was also observed at higher pressure drops obtained by increasing the inlet pressure [8]. Kumar and Pandit [64] showed also that with an increase in the Venturi inlet pressure, the pressure drop across the Venturi also increased, resulting in an increase in the cluster collapse pressure.

5.2.3. Influence of cavitation number

Cavitation number is inter-correlated with the other two parameters previously described: flow velocity and inlet pressure. Up to now, many studies on the influence of cavitation number on effectiveness of cavitation were carried out. However, missing or inaccurate information about the position at which the pressure and the flow velocity were measured or calculated implies that researchers commonly tend to use inappropriate values of cavitation number, taking advantage that there are no standards methods for its determination [44]. Most of the studies on HC are not repeatable because of a poor definition of the cavitation number in the manuscripts. Nevertheless, for completeness of the contents of this work, some results on the influence of cavitation number on the HC effectiveness are here reported.

Saharan et al. [43] used a Venturi system to degrade Reactive Red 120 dye. It was observed that the rate of degradation increased with a reduction in cavitation number, reaching a maximum and then dropping. The authors explained this finding by considering two separate stages depending on the cavitation number value. In the first stage, a decrease in cavitation number allowed an increase in the number of generated cavitation bubbles. Then, the increase in the number of cavitation collapse pressure pulses as well as of generated $\cdot\text{OH}$ radicals resulted into an increased degradation rate. On the contrary, in the second stage, the degradation rate decreased with a further decrease in cavitation number. This may be because of reduced cavitation intensity due to excess numbers of cavities inside the Venturi at very low cavitation number. Indeed, when there is a large number of cavities, these can start coalescing to form a larger cavitation bubble that can escape the liquid without collapsing or result into an incomplete collapse, resulting in a reduction of generated $\cdot\text{OH}$ radicals. Gore et al. [60] investigated the influence of the cavitation number, ranged from 0.210 to 0.095 on

degradation of reactive orange 4 dye using a Venturi system. It was found that the decolourisation rate increased with a decrease in cavitation number reaching to the maximum at 0.15 and then decreased. Authors attributed these findings to an increase in number of cavities and thus in number of collapsing events, resulting into a generation of more $\cdot\text{OH}$ radicals. However, a further decrease in cavitation number under 0.15 implied a decrease in the extent of degradation due to the occurrence of choked cavitation/supercavitation condition. Under choked cavitation conditions, cavities no longer behaved as individual cavities. They coalesced with each other to form larger vaporous bubbles, which were carried away with the flowing liquid without collapsing.

Therefore, for a decrease in cavitation number, an increase in number of cavities is expected, resulting in an increase in overall collapse intensity of cavities. However, depending on the specific HC device configuration, after certain value of cavitation number, the number of cavities can become very high, so these cavities can start coalescing with each other and form a cavity cloud. Energy produced by the collapse of some cavities can be taken up by the neighbouring cavities, resulting in cavity cloud formation (choked cavitation). Hence, the importance of optimizing HC cavitation devices in order to operate between these two limits, i.e. cavitation inception and choked cavitation/supercavitation to get the maximum effect.

Furthermore, it should be noticed that in order to compare two or more HC systems each other, rather than cavitation number other parameters, such as the vibrations and noise measurements, and indexes (see section 6) can be used to measure the intensity and efficiency of HC system.

5.2.4. Influence of liquid temperature

The influence of temperature on HC is complex, which has positive and negative effects on HC treatment efficiency. Temperature affects the dynamics of the cavity through the properties of the liquid such as vapour pressure, viscosity, surface tension, gas solubility. As shown in the phase diagram of water (*Fig. 2*), the vapour pressure of a fluid is dependent on its temperature and it increases exponentially with temperature. Thus, an increase in the operative temperature can enhance the probability of vaporous cavities generation due to entrapment of the vapours and influence the kinetic rate. The increase of temperature implies a decrease of the viscosity and surface tension, leading to an easier bubble formation [51]. However, these generated bubbles are richer in vapour content, which cushioning their implosion, reducing the intensity of bubbles collapse [51]. A rise in temperature reduces the gas solubility, which is the chief source of cavity nuclei and thus reduces the rate of occurrence of cavitation event.

It is then likely that an optimum operative temperature might exist for specific conditions. When the temperature of the solution increases beyond the optimum value, the increase in the vapour pressure of the liquid might result in higher vapour content in the cavitating bubbles leading to a cushioning effect and thus to a HC effectiveness reduction.

With this background, Wang and Zhang [62] reported a positive effect on the degradation of alachlor with an increase in temperature from 30 to 40 °C, but the degradation rate decreased with a further increase in the temperature over a range of 40-60 °C. Joshi and Gogate [61] investigated the effect of operative temperature over the range of 31-39 °C. In their experiments on degradation of dichlorvos, the maximum degradation rate was achieved at the lowest temperature. Mancuso et al. [9] investigated the influence of temperature, ranged from 20 to 35 °C, on sludge disintegration. The authors observed that in this temperature range, HC efficiency was more efficient in terms of sludge solubilisation at higher temperatures. Šarc et al. [44] demonstrated that the magnitude of pressure oscillations, which occur due to cavitation bubbles collapse, increased for temperature up to 40 °C, but then dropped significantly for higher temperatures.

5.2.5. Influence of liquid pH

Typically, acidic or basic conditions can be favourable to the degradation of chemical pollutants using HC reactors. The optimal pH value depends on the pollutant to be treated. Many studies were carried out to remove dye pollutants from wastewaters. Their degradation is strongly dependent on medium pH, as pH can both influences the presence of $\cdot\text{OH}$ free radicals available for pollutants removal and changes pollutants structure resulting in a more biodegradable form, which can be easily attacked by $\cdot\text{OH}$ free radicals. Usually, acid conditions are recommended for pollutants degradation by HC, because such conditions favour the generation of hydroxyl radicals and impede the recombination reaction among free radicals [60].

Joshi and Gogate [61] investigated the influence of the solution pH on the degradation of dichlorvos by using an orifice plate as cavitating device. Among the investigated pH, lower pH provided a higher extent of degradation. Gore et al. [60] investigated on the effect of the solution pH on degradation of reactive orange 4 dye using a Venturi system, ranging from 2 to 10. Authors observed that the decolourisation rate increased with both a decrease and an increase in solution pH starting from a neutral polluted solution. However, the highest extent of degradation was obtained for lower pH solutions, indicating a lower rate of recombination of generated $\cdot\text{OH}$ radicals in acid conditions and hence the presence of more $\cdot\text{OH}$ radicals available for the oxidation of the dye. Moreover, under acidic

conditions the state of the orange 4 molecules changes from ionic to molecular. This alteration in the state of the molecules makes them hydrophobic and more easily attacked by $\cdot\text{OH}$ free radicals. On the contrary, in the basic medium, the extent of degradation of orange 4 was not so high as in acid conditions because its molecules remained in ionic state, resulting in an increase in their hydrophilic behaviour that implied their persistence in the liquid bulk. Same behaviours were reported for Rhodamine B degradation. Mancuso et al. [8] treated polluted aqueous solutions by Rhodamine B using a multi hole orifice plate system; they observed the highest degradation rate of the dye at pH 2.0, while it dropped significantly and remained constant in the pH range of 5.0-8.0. This was due to the prevalence in acid conditions of Rhodamine B in the cationic form rather than the zwitterionic form [65]. Previous studies on Rhodamine B reported that the cationic form is easier to degrade [66], and thus at low values of pH the oxidation of Rhodamine B is higher. Similar results were obtained by Mishra and Gogate [67] using a Venturi device and by Wang et al. [66] using a swirling jet-induced cavitation system, respectively. Saharan et al. [43] investigated on the effect of medium pH on Reactive Red 120 dye degradation by carrying out experiments at different pH in the range of 2-11. Their results indicated that the rate of degradation increased with a decrease in solution pH confirming that acidic medium was more favourable for the degradation of Reactive Red 120 dye. Treating sludge, alkaline conditions are preferable to enhance the organic hydrolysis [68]. Optimal results in terms of organic matter release were obtained when HC was assisted with NaOH pre-treatment, working at pH of 9- 10, favouring the biogas production by means of anaerobic digestion process [69].

5.3. Properties of the liquid medium

This last group includes parameters characterising the properties of the liquid medium, in the main: pollutant concentration, viscosity of the liquid, the surface tension and the dissolved gas content.

5.3.1. Influence of pollutant concentration

When the cavitation conditions are constant, the amount of $\cdot\text{OH}$ radicals produced in the HC system would be constant as well. Therefore, for an increase in initial pollutant concentration a decrease in pollutant removal rate is expected as hydroxyl radicals may not be sufficient to destruct the pollutant completely.

This is true in the case of removal of chemical pollutants dissolved in water solutions. Parsa et Zonouzian [53] studied the effect of dye initial concentration on degradation of Rhodamine B by using

a submerged multi hole orifice plate system. In their experiments, the initial dye concentration was ranged from 2 to 14 mg L⁻¹. They found that the efficiency of process was inversely proportional to the initial dye concentration. In justifying this result, authors explained that it might be imputed to an increase in the total amount of dye molecules while the total amount of free hydroxyl radicals remained constant. These findings are in agreement with the studies on Rhodamine B degradation by Mancuso et al. [8] and Wang et al. [66,70], respectively, where authors observed an increase in the extent of dye degradation with a decrease in initial dye concentration.

However, when sludge, characterized by the presence of particulate organic matter, is treated in order to increase its solubilisation, higher initial total solid concentrations (TS) can positively influence the sludge disintegration degree. Kim et al. [52] investigated the influence of initial sludge concentration, ranged from 5 to 40 g L⁻¹ on sludge solubilisation by using a Venturi system as cavitating device. Authors observed an increase in sludge solubilisation increasing the initial TS concentration. These results are in agreement with the study by Mancuso et al. [9], where authors, ranging the initial sludge concentration from 7 to 40 g L⁻¹, observed the highest COD solubilisation for the highest initial sludge concentration. The increase in TS content provides more cells and aggregates and thus a higher viscosity of the sludge, due to the inter- and intra- particle interactions. Even if both growth and collapse of bubbles are slowed down by viscosity in HC [46], the increase in TS enhances the collisions between sludge flocs and cavitation bubbles, allowing the subsequent increase in sludge disintegration. Thus, the negative effect of high TS concentration was negligible compared to the positive effect of TS concentration on the sludge disintegration.

The presence of solids can also decide the initial size of the nuclei and the effect of initial radius must also be considered while choosing a particular liquid medium and the process conditions.

5.3.2. Influence of liquid viscosity

Viscosity is the main characteristic reflecting the rheology of the treated matter. This important parameter can influence the HC intensity and the way in which polluted liquids flow into HC devices. Viscosity affects both the distribution of nuclei and bubble dynamics. Usually, an increase in viscosity, both in Newtonian and non-Newtonian fluids, reduces the efficiency of the cavitation effect, resulting in a slowdown in both growth and collapse of bubbles in HC [46]. Indeed, in most of the applications, water is used as the liquid medium due to its low viscosity, which assists the occurrence of cavitation. However, HC process was also used as pre-treatment for sludge from wastewater treatment plants, which viscosity increases with the increase of TS concentration, due to the inter- and intra-particle

interactions [52]. Experimental results showed that the negative effect of viscosity on the sludge solubilisation is negligible compared to the positive effect of sludge concentration for cavitation development [9,52].

Furthermore, it is interesting to underline that, when sludge is treated by HC process its viscosity decreases indicating possible reductions of energy requirements for the anaerobic digestion heating, mixing, and pumping [71]. Kim et al. [52], using a Venturi system as cavitating device, observed that sludge viscosity decreased significantly during the first 30 min treatment and then stayed relatively constant after 1 h treatment. The decrease in viscosity was mainly attributed to the increase in temperature, shear forces and cavitation bubble collapse. These results are in agreement with the study by Mancuso et al. [9] where a swirling jet-induced cavitation was used to increase the sludge solubilisation. During their HC tests, authors progressively reduced the frequency of the pump inverter in order to keep constant the inlet pressure value, and thus the flow rate and flow velocity. This was due to a progressive alteration of the rheology of the sludge, resulting in a decrease of the viscosity of the sludge during the HC treatment. Similarly, Prajapat and Gogate [59] investigated the effect of inlet pressure on depolymerisation of aqueous polyacrylamide solution by using a Venturi system. Their experimental results showed an increase in intrinsic viscosity reduction with an increase in the inlet pressure.

5.3.3. Influence of surface tension

Surface tension has an effect on the nucleation stage of the HC process by controlling the number and the size of the stable gas or vapour nuclei that are present in the liquid, which influence the HC process efficiency [72]. For a bubble at stable equilibrium with the surrounding liquid, the pressure inside the bubble is equal to the sum of external liquid pressure and surface tension forces. Before being subjected to cavitation, for higher surface tensions, the dissolution of the gas nuclei into the liquid due to surface tension forces will be faster and the number of gas nuclei present in the liquid at any instant will be smaller. Thus, at the start of the HC process, the nuclei may not be present in sufficient numbers to get any significant impact on cavitation. However, during collapse, the cavities become fragmented at high implosive velocities and these fragments can subsequently become nuclei for the next cycle. Thus, over a period, the nuclei become sufficient in number and the cavitation effect can be observed.

The surface tension depends on the type of liquid and temperature; a rise in temperature causes a fall in the surface tension, which means easier evaporation [51]. The presence of a small amount of

surfactant allows to reduce the surface tension and thus to greatly reduce the cavitation threshold and facilitate the generation of bubbles and, therefore, the production of hydroxyl radicals.

However, while a decrease in the surface tension of the liquid makes generation of cavitation easier, it should also be noticed that a decrease of surface tension affects the collapse of cavities, which would be less violent.

5.3.4. Influence of dissolved gas content

The presence of dissolved gases significantly enhances the cavitation effect by supplying the nuclei for the HC process; in addition, the quantity of the gas inside the cavity significantly affects the final collapse temperature and pressure [72]. Most of the HC applications are carried out in the presence of gas atmosphere; however the effect of presence of various gases (i.e. argon) was also investigated [73]. It was observed that different properties of the dissolved gases significantly affect the cavitation process, such as the gas solubility [72].

6. Methods to evaluate cavitation efficiency

In the last years, in order to investigate the efficiency of different HC systems in terms of both treatment removal efficiency and total energy supplied to the system, many parameters were proposed, mainly depending upon the treated matter characteristics.

6.1. Pollutants degradation in wastewaters

HC technique was recently used alone or in presence of additives to degrade toxic and carcinogenic dyes in polluted water bodies. In different studies, the degree of the degradation of dyes, such as Rhodamine B (RhB) [8,13,66,67,70], orange 4 dye [60], orange acid II [74], brilliant green [74], reactive brilliant red K-2BP [75], pharmaceuticals [76] and pharmaceutical micro-pollutants [76,77] was evaluated by considering the extent of degradation (ED), as a percentage of removal. ED was calculated as reported in Eq. 4:

$$ED (\%) = \frac{(C_0 - C)}{C_0} \times 100 \quad \text{Eq. 4}$$

where c_0 [mg L^{-1}] is the initial value of pollutant concentration and c [mg L^{-1}] is the residual pollutant concentration at the generic instant. HC efficiency was more efficient in terms of extent of dye degradation at higher ED.

Another parameter that was taken into account is the cavitation yield C.Y. [8,13,60,66,74,78], calculated as in Eq. 5 and defined as the ratio of the observed cavitation effect, in terms of amount of degraded pollutant (usually expressed in mg L^{-1}) by using HC, to the total energy supplied to the system:

$$\text{C.Y.} = \frac{\text{Degraded matter}}{\text{Power density}} \quad \text{Eq. 5}$$

where the degraded matter is the amount of dye in $[\text{mg L}^{-1}]$ removed in the experiment, while the power density, in $[\text{J L}^{-1}]$, is represented by the following equation Eq. 6:

$$\text{Power density} = \frac{P_{\text{abs}} \cdot t}{V} \quad \text{Eq. 6}$$

where V is the volume of the treated matter $[\text{L}]$, P_{abs} the pump absorbed power by HC system $[\text{W}]$ and t the treatment time $[\text{sec}]$. The higher the C.Y. value, the more efficient the HC treatment, in terms of both degradation and total energy supplied to the HC system, was.

Treating the same pollutant, C.Y. can be used to compare two or more different HC systems with each other.

6.2. Biological wastewater treatments

Recently, HC technique was successfully applied in the field of wastewaters to treat sludge, manure and biomass, resulting in an intensification and improvement of organic matter solubilisation.

Cavitation acts by destroying bacterial cell walls and membranes resulting in a release of intracellular and extracellular matter [79]. Many of the intracellular constituents, including cytoplasm and nucleic acids, are readily biodegradable, resulting either in acceleration of both aerobic and anaerobic digestion processes in the sludge treatment or in promoting denitrification in the wastewater treatment process [9].

In this case, HC efficiency can be evaluated by measuring (i) the improvement of solubilisation of sludge in terms of the soluble chemical oxygen demand (SCOD)- increase, Eq. 7, (ii) the ratio of change in soluble chemical oxygen demand (SCOD) after cavitation to particulate chemical oxygen demand ($\text{PCOD}_0 = \text{TCOD} - \text{SCOD}_0$), Eq. 8, and (iii) the ratio of change in ammonia after cavitation to initial organic nitrogen content ($\text{Norg}_0 = \text{TKN}_0 - \text{NH}_4 + \text{N}_0$), Eq. 9:

$$\Delta\text{SCOD} (\%) = \text{SCOD}_{\text{cav}} - \text{SCOD}_0 \quad \text{Eq. 7}$$

$$DD_{PCOD} (\%) = \frac{SCOD_{cav} - SCOD_0}{PCOD_0} \times 100 = \frac{SCOD_{cav} - SCOD_0}{TCOD - SCOD_0} \times 100 \quad Eq. 8$$

$$DD_N (\%) = \frac{NH_4^+ - N_{cav} - NH_4^+ - N_0}{Norg_0} \times 100 = \frac{NH_4^+ - N_{cav} - NH_4^+ - N_0}{TKN_0 - NH_4^+ - N_0} \times 100 \quad Eq. 9$$

where $SCOD_{cav}$ is the soluble COD of the treated sludge by using HC [$mg L^{-1}$] at the time t , $SCOD_0$ is the soluble COD of the untreated sludge [$mg L^{-1}$], $TCOD$ is the total COD of the untreated sludge [$mg L^{-1}$], $NH_4^+ - N_{cav}$ is the ammonia content of the treated sludge by using HC [$mg L^{-1}$] at the time t , $NH_4^+ - N_0$ and TKN are the ammonia and total Kjeldahl nitrogen content of the untreated sludge [$mg L^{-1}$]. Another index of importance in sludge disintegration is the sludge disintegration degree calculated as the ratio of SCOD-increase by cavitation to the SCOD increase by the chemical disintegration, *Eq. 10*:

$$DD_{COD NaOH} (\%) = \frac{SCOD_{cav} - SCOD_0}{SCOD_{NaOH} - SCOD_0} \times 100 \quad Eq. 10$$

where $SCOD_{NaOH}$ [$mg L^{-1}$] is the soluble COD of the reference sample obtained with a strong alkaline disintegration (NaOH digestion).

Furthermore, indexes that take into account the energy consumption can be calculated for each HC system. Many studies report the specific supplied energy (SE), where the energy required by the HC system is divided by the initial amount of total solids:

$$SE \left(\frac{kJ}{kg TS} \right) = \frac{P_{abs} \times t}{V \times TS} \quad Eq. 11$$

where P_{abs} is the pump absorbed power [W], t is the treatment time [sec], V is the volume of the treated sludge [L] and TS is the solids content [$g L^{-1}$].

Moreover, the energy efficiency (EE), expressed as $mg DSCOD kJ^{-1}$, can be calculated as the mg of SCOD-increase per unit of energy supplied, *Eq. 12*, [80]. Higher EE values correspond to higher removal efficiencies.

$$EE \left(\frac{mg \Delta SCOD}{kJ} \right) = \frac{V \times \Delta SCOD}{P_{abs} \times t} \times 1000 \quad Eq. 12$$

7. Conventional scheme of a HC experimental system

Different scheme of HC experimental system were applied in wastewater treatment field. Among available experimental studies, the most common experimental configurations used for HC are closed

loop circuits. Among them, the continuous HC test rig (*Fig. 13*) is the most applied [8,9,13,20]. It comprises a reservoir (1), a pump (2), control valves at appropriate places (V_1, V_2, V_3, V_4, V_5), a cavitation reactor (4), sampling port (5) and measurement gauges (P_1, P_2). Control valves (V_1, V_2, V_3) are provided at appropriate places to control the flow rate through the mainline, [13]. Optionally, an inverter (3), instead of control valves can be used to control the pump flow rate by adjusting the frequency [8,9]. Using control valves, water is pumped from the reservoir branches into two lines, i.e., a main line where HC takes place and a by-pass line that is used to control the flow rate and the pressure. Using the inverter, the solution to treat is directly pumped from the reservoir to a channel internally accommodating the cavitating device. The solution treated by HC, is then recirculated and entered again into the reservoir. Pump can be a mono screw pump [8,9], and in this case the suction side of the pump is connected to the bottom of the reservoir, or a centrifugal pump [13].

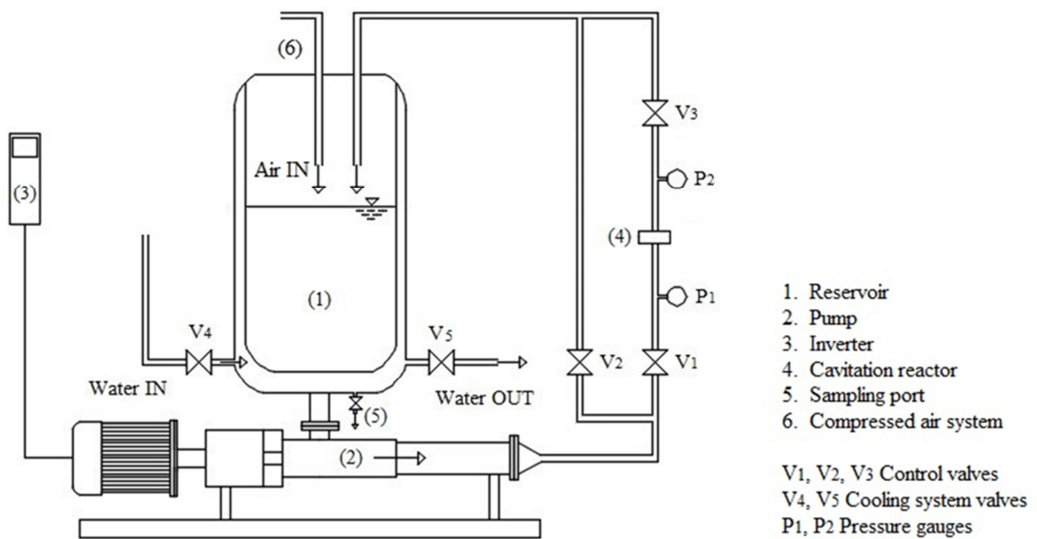


Fig. 13- Schematic representation of the experimental setup of a continuous HC reactor (closed loop), (adapted from [8,9,13,20]).

As temperature has a significant effect on cavitation, a cooling system is usually provided to control the liquid temperature.

Optionally, instead of the pump, a compressed air system (6) at high pressure (about 5 atm) flow can be present to adjust the flow rate [20]. Using the compressed air system, by opening the valve, compressed air at high pressure flows into the reservoir and forces water to flow through the cavitating device. Since this configuration does not have the pump, the water temperature cannot

increase significantly and no temperature control is needed.

However, in order to have a more accurate evaluation of the cavitation phenomenon and the number of passes, two reservoirs can be used instead of a closed loop, as proposed by Dular et al. [20] in a pulsating HC reactor configuration (*Fig. 14*). A pump, the main heat source in the loop, was not included in the experimental set-up, and pressure due to a compressed air system was used to force the treated water from one reservoir to the other. It operated in cycles. Water was introduced into the reservoir 1, while the reservoir 2 remained empty. By opening the valve, compressed air at high pressure flowed into the reservoir 1 and forced water to flow through the symmetrical cavitating device (i.e. symmetrical Venturi pipe) into the second reservoir, where constant pressure was maintained at 1 bar. As the flow passed through the cavitating device, it accelerated, causing a drop in the static pressure, which resulted in cavitation. The 3- way valve was electrically controlled – when a signal that the reservoir 1 was empty was received, it closed and then opened the path for the compressed air to flow into the reservoir 2 and for water to flow in the opposite direction and consequently cavitation was achieved at the other side of the cavitating device.

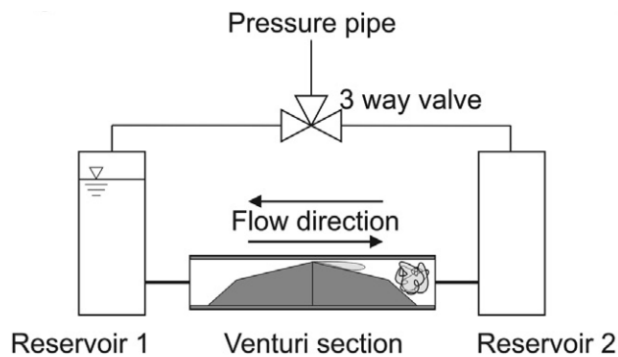


Fig. 14- Schematic representation of the experimental setup of a pulsating HC reactor (closed loop) (reported by [20]).

However, the full-scale application of HC process in a wastewater treatment plant needs to move from closed loop to other configurations that allow a continuous treatment (*Fig. 15*). The scheme reported in *Fig. 15 a*, is an adaption of a closed loop, where a small flow rate of the solution to treat is continuously fed to the reservoir and simultaneously discharged, ensuring a proper retention time. This scheme can be applied when HC devices, which transfer low high energy levels are used, requiring that the solution is treated several times. On the contrary, the scheme reported in *Fig. 15 b* is a one shot treatment, without any recirculation of the solution to treat, and it requires a HC device

able to transfer high energy levels during the single passage.

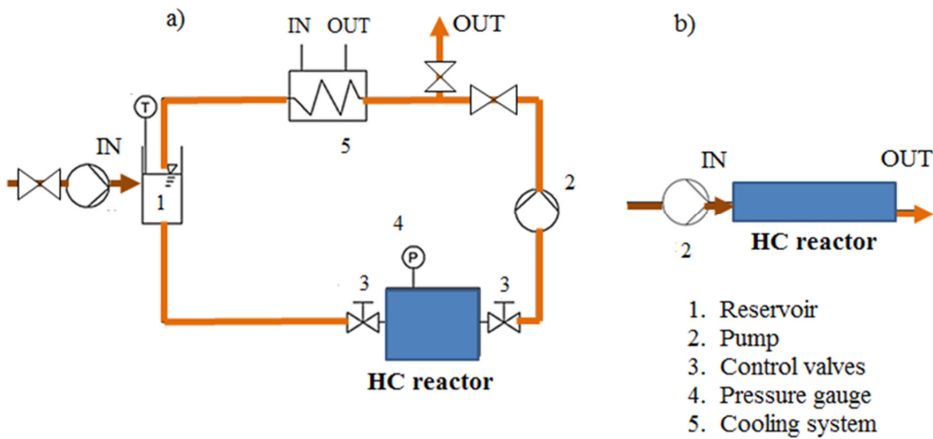


Fig. 15- Schematic representation of opened loops.

8. Reactor used for generation of cavitation in wastewater treatment field

From an engineering point of view, the HC process applied in wastewater treatment field should aim to be a simple energy efficient way of degrading substances. During the last few decades, a number of new cavitation configurations were developed, each of which offers the hope of providing higher pollutant removal efficiencies with the lowest energy consumption.

A first classification was provided by [81,82]:

- *high pressure homogenizer*, which is a high pressure positive displacement pump with a throttling device designed to operate at pressure ranging from 50 atm to as high as 300 atm;
- *low pressure HC reactor*, where the flow through the main line is forced to pass through a geometric constriction (Venturi Fig. 16 b, single-hole orifice, multiple holes on an orifice plate Fig. 16 a) where the local velocities suddenly increase due to a reduction in the flow area resulting in lower pressures;
- *high speed homogenizer*, which consist of a stator-rotor assembly (Fig. 16 c) that operates at rotating speeds of 4,000 rpm to as high as 20,000 rpm, causing a pressure drop near the periphery of the rotor.

Furthermore, other configurations of HC reactor were developed and discussed in details [72], underlining the principles and differences.

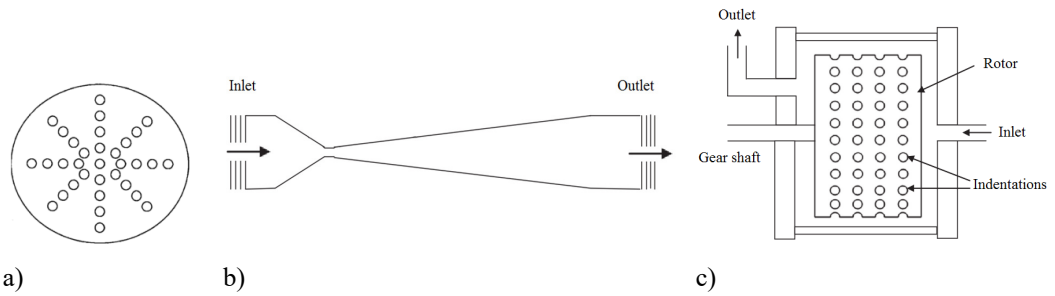


Fig. 16- HC devices: a) hole orifice plates; b) Venturi systems; c) rotor-stator systems.

9. Main fields of application of cavitation in a wastewater treatment plant

In a wastewater treatment plant, HC can be applied to both water and sludge treatment lines (Fig. 17).

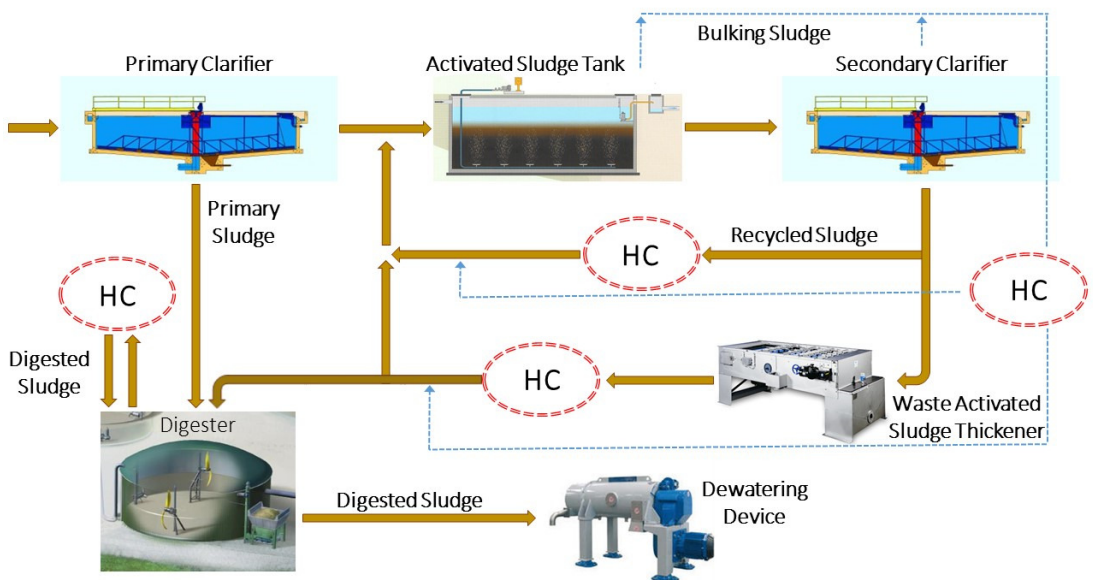


Fig. 17- Main fields of application of HC in a wastewater treatment plant.

In the sludge treatment line, it can be used as pre-treatment technique in both anaerobic and aerobic digestion in order to increase the biogas production [58], and the activated sludge solubilisation and the aerobic sludge biodegradability [9], respectively. HC can be also used to promote the denitrification process. Among other benefits, cavitation process may counteract the formation of activated sludge bulking and foam, resulting in improved sludge sedimentation properties [83]. Moreover, HC can improve the sludge rheology, resulting in a decrease in pumping and dewatering

costs. In the water treatment line, HC can be used as water disinfection process.

10. Modelling

In the past years, HC was deeply studied by many researchers worldwide. As reported in Sections 5 and 6, it was observed that essential parameters and operative conditions can deeply influence the cavitation intensity and the way in which it is generated. Due to both turbulent flow in cavitation conditions and complexity of the geometry of cavitating devices, some of these parameters such as flow velocity and flow pressure are always more often difficult to measure. As observed by Šarc et al. [44], large inconsistencies in defining values of these parameters in the scientific reports exist. Then, only an accurate measurement of these variables could lead to repeatable results. However, it was observed that flow velocity and flow pressure measurements can be easier made in simpler geometries such as hole orifice plates, nozzles or Venturi systems. On the contrary, in cavitating devices with a more complex geometry, it is rather difficult to perform measurements on these variables, resulting in an incomplete or incorrect characterization of cavitation process. For this reason, in the last years there is an increasingly interest in developing mathematical models with the main goal to define a powerful tool able to provide information on hydraulic parameters and on the fluid dynamic inside cavitating devices.

Many researchers are focusing on mathematical modelling of different HC devices such as orifice plates, nozzles, Venturi, swirling jet or rotor-stator systems. Numerical investigations were conducted to predict cavitation and to determine whether computational methods can be used as a reliable tool to evaluate the performance characteristics of the cavitating devices. However, the definition of the mathematical problem can be difficult because it can include very complex geometries of HC devices in addition to the presence of turbulent flows and cavitating conditions. Palau-Salvador et al. [84] performed numerical predictions of cavitation flows based on computational fluid dynamic (CFD) for simple geometries, such as orifices, nozzles and Venturi systems, using the commercial CFD code FLUENT 6.1. Navickas and Chen [85] studied cavitating Venturi internal flow characteristics by means of the FLOW-3D three-dimensional fluid flow program. Their results indicated that numerical methods are effective in obtaining relative magnitudes of significant parameters affecting the performance of the cavitating device. In order to optimize a multi-hole injector nozzle, He et al. [86] modelled the three-dimensional nature of the nozzle flow investigating the effect of the geometry and dynamics factors on the spray characteristics in turbulent and cavitating conditions. Müller et Kleiser [87] developed a numerical method for the vortex breakdown in a compressible swirling jet non-cavitating

flow. Ashrafizadeh and Ghassemi [88] performed an experimental and numerical investigation on the performance of small-sized cavitating Venturi. Badve et al. [63] made a mathematical model describing the shear rate and pressure variation in a complex flow field created in a rotor-stator type HC reactor.

Thanks to the quick development of computational resources, there were attempts to model the flow unsteadiness during cavitation using the Large Eddy Simulation (LES), which represent an alternative way of improving qualitative and quantitative aspects of complex turbulent flow predictions for both research and engineering purposes. The main aim of LES is to explicitly simulate the large scale of a turbulent multiphase flow while modelling the small scales. Despite some yet unresolved issues, LES is currently considered the most promising method for studying complex multiphase flows. Moreover, numerical results of studies on HC by using LES showed a very good agreement between mathematical models and the experimental data [87,88].

Therefore, an accurate mathematical model could be a useful tool to optimize parameters, operative conditions and geometry of the cavitating device with the main aim to improve cavitating devices performances in terms of generated cavitation intensities.

11. Concluding comments

HC appears to be very effective for intensification of chemical and mechanical processing in the specific area of wastewater treatment. Among mechanical treatments, this process is taking a more prominent role, mainly due to the ease of operation, flexibility and capability to vary the required intensities of cavitation conditions. In the present work, the importance of HC phenomenon in wastewater treatments engineering was exemplified, explaining the basic principles of the process and critically examining the aspects related to the use of different types of HC. The efficiency of HC reactors were reported as function of several parameters that characterize the HC device and the wastewater to be treated. The optimum selection of the HC device and of the operative parameters will help to obtain more overall advantages for each application. According to the reviewed literature, there is still no fully comprehensive method to evaluate the efficiency of HC. However, some main methods commonly used for this purpose were reported.

This work provides a useful guideline for HC applied to wastewater treatment and acts as a starting point for HC optimization. Moreover, the provided framework could form an origin for future modeling studies.

Chapter 2

Decolourization of Rhodamine B: A swirling jet-induced cavitation combined with NaOCl

This chapter was based on:

G. Mancuso, M. Langone, M. Laezza, G. Andreottola, *Decolourization of Rhodamine B: A swirling jet-induced cavitation combined with NaOCl*, *Ultrason. Sonochem.* 32 (2016) 18-30.

Chapter 2

Decolourization of Rhodamine B: A swirling jet-induced cavitation combined with NaOCl

Giuseppe Mancuso, Michela Langone, Marco Laezza, Gianni Andreottola

Department of Civil, Environmental and Mechanical Engineering, University of Trento, via Mesiano 77, 38123, Italy

Abstract

A hydrodynamic cavitation (HC) reactor (Ecowirl) based on swirling jet-induced cavitation was used in order to allow the degradation of a waste dye aqueous solution (Rhodamine B, RhB). Cavitation generated by Ecowirl reactor was directly compared with cavitation generated by using multiple hole orifice plates. The effects of operative conditions and parameters such as pressure, pH of dye solution, initial concentration of RhB and geometry of the cavitating devices on the degradation rate of RhB were discussed. In similar operative conditions, higher extents of degradation (ED) were obtained using Ecowirl reactor rather than orifice plate. An increase in the ED from 8.6% to 14.7% was observed moving from hole orifice plates to Ecowirl reactor. Intensification in ED of RhB by using HC in presence of NaOCl as additive was studied. It was found that the decolourization was most efficient for the combination of HC and chemical oxidation as compared to chemical oxidation and HC alone. The value of ED of 83.4% was reached in 37 min using Ecowirl combined with NaOCl (4.0 mg L^{-1}) as compared to the 100 min needed by only mixing NaOCl at the same concentration. At last, the energetic consumptions of the cavitation devices were evaluated. Increasing the ED and reducing the treatment time, Ecowirl reactor resulted to be more energy efficient as compared to hole orifice plates, Venturi and other swirling jet-induced cavitation devices, as reported in literature.

Keywords: Energy efficient, Rhodamine B degradation, Swirling jet-induced cavitation, Sodium hypochlorite, Synergetic effect

1. Introduction

Dye pollutants are extensively employed to impart colour in various industrial processes, such as textile, plastic, leather, food, dyeing, paper, printing, pharmaceutical and cosmetic industries [89–91]. Even a very low concentration of dyes in the effluents is highly visible and undesirable. Many of these are toxic, carcinogenic or even mutagenic to life forms [92–94]. Moreover, the presence of these contaminants in water bodies reduces the light penetration and the oxygen transfer, hence affecting aquatic life [95]. In consequence, occurrence of dyes in wastewaters leads to serious environmental and human health issues [96].

The dye under consideration in this study is Rhodamine B (RhB, tetramethylrhodamine, molecular formula: $C_{28}H_{31}N_2O_3Cl$; molecular weight: 479.01 g mol⁻¹; colour: basic violet 10). RhB, a basic dye of xanthene class, non-volatile and highly soluble in water, methanol and ethanol, is commonly used for dyeing textiles, paper, soap, leather, jute, food and drugs. Furthermore, as RhB shows a high degree of persistence, it is commonly used as a systemic marker in a variety of animals [97] and as a water fluorescent tracer for wildlife studies [98,99]. The colour of the dye is bright reddish violet.

Both carcinogenicity [100] and toxicity [101] of RhB towards human and animals and genotoxicity in plant systems [94] were experimentally proved. Furthermore, more and more stringent environmental legislations required many efforts to develop technologies that are able to remove dyes and minimize hazardous effects caused by industrial wastewaters. As reviewed by Robinson et al. [96], various techniques were proposed for removing dyes from wastewaters, such as biological [95], physical [102–104] and chemical [48,102,105] processes.

Recently, cavitation process [12] has been attracting attention among the advanced oxidation processes (AOPs), due to its elevated oxidative capability, linked to its ability of generating highly reactive free radicals [34]. There are four types of cavitation depending on the mode of its generation: acoustic, hydrodynamic, optic and particle cavitation. Among the cavitation techniques mentioned, acoustic [65] and HC [66,67] were the most studied and applied to dyes treatments, mainly due to the ease of operation, flexibility and capability to vary the required intensities of cavitation conditions. In particular, HC requires less energy than the acoustic one [13,74]. For this reason, there is a great interest in developing innovative HC devices in order to optimize the wastewaters treatments as well as reduce the energy requirements. Recently, HC was successfully used for remediation of polluted aqueous solutions containing persistent pollutants as pesticides [61], pharmaceutical drugs [77,106] and dyes [43,55,60,75,107,108].

Cavitation process involves the dissociation of vapours trapped in the cavitating bubbles, resulting in the generation of free radicals, such as $\cdot H$ and $\cdot OH$, which are very strong and not specific oxidizing species, efficiently decomposing and destroying both organic and inorganic compounds. This effect works on water clusters, agglomerations of fibres and molecules. Given that $\cdot OH$ radical is the most oxidising free radical, the production rate of $\cdot OH$ radicals strongly influence the oxidation efficiency of contaminants. Among dyes, a great interest has grown on decolourization of RhB by using acoustic cavitation [65,107,108] and HC [13,53,66,67,70], where the controlling mechanism of RhB degradation is the free radical attack [65,70].

As reviewed by Gogate et al. [109], several design configurations of the HC reactor were proposed in

order to optimize dyes degradation; all of them based on a closed loop circuit. A commonly used device for RhB removal is the HC unit based on orifice plate [13]. Sivakumar and Pandit [13], studying six types of plates with different diameter and number of holes, evaluated the effect of the geometry of the orifice plates on the RhB degradation. Mishra and Gogate [67] investigated the effect of inlet pressure (over a range 2.9-5.8 atm), operative temperature (30 and 40 °C) and pH (over a range 2.5-11) on the RhB degradation by using two different cavitating devices viz. orifice plate and Venturi. Gore et al. [60] studied the degradation of orange 4 dye by using a circular Venturi as cavitating device. Wang et al. [66] discussed the effect of operative conditions on RhB degradation by using a swirling jet-induced cavitation system. A liquid whistle reactor, comprising an orifice and a blade, was used to treat chemical manufacturing wastewaters by HC [110]. A low-pressure pilot scale HC reactor using fixed scrap iron sheets as heterogeneous catalyst was used for decolourization of RhB [53]. A HC device comprising a stator and rotor assembly was used by Badve et al. [111] and Petkovšek et al. [45] to study the treatment of a wastewater from wood finishing industry and pharmaceutical industry, respectively.

Furthermore, several researchers investigated the intensification of degradation of RhB using HC in the presence of additives. Hydrogen peroxide (H_2O_2), Fenton chemistry ($FeSO_4:H_2O_2$ in the ratio of 1:5) and Chloroalkanes (CCl_4) were investigated as useful additives in improving the efficacy of HC reactor by Mishra and Gogate [67]. The only use of H_2O_2 combined with HC was studied by Wang et al. [70]. Ozone was used combined with HC to degrade orange 4 dye [60]. Sodium hypochlorite (NaOCl) was used to promote degradation of Rhodamine B using sonochemical cavitation [112] and the degradation of orange acid II and brilliant green dye using HC [74].

To date, it appears that the processes based on HC have to be improved for dyeing industrial application. A good design and fabrication of a hydrodynamic set-up differing in flow field, turbulence characteristics and geometry are needed to enhance the use of this process as a sustainable supplement process for wastewaters treatment.

The present work was dedicated to study and compare the effectiveness of two modes of industrial HC device viz. an orifice plate and a modified swirling jet-induced reactor, named Ecowirl reactor [56]. Due to its presence in water distribution systems as residual chlorine, the use of NaOCl as additive to intensify the extent of degradation of RhB was investigated. Furthermore, the study was devoted to maximize the hybrid treatment scheme based on HC and NaOCl, concentrating on the optimization of operative parameters of the hybrid system (inlet pressure, pH, concentration of RhB and NaOCl) and the geometry of the constriction chamber (using both orifice plate and Ecowirl reactor). The

energetic consumptions of the cavitation devices were evaluated.

2. Materials and Methods

2.1. Reagents

RhB was obtained from Sigma-Aldrich Co. LLC, and was 95% pure. A stock solution 10.0 g L^{-1} of RhB was prepared by dissolving the dye in distilled water. Afterwards, it was diluted obtaining a working standard solution in the range of $2.0\text{-}5.0 \text{ mg L}^{-1}$. Both distilled water and tap water were used. Tap water contained a residual chlorine in the range of $0.1\text{-}0.2 \text{ mgCl}_2 \text{ L}^{-1}$. NaOCl solutions were prepared by dilution of the commercial product (13% w/v, Acros Organics); concentrations are reported as mg NaOCl L^{-1} . Sulphuric acid H_2SO_4 (0.1 mol L^{-1}) and sodium hydroxide NaOH (0.1 mol L^{-1}) were used to adjust the pH of the dye solution. All chemicals used were of analytical grade (Sigma).

2.2. HC system

Fig. 18 shows a schematic representation of the experimental configuration used for HC.

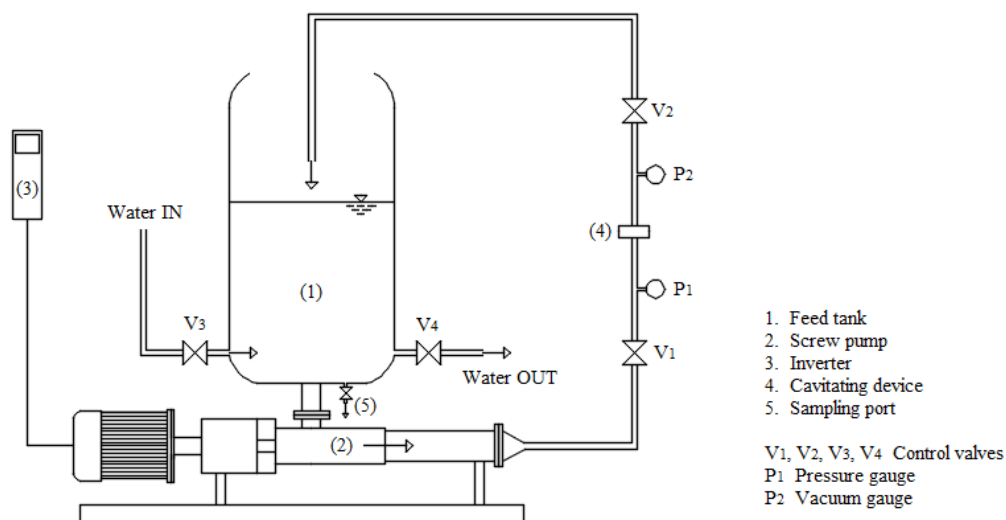


Fig. 18- Schematic representation of the experimental setup.

It was a closed loop circuit designed to draw an RhB dye solution from a feed tank of 50 L volume, then taking it into a flow channel internally accommodating the cavitating device and then discharging the treated solution back to the tank with a pump. The solution to treat was recirculated and entered again into the feed tank. The suction side of the pump was connected to the bottom of the tank. The

flow channel terminated well inside the feed tank, below the liquid level in order to avoid any introduction of air into the system.

Details are as follows: (1) a feed tank; (2) a mono screw pump (3.0 kW, Netzsch Pumps & Systems GmbH Germany); (3) an inverter (Bonfiglioli Vectron – Active) used to control the pump flow rate (in the range of $0.5\text{--}6\text{ m}^3\text{ h}^{-1}$) and the inlet pressure (about 0.5-12 bar) of the liquid by adjusting the frequency, (4) a cavitating device; (5) a sampling port; a system of control valves at appropriate places (V1, V2, V3, V4); a pressure gauge to measure the inlet pressure (P1); a vacuum gauge to measure the vacuum after the cavitating device (P2). During each experimentation, valves V1 and V2 were always kept fully open, while valves V3 and V4 were used at the beginning and at the end of each experiment, in order to fill and draw the feed tank, respectively.

Two different cavitation devices were used viz. an orifice plate and a modified swirling jet-induced reactor. The orifice plate used in this study was circular with a diameter of 40 mm and 33 holes of 2 mm diameter each (*Fig. 19 a*). Four orifice plates, with different thickness (1, 2, 3 and 4 mm) were considered. The plates were made of stainless steel (AISI 316).

A modified swirling jet-induced reactor device, named Ecowirl [56], patented by Econovation GmbH, Germany and commercialized and optimized by Officine Parisi S.R.L., Italy, was used as innovative HC device (*Fig. 19 b*). Ecowirl is a full-scale HC reactor, made of stainless steel (AISI 316) and based on a particular geometry of constrictions which create multi-dimensional vortices of liquid that never hit the walls of the reactor, avoiding problems of erosion, allowing to harness the impressive effects of HC for chemical-physical transformations.



Fig. 19- (a) Orifice plate; (b) Ecowirl reactor.

Fig. 20 shows as this device operates like a swirling jet-induced reactor, in which cavitation is generated by using a multi-dimensional vortices generator, consisting of (i) a frustum-conical pre-swirling chamber with six injection slots at the vertex through which the flow enters and (ii) a double cone chamber where cavitation mainly occurs, resulting in an increase in the extent of cavitation.

Injection slots (upstream diameter 10 mm - downstream diameter 8 mm) divide the radial vortex in six single vortices generating a braided stream along the jet axis with a helical shape. Due to centrifugal forces, the pressure in the core of the braided stream is lower than the vapor pressure of water, and cavitation bubbles are expected to generate. The frustum-conical pre-swirling chamber both accelerates the braided stream and shakes the solution to treat. Then, the braided stream is ejected from the conical pre-swirling chamber to the double-cone chamber and impacts to a perpendicular insert to the braided stream where the pressure is risen rapidly and the cavitation bubbles collapse. The field of helical vortex produces more than 1000 pulses per second.

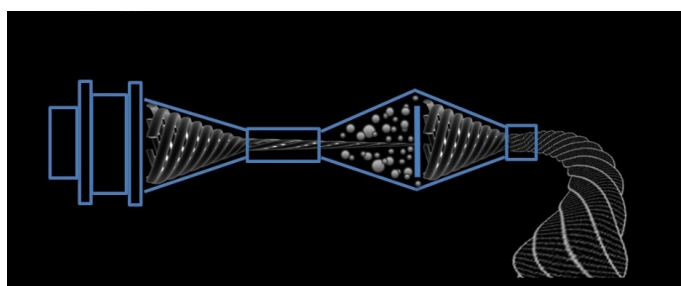


Fig. 20- Schematic representation of the operation of Ecowirl reactor.

2.3. Procedures

In a typical experiment, 50 L aqueous solutions of RhB were subjected to cavitation. The degradation of the contaminants by using HC is carried out for successive cycles. For this reason, each experiment included the recirculation of RhB dye solution. Initially, the degradation of RhB by using HC alone was investigated. For this purpose, two different cavitating devices, orifice plate and modified swirling jet-induced reactor (Ecowirl reactor with standard double cone chamber), were used separately to treat the contaminated dye solution.

Afterwards, the effect of NaOCl as additive to intensify the degradation of RhB using HC was studied. Treating an aqueous solution with an initial content of $3.0 \text{ mg RhB L}^{-1}$, the effects of sodium hypochlorite at 0.5 and 4.0 mg L^{-1} in a mixing system and in the hybrid scheme were investigated. Hence, the investigation of a progressive increase in the concentration of NaOCl ($0.5, 1.0, 2.0, 3.0, 4.0 \text{ mg L}^{-1}$) was carried out using the Ecowirl reactor (standard type). Tap water containing a residual chloride in the range of $0.1\text{-}0.2 \text{ mg L}^{-1}$ and RhB was also tested.

Using the Ecowirl reactor, the effects of inlet operative pressure ($2.0, 3.0, 4.0 \text{ bar}$) and geometry of the double-cone chamber (Type standard, type A, B and C) on the degradation rate of RhB were

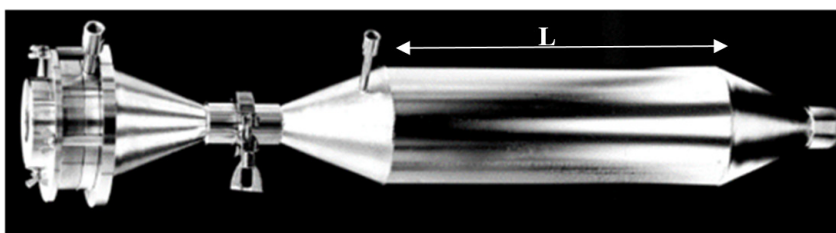
studied in the hybrid scheme based on HC and NaOCl chemistry. At the same time, using the orifice plate, the effects of operative conditions such as inlet operative pressure (2.0, 3.0, 4.0 bar), thickness of the plate (1, 2, 3, 4 mm), initial concentration of RhB (2.0, 3.0, 4.0 mg L⁻¹) and pH of solution (2.0, 3.0, 4.0, 5.5, 7.0, 8.0, 9.0, 10.0, 11.5) were studied in the hybrid scheme.

Table 1 shows parameters and operative conditions that were varied during the experiments.

Table 1 - Parameters and operative conditions for the two different cavitating devices used.

Orifice plate					Ecowirl reactor				
Pressure (bar)	pH	Thickness (mm)	[RhB] (mg L ⁻¹)	[NaOCl] (mg L ⁻¹)	Pressure (bar)	pH	Double-cone (Type)	[RhB] (mg L ⁻¹)	[NaOCl] (mg L ⁻¹)
2	4.0	2	3.0	0.0 → 4.0	2	4.0	Std	3.0	0.0 → 4.0
2-3-4	4.0	2	3.0	0.5	2-3-4	4.0	Std	3.0	0.5
2	4.0	1-2-3-4	3.0	0.5	2	4.0	A, B, C, Std	3.0	0.5
2	2.0 → 11.5	2	3.0	0.5					
2	2.0	2	2.0-3.0-4.0	0.5					

The geometry of the double cone chambers differed for the length of the cylinder in the middle of the double cone. Type C is illustrated in *Fig. 21*.



Type Std → L = 0 cm; Type A → L = 20 cm; Type B → L = 40 cm; Type C → L = 60 cm

Fig. 21- Geometry of double cone type C in the Ecowirl reactor.

The resultant flow rate through the system, and thus the applied frequency of the inverter, the absorbed power and the treatment time changed as a function of the installed cavitating device and the inlet operative pressure are reported in *Table 2*.

The desired inlet pressure value was fixed by setting the number of revolutions of the pump through the inverter.

A base for comparison was taken to be the 260th cycle, even though the complete degradation was not obtained during the corresponding treatment time. Through a sampling valve on the bottom of the feed tank, samples were taken out at an interval of 20 cycles for an analysis of the progress of degradation. The collected samples were analysed at the maximum absorption wavelengths of RhB

(553 nm) by using a DR/2010 spectrometer (Hach Lange). RhB concentration was determined from the measured absorbance, using a pre-calibrated chart. Concentrated H₂SO₄ and NaOH were used for the pH adjustments. The temperature at the beginning of each run was fixed around at 20 °C, while it was allowed to vary during the experiment. Throughout each run, temperature and pH were monitored. All experiments were repeated at least two times and the reported values are an average of the different experimental runs. The experimental errors were within 2-3% of the reported value of the extent of degradation.

Table 2 - Flow characteristics for the two different cavitating devices used.

Orifice plate					Ecowirl reactor				
Pressure (bar)	Frequency (Hz)	Flow rate (m ³ h ⁻¹)	Corresp. time to 260 cycles (min)	Absorbed power (kW)	Pressure (bar)	Frequency (Hz)	Flow rate (m ³ h ⁻¹)	Corresp. time to 260 cycles (min)	Absorbed power (kW)
2	59.0	6.0	130	0.8	2	47.0	4.6	169	0.8
3	72.0	7.2	110	1.3	3	59.0	5.7	137	1.1
4	83.0	8.4	92	1.8	4	69.0	6.6	118	1.4

2.4. Calculations

There are several parameters able to evaluate the degree of the gradual degradation of RhB by using an HC process. In order to estimate the extent of degradation (ED) of RhB, a percentage of removal was considered. The ED was calculated using the following equation *Eq. 13*:

$$ED(\%) = (C_0 - C) / C_0 \cdot 100 \quad \text{Eq. 13}$$

The initial value of RhB concentration is denoted as C_0 [mg L⁻¹], the residual RhB concentration at the generic instant is written as C [mg L⁻¹].

Another parameter used for the characterization of the cavitation systems is the cavitation yield (C.Y.), defined as the ratio of the observed cavitation effect, in terms of RhB degradation, to the total energy supplied to the system. C.Y. was calculated from the *Eq. 14* [78]:

$$C.Y. = \text{RhB degraded} / \text{Power density} \quad \text{Eq. 14}$$

where RhB degraded is the amount of dye in mg L⁻¹ removed in the experiment, while power density, in J L⁻¹, is represented by the following equation *Eq. 15*:

$$\text{Power density} = (P_{\text{abs}} \cdot t) / V \quad \text{Eq. 15}$$

where V is the volume of liquid [L], P_{abs} the pump absorbed power [W] and t the time of treatment [sec]. Finally, the pressure difference (ΔP_{HC}), between the inlet operative pressure upstream of the constriction (P_{inlet}) and the operative pressure downstream of the constriction (P_{outlet} , where the vacuum is achieved), was calculated for each test.

3. Results and discussion

3.1. Degradation using HC alone

Degradation of RhB was investigated using two different cavitating devices viz. orifice plate and modified swirling jet-induced reactor. Experiments were performed using $3.0 \text{ mg RhB L}^{-1}$ aqueous solutions obtained using distilled water and two approaches were put forward: (1) using orifice plate (33 holes \times F = 2 mm, plate thickness = 2 mm); (2) using swirling jet-induced cavitation device (Ecowirl reactor - standard type, L = 0 cm). The frequency of the inverter was adjusted to provide an inlet pressure of 2.0 bar, corresponding to a flow rate of $6.0 \text{ m}^3 \text{ h}^{-1}$ and $4.6 \text{ m}^3 \text{ h}^{-1}$ for the orifice plate and Ecowirl reactor, respectively. Each test lasted 260 passes through the cavitation system, which corresponded to 130 min and 169 min using orifice plate and Ecowirl reactor, respectively. Other experimental conditions involved the solution temperature $20.0 \pm 1.0 \text{ }^\circ\text{C}$ and pH 4.0. The results are showed in Fig. 22.

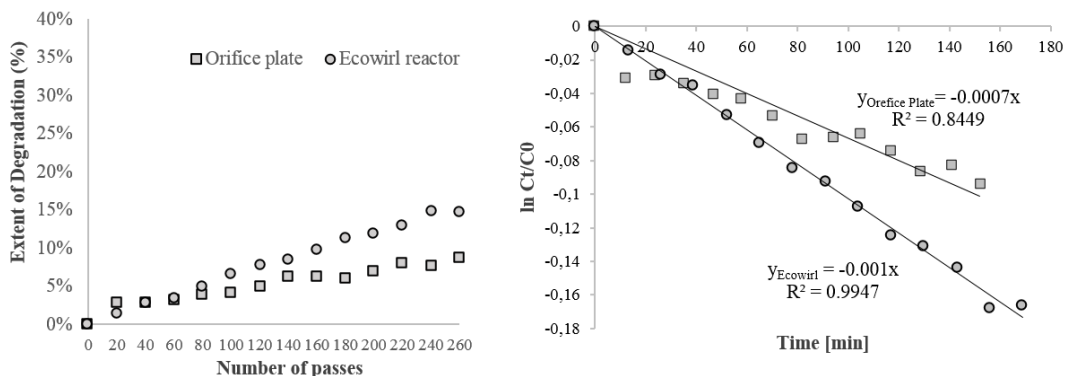


Fig. 22- Comparison between different HC devices alone (volume 50 L; initial RhB concentration 3.0 mg L^{-1} ; pH 4.0; inlet pressure 2.0 bar; initial temperature $20.0 \pm 1.0 \text{ }^\circ\text{C}$).

Comparing the two cavitating devices used in the present work, it can be seen from the Fig. 22 that, at similar operative conditions, higher extents of degradation were obtained using Ecowirl reactor rather than orifice plate. ED of 15% and 9% were achieved using Ecowirl reactor and orifice plate,

respectively. Up to date, other studies demonstrated the low efficiency of orifice plate as compared with other HC devices. Mishra and Gogate [67] found higher extents of RhB degradation using Venturi rather than orifice plate. In their study, authors attributed the greater efficiency of Venturi to the higher velocities in the reactor and hence to the higher number of passes through the cavitating zone for the same time of operation, resulting into higher degradation rates. In our study, for the same number of passes we achieved a higher ED using the Ecowirl reactor as compared to the orifice plate. The obtained results can be attributed to the fact that the operative pressure downstream the Ecowirl reactor was lower (-0.85 bar) as compared to the value downstream of the orifice plate (0.30 bar) at similar inlet operative pressure (2.0 bar), resulting in a higher pressure drop. ΔP_{HC} values of 2.85 and 1.7 bar were measured for the Ecowirl reactor and the orifice plate respectively (*Table 3*).

The efficiency can be also compared based on cavitation yield (C.Y.). It can be noticed that the Ecowirl reactor gives 1.3 times more cavitation yield as compared to the orifice plate, when operated individually under the same operative conditions (*Table 3*). Thus, even if the treated flow rate was lower using Ecowirl reactor, the corresponding C.Y. was greater mainly due to the higher extent of degradation, showing that Ecowirl reactor was the most performing cavitation device.

Finally, it was found that the concentration of RhB in aqueous solutions by using orifice plate and Ecowirl reactor decreased exponentially with reaction time, following a pseudo first order kinetic reaction. The degradation rate can be expressed by the following equation *Eq. 16*:

$$C = C_0 \exp(-kt) \text{ or } \ln(C/C_0) = -kt \quad \text{Eq. 16}$$

where C is the concentration of RhB at time t, C_0 is initial concentration, k is degradation rate constant, and t is degradation time. The degradation rate constants (k) were $0.7 \cdot 10^{-3}$ ($R^2 = 0.8449$) and $1.0 \cdot 10^{-3}$ ($R^2 = 0.9947$) min^{-1} for orifice plate and Ecowirl reactor, respectively.

3.2. Synergetic effect between HC and NaOCl

Sodium hypochlorite (NaOCl), known as bleaching agent, is commonly used as a disinfectant for treating wastewaters. If used individually, the efficiency of NaOCl in oxidizing the RhB is high but extremely slow because sodium hypochlorite decomposition is usually a very slow process under room temperature conditions. Nevertheless, the efficiency of NaOCl in degrading RhB can be enhanced significantly if used in combination with HC.

Table 3 - Operative parameters and efficiency measured at the end of each test.

Orifice plate										
P _{inlet} (bar)	pH	Thickness (mm)	[RhB] (mg L ⁻¹)	NaOCl (mg L ⁻¹)	ED after 260 cycles (%)	P _{outlet} (bar)	ΔP _{HC} (bar)	RhB degraded (mg L ⁻¹)	Power density (kJ L ⁻¹)	CY (mg J ⁻¹)
2.0	4.0	2	3.0	0	8.6	0.30	1.70	0.258	124.80	2.07·10 ⁻⁶
2.0	4.0	2	3.0	0.5	18.8	0.30	1.70	0.564	124.80	4.52·10 ⁻⁶
3.0	4.0	2	3.0	0.5	24.3	0.35	2.65	0.729	171.60	4.25·10 ⁻⁶
4.0	4.0	2	3.0	0.5	21.7	0.40	3.60	0.651	198.72	3.28·10 ⁻⁶
2.0	4.0	1	3.0	0.5	24.3	0.28	1.72	0.729	145.92	5.00·10 ⁻⁶
2.0	4.0	2	3.0	0.5	18.8	0.30	1.70	0.564	124.80	4.52·10 ⁻⁶
2.0	4.0	3	3.0	0.5	20.0	0.32	1.68	0.66	131.76	5.00·10 ⁻⁶
2.0	4.0	4	3.0	0.5	22.9	0.35	1.65	0.687	138.00	4.98·10 ⁻⁶
2.0	2.0	2	3.0	0.5	65.0	0.30	1.70	1.950	124.80	15.63·10 ⁻⁶
2.0	3.0	2	3.0	0.5	32.4	0.30	1.70	0.972	124.80	7.79·10 ⁻⁶
2.0	4.0	2	3.0	0.5	18.8	0.30	1.70	0.564	124.80	4.52·10 ⁻⁶
2.0	5.5	2	3.0	0.5	3.5	0.30	1.70	0.105	124.80	0.84·10 ⁻⁶
2.0	7.0	2	3.0	0.5	5.2	0.30	1.70	0.156	124.80	1.25·10 ⁻⁶
2.0	8.0	2	3.0	0.5	3.6	0.30	1.70	0.108	124.80	0.87·10 ⁻⁶
2.0	9.0	2	3.0	0.5	1.7	0.30	1.70	0.051	124.80	0.41·10 ⁻⁶
2.0	10.0	2	3.0	0.5	3.9	0.30	1.70	0.117	124.80	0.94·10 ⁻⁶
2.0	11.5	2	3.0	0.5	7.4	0.30	1.70	0.222	124.80	1.78·10 ⁻⁶
2.0	2.0	2	2.0	0.5	76.1	0.30	1.70	1.52	124.80	12.20·10 ⁻⁶
2.0	2.0	2	3.0	0.5	65.0	0.30	1.70	1.95	124.80	15.63·10 ⁻⁶
2.0	2.0	2	4.0	0.5	61.3	0.30	1.70	2.45	124.80	19.65·10 ⁻⁶
Ecowirl reactor										
P _{inlet} (bar)	pH	D. cone (Type)	[RhB] (mg L ⁻¹)	NaOCl (mg L ⁻¹)	ED after 260 cycles (%)	P _{outlet} (bar)	ΔP _{HC} (bar)	RhB degraded (mg L ⁻¹)	Power density (kJ L ⁻¹)	CY (mg J ⁻¹)
2.0	4.0	Std	3.0	0	14.7	-0.85	2.85	0.441*	162.24*	2.72·10 ^{-6*}
2.0	4.0	Std	3.0	0.5	24.9	-0.90	2.90	0.747*	162.24*	4.60·10 ^{-6*}
2.0	4.0	Std	3.0	1.0	39.8	-0.90	2.90	1.194	162.24	7.36·10 ⁻⁶
2.0	4.0	Std	3.0	2.0	61.5	-0.90	2.90	1.845	162.24	11.37·10 ⁻⁶
2.0	4.0	Std	3.0	3.0	76.5	-0.90	2.90	2.295	162.24	14.15·10 ⁻⁶
2.0	4.0	Std	3.0	4.0	93.6	-0.90	2.90	2.808	162.24	17.31·10 ⁻⁶
2.0	4.0	Std	3.0	0.5	29.8	-0.85	2.85	0.894	162.24	5.51·10 ⁻⁶
3.0	4.0	Std	3.0	0.5	26.0	-0.90	3.90	0.754	180.84	4.17·10 ⁻⁶
4.0	4.0	Std	3.0	0.5	22.1	-0.95	4.95	0.663	198.24	3.34·10 ⁻⁶
2.0	4.0	Std	3.0	0.5	29.8	-0.85	2.85	0.894	162.24	5.51·10 ⁻⁶
2.0	4.0	A	3.0	0.5	18.5	-0.95	2.95	0.555	162.24	3.42·10 ⁻⁶
2.0	4.0	B	3.0	0.5	13.4	-0.95	2.95	0.402	162.24	2.48·10 ⁻⁶
2.0	4.0	C	3.0	0.5	9.0	-0.80	2.80	0.270	162.24	1.66·10 ⁻⁶

C.Y. was calculated after 260 number of passes
* Calculations reported in Appendix A

In this study, degradation of RhB was investigated using Ecowirl reactor (standard type) in combination with NaOCl, at concentration of 0.5 mg L⁻¹ and 4.0 mg L⁻¹. Experiments were conducted using 3.0 mg RhB L⁻¹ aqueous solutions, at 20.0 ± 1.0 °C, pH 4.0 and inlet pressure of 2.0 bar. Control experiments in the absence of HC were performed with NaOCl, at concentration of 0.5 mg L⁻¹ and 4.0 mg L⁻¹, only mixing.

It can be seen from *Fig. 23* that there is an obvious synergetic effect between HC and NaOCl for the degradation of RhB. The combined process HC and NaOCl at 0.5 mg L⁻¹ increased the efficiency of RhB

degradation of about 45-50% in 260 number of passes (169 min of operation time) as compared to the HC alone. Similar results were achieved using the orifice plate as cavitating device (data not showed).

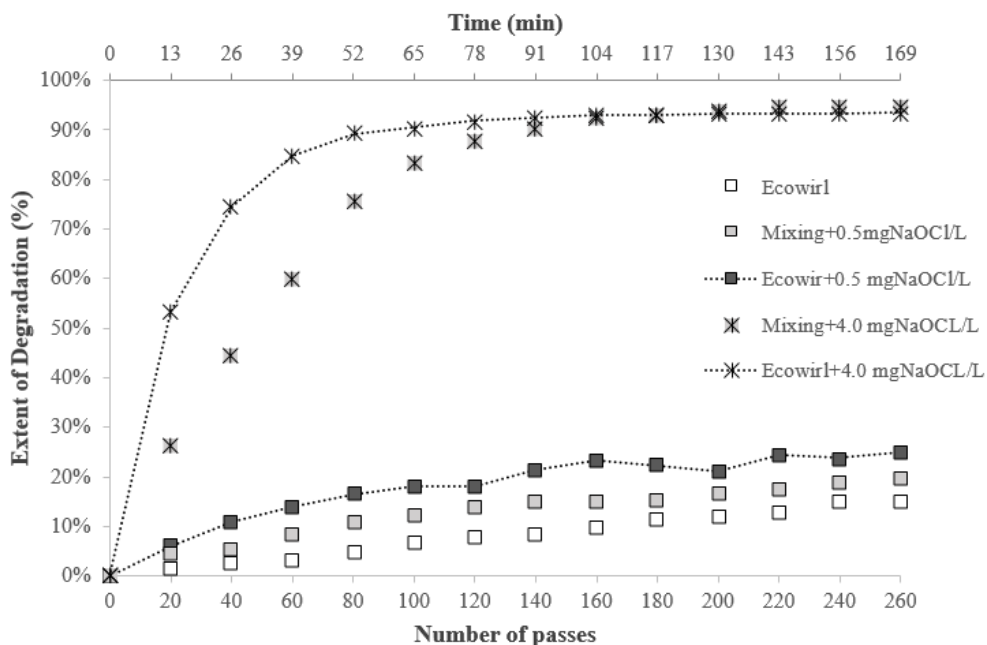


Fig. 23- Synergetic effect between HC and NaOCl on degradation of RhB (volume 50 L; initial RhB concentration 3.0 mg L⁻¹; pH 4.0; inlet pressure 2.0 bar; initial temperature 20.0 ± 1.0 °C).

Furthermore, the acceleration of the kinetic of RhB degradation promoted by the HC is clear. In absence of HC, 75% of the RhB content is lost in ca. 52 min, whereas only 26 min (40 number of passes through the Ecowirl reactor) are needed when using the hybrid treatment based on HC + NaOCl (4.0 mg L⁻¹). As known, HC in water causes the formation of $\cdot\text{OH}$ radicals which are very strong and non-specific oxidizing species. Since $\cdot\text{OH}$ radicals are major free radicals and important precursors for many products formed in degradation process, the production rate of $\cdot\text{OH}$ radicals strongly influence the oxidation efficiency of pollutants. On the other hand, hypochlorite bleaches via the oxidising OCl^- ion, which in aqueous solution is in equilibrium with the strongly oxidising hypochlorous acid HClO , so that the reactions are pH dependent. When the pH is between 2 and 7, the equilibrium favours HClO . As the pH falls below 2, the main form is Cl_2 . At a pH of 7.4, HClO and OCl^- are about equal, and as the pH goes above 7.4, increasing proportions of OCl^- are present. Thus, at pH of 4.0, the strongly oxidising HClO is the dominant form. Tiong and Price, [112], suggested that undissociated

hypochlorous acid could also evaporate into a cavitation bubble and undergo sonolysis, also producing $\cdot\text{OH}$ radicals, resulting in higher concentrations of these highly oxidising species, contributing to the acceleration of the degradation process. Zeng et al. [113], also hypothesized that the presence of HClO could result in the production of more hydroxyl radicals to accelerate the degradation of aqueous dyestuffs. This suggests that the synergetic effect between HC and NaOCl for the degradation of RhB could be mainly due to the contribution of additional $\cdot\text{OH}$ radicals production.

3.3. Effect of NaOCl concentration

The effect of the NaOCl concentration ranging from 0.5 to 4.0 mg L⁻¹, corresponding to 0.3-3.7 mg OCl⁻ L⁻¹, on the degradation of RhB was investigated using a 3.0 mg L⁻¹ RhB aqueous solution at 20 °C, pH 4.0, inlet pressure of 2.0 bar and Ecowirl reactor (standard type) as cavitation device. Fig. 24 shows that an increase in NaOCl concentration involved an intensification of the extent of degradation of RhB.

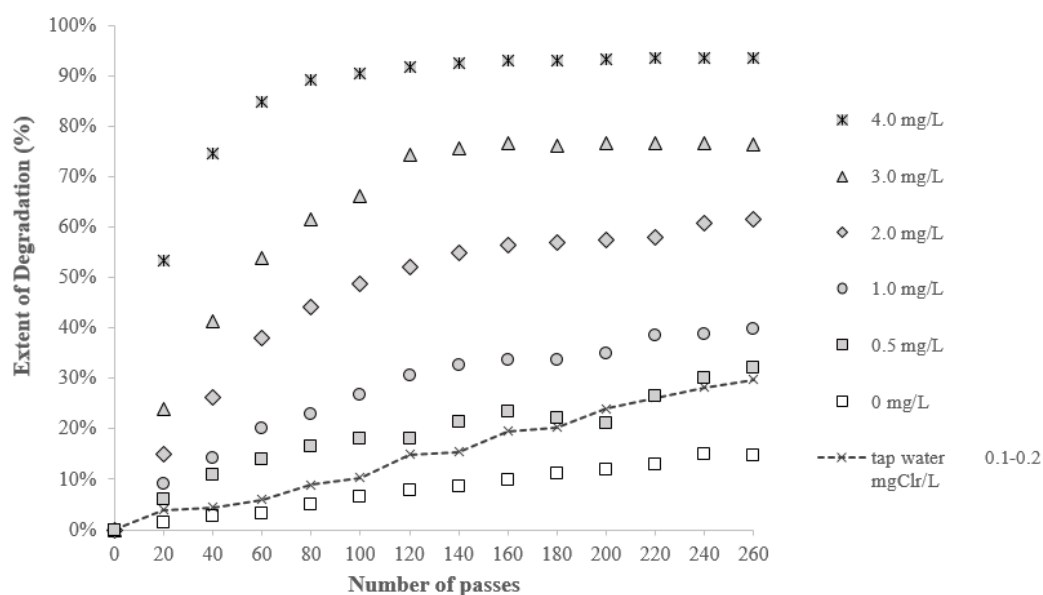


Fig. 24 - Effect of HC using Ecowirl in presence of NaOCl on degradation of RhB (volume 50 L; initial RhB concentration 3.0 mg L⁻¹; pH 4.0; inlet pressure 2.0 bar; initial temperature 19.0 ± 1.0 °C; mg NaOCl L⁻¹).

As mentioned above, the enhancement of ED could be mainly due to the formation of hypochlorous acid (HClO) and to the production of additional $\cdot\text{OH}$ radicals. Quantitatively speaking, about 94% RhB

degradation was obtained at the maximum oxidant loading of 4.0 mg NaOCl L⁻¹ within 169 min of treatment time. At the minimum loading (0.5 mg NaOCl L⁻¹), the extent of decolourization was about 31% at the end of 169 min, which is higher as compared to HC alone.

When tap water solution characterized by a residual chloride content of 0.1-0.2 mg L⁻¹ was used, an ED of 29% was achieved, showing the possibility to use the residual chlorine in waters as a possible way to spare the chemical consumption. In order to meet residual chloride discharge limits of 0.2 mg L⁻¹, and simultaneously benefit of the synergic effect of the hybrid treatment scheme based on HC and NaOCl, a value of 0.5 mg NaOCl L⁻¹ was selected as the sustainable NaOCl addition dose in the present research.

3.4. Effect of the pressure

The effect of fluid pressure on the degradation ratio of RhB was also investigated in the hybrid treatment scheme based on HC and NaOCl (0.5 mg L⁻¹), using the two different cavitating devices viz. orifice plate (plate thickness: 2 mm) and Ecowirl reactor (standard type). The experiments were carried out at three different inlet pressure, 2.0, 3.0 and 4.0 bar. The experiments were conducted in aqueous solution at 3.0 mg L⁻¹ RhB, an initial temperature of 19.0 ± 0.5 °C and pH 4.0. The obtained results were depicted in *Fig. 25 a* for orifice plate as the cavitating device and in *Fig. 25 b* for Ecowirl reactor.

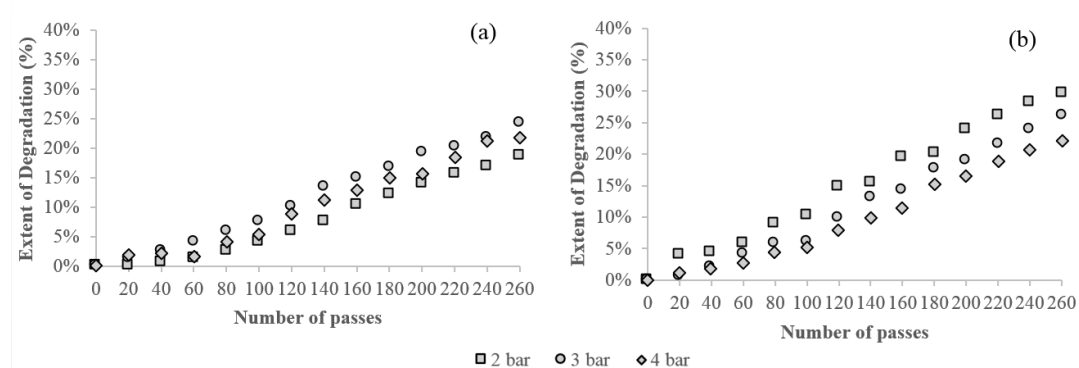


Fig. 25- Effect of inlet pressure on degradation of RhB by using (a) orifice plate and (b) Ecowirl reactor (volume 50 L; initial dye concentration 3.0 mg L⁻¹; pH 4.0; initial temperature 19.0 ± 0.5 °C; 0.5 mg NaOCl L⁻¹; inlet pressure).

Using the orifice plate, the degradation rates increased with an enhance in the inlet pressure until an optimum value of 3.0 bar, where an ED of 24.3% was reached. At 4.0 bar pressure, the extent of

degradation was observed to drop marginally.

Mishra and Gogate [67] both using Venturi and orifice plate as cavitating devices, treating a 10 mg RhB L⁻¹ solution at 30-40 °C, obtained a decrease in ED at a high inlet pressure of 5.9 atm. In their study the authors attributed this phenomenon to the onset of super cavitation i.e. indiscriminate growth of the bubbles downstream of the constriction resulting in splashing and vaporization of the flow and enhancing phenomena of coalescence that produce less effective bubbles in terms of degradation. In our study, the inlet pressure was lower, however the ΔP_{HC} values measured using the orifice plate were 1.70, 2.65 and 3.60 bar, at 2.0, 3.0, and 4.0 bar, respectively (*Table 3*). Thus, a pressure drop of 3.6 bar was the ΔP_{HC} value for which the super cavitation may occur using the specific orifice place and the RhB solution.

Using Ecowirl reactor, instead, it was found that the extent of degradation decreased at increasing the operative inlet pressure from 2.0 to 4.0 bar. In the case of Ecowirl reactor, a ΔP_{HC} of 2.85 bar was measured at 2.0 bar. Increasing the inlet operative pressure the ΔP_{HC} increased up to 3.90 and 4.95 bar at 3.0 and 4.0 bar, respectively. Similarly to the results of the orifice plate experiments, a pressure drop of 3.90 bar was the ΔP_{HC} value for which the super cavitation may occur using the specific swirling jet reactor and the RhB solution.

Different results were achieved by using a swirling jet-induced cavitation device, where the increase of degradation rates of RhB were observed with the increase of the inlet pressure, from 2.0 to 6.0 bar [66,70]. However, different operative conditions were used in terms of temperature and concentration of RhB. In a swirling jet-induced cavitation device, treating a 5.0 mg RhB L⁻¹ solution at 6.0 bar and 40 °C, a maximum ED of 60% was achieved [66]. Using H₂O₂ as additive, in a swirling jet-induced cavitation, treating a 10.0 mg RhB L⁻¹ solution at 6.0 bar and 50 °C, a maximum ED of 95% was achieved [70]. Finally, in a swirling jet-induced cavitation, treating reactive brilliant red K-2BP solution (20 mg L⁻¹) at 6.0 bar and 50 °C, where a maximum ED of 75% was achieved, a ΔP_{HC} of about 5.9 bar can be calculated [55] that is comparable with the pressure drop that we measured in our experiments.

However, as recently reviewed by Bagal and Gogate [114], the effect of operative pressure is strongly dependent on the geometry of the cavitation chamber as well as on the pollutant nature and fluid dynamic characteristics of the solution to treat. Hence, the optimization of the inlet pressure is indispensable to obtain maximum cavitation effects.

Table 3 shows the operative parameters and the extent of degradation of RhB, in terms of ED and C.Y., by using orifice plate and Ecowirl reactor and by varying the inlet pressure on cavitating system. In

the case of orifice plate, the C.Y. is almost the same value at 2.0 and 3.0 bar, then decreases at 4.0 bar. This is due mainly to the fact that up to 3.0 bar both the flow rate and ED increased, thus increasing the amount of RhB degraded. After 3.0 bar, even if the flow rate increased with the increasing of the inlet operative pressure, ED decreased causing a lower amount of degraded dye molecules. Furthermore, increasing the inlet operative pressure, the power density increased as well, thus resulting in a decrease in mg of pollutant degraded to the total energy input to the system. Concerning Ecowirl reactor, as the operative pressure increased, even if the flow rate increased, the ED decreased, resulting in a decreasing amount of RhB. On the other hand, even if the treatment time decreased, the adsorbed power increased causing an increasing power density. The resulting C.Y. decreased with the increase of inlet operative pressure.

3.5. Effect of geometry

Based on the geometrical configuration of the cavitating system, it is possible to achieve different values of the extent of degradation of RhB. Concerning orifice plate, while many studies were carried out on holes number and diameter, and consequently, on cross-sectional area and perimeter [13], only few studies were performed on the thickness of orifice plates. Furthermore, no studies are present on the geometry of Ecowirl reactor. The effect of the geometry was investigated in the hybrid treatment scheme based on HC and NaOCl (0.5 mg L^{-1}).

3.5.1. Effect of the orifice plate thickness

In the present study, the influence of thickness of the orifice plate (the orifice length or holes depth) on the RhB degradation was analysed. The tests were carried out at a thickness of 1, 2, 3 and 4 mm, using an aqueous solution at initial dye concentration of 3.0 mg L^{-1} , pH 4.0, an inlet pressure of 2.0 bar, a temperature of $19.0 \pm 1.0 \text{ }^\circ\text{C}$ and $0.5 \text{ mg NaOCl L}^{-1}$.

Even if no significant difference in ED was found for the different orifice plates investigated, the highest ED was achieved for the plate characterized by the lowest thickness (1 mm), and thus the lowest unit length to diameter ratio, for which an ED of 24.3% was reached (*Table 3*). The experiments of the present study confirmed the results observed by Parsa and Zonouzian [53], who used two different types of orifice plates (type A: 1 mm of thickness, ED = 71.0%; type B: 2 mm of thickness, ED = 64.8%). The authors suggested that the thicker plate (plate type B) had a higher inlet pressure and a lower flow rate, and consequently, fewer intense collapses and lower ED [115]. Unlike Parsa and Zonouzian, we worked at constant inlet operative pressure and constant flow rate. In the present

study, the pressures downstream of the orifice plate increased from 0.28, 0.30, 0.32 to 0.35 bar using the 1, 2, 3 and 4 mm thickness orifice plates, respectively. From those results, it seems that the higher efficiency could be linked to the lowest outlet pressure measured downstream of the orifice plate, and thus at the highest ΔP_{HC} , equal to 1.72 bar. Thus, working at the same inlet operative pressure, it means that a higher HC effect can be obtained using the 1 mm thickness orifice plate.

3.5.2. Effect of the double cone

In the Ecowirl reactor, the geometry of double cone chamber was investigated. The interest in studying this zone of the reactor was due to the cavitation phenomenon that occurs in this region of space. The tests were conducted considering four different types of cavitation chambers, type standard, type A, B and C, different for the length of the cylinder in the middle of the double cone, using an aqueous solution at initial dye concentration of 3.0 mg L^{-1} , pH 4.0; 2.0 bar, $19.0 \pm 2.5 \text{ }^\circ\text{C}$ and $0.5 \text{ mg NaOCl L}^{-1}$. The results, shown in *Fig. 26*, confirmed that choosing different geometric configurations of the double cone chamber it is possible to obtain different extent values of the extent of degradation of RhB. For all new types considered, the extent of degradation on RhB was lower than the values measured using the standard double cone chamber (*Table 3*).

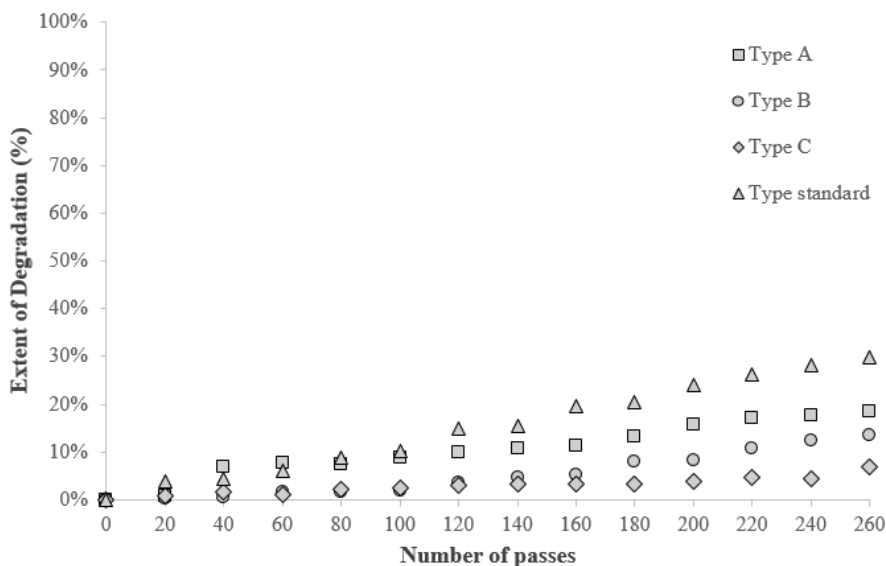


Fig. 26- Effect of the geometry of the double cone chamber of Ecowirl reactor on degradation of RhB (volume 50 L; initial RhB concentration 3.0 mg L^{-1} ; pH 4.0; inlet pressure 2.0 bar; initial temperature $19.0 \pm 2.5 \text{ }^\circ\text{C}$; $0.5 \text{ mg NaOCl L}^{-1}$; double cone).

The ED decreased with the increasing of the length of the cylinder. The lower efficiency associated to the configuration A, B and C could be related both to the high measured ΔP_{HC} value of 2.95 bar as compared to the standard type (2.85 bar), which could increase the phenomenon of coalescence, and lead to a less violent implosion of the bubbles, due to the fact that they are subjected to a slower pressure increase in the longer double cones as compared to the standard double cone, where a very rapid pressure increase occurred. Hence, the need for further studies on the definition of new geometries of the Ecowirl reactor, able to induce an appropriate ΔP_{HC} value and a rapid pressure increase, that may increase the intensity of cavitation and thus ensure greater degradation of the dye.

3.6. Effect of operative pH

In cavitation process, the pH of the medium is an important parameter on the degradation of chemical pollutants. Indeed, it can heavily influence the chemical state of the compound to remove. Moreover, using NaOCl, the pH influences the distribution of free chlorine species in aqueous solutions.

In this study, the effect of pH in a range between 2.0 and 11.5 was investigated on a 3.0 mg L⁻¹ RhB solution by using the hybrid system based on HC and 0.5 mg NaOCl L⁻¹. Orifice plate (plate thickness: 2 mm) was used as cavitating device. Other experimental conditions involved the solution temperature 18.2 ± 2.6 °C and the inlet fluid pressure 2.0 bar. The ΔP_{HC} value was the same for the all the performed tests and equal to 1.7 bar. The obtained results were depicted in Fig. 27.

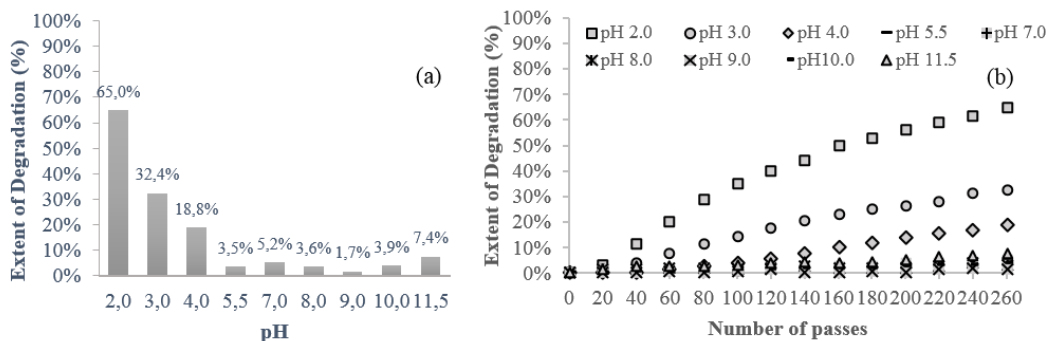


Fig. 27 - (a) Effect of pH on degradation of RhB by using orifice plate, (b) Degradation kinetics (volume 50 L; initial RhB concentration 3.0 mg L⁻¹; initial temperature 18.2 ± 2.6 °C; inlet pressure 2.0 bar; 0.5 mg NaOCl L⁻¹; pH).

According to results from other studies [65–67], our results confirmed the degradation of RhB was strongly dependent on the pH solution. It can be seen from the Fig. 27 a that the highest ED of RhB

was reached for strongly acid pH (2.0-4.0). The maximum degradation of 65.0% was observed at pH value of 2.0, while it significantly dropped and remained constant at neutral pH (5.0-8.0). The lowest ED was observed at pH 9.0, while it slightly increased again for very basic pH (11.5), reaching a degradation of 7.4% at pH of 11.5.

The same degradation trend at acid pH was observed by Mishra and Gogate [67], using a Venturi device to treat a solution with an initial RhB concentration of 10.0 mg L⁻¹, at 30-40 °C and 4.9 bar and by Wang et al. [66], using a swirling jet-induced cavitation system to treat a solution with an initial RhB concentration of 5.0 mg L⁻¹ at 40 °C and 6.0 bar. Furthermore, this result is correspondent closely with that reported for the degradation of RhB by ultrasonic cavitation [116].

The different value of the extent of degradation of RhB by varying the pH of the contaminated solution is due to the possibility for the dye to assume two different forms that can react differently in contact with •OH free hydroxyl radicals made by cavitation process. At low pH prevails the cationic form of RhB while at high values prevails the zwitterionic form, [65]. It was reported that the cationic form is easier to the degradation [66], and thus at low values of pH the oxidation of RhB is higher. The acidity of the medium, which results in modification of the physical properties of molecules, plays an important role in the degradation of chemical pollutants. Similar results were also obtained for other dyes. Furthermore, as suggested by Wang et al. [66], the increasing of the oxidation potential of •OH in the acidic solution might be another reason for the degradation rate increase. Using NaOCl as additive, at acid pH prevails the undissociated hypochlorous acid, HClO. It is both a strong oxidants and it could evaporate into a cavitation bubble and undergo HC, also producing •OH radicals, resulting in an acceleration of the RhB degradation process [112]. Furthermore, in the present study, the slight increase in ED observed at basic pH could be justified by the prevalence at pH > 9.0 of the oxidising OCl⁻ ion. *Fig. 27 b* clearly shows how the kinetics of degradation are higher for lower pH compared to higher ones.

3.7. Effect of initial dye concentration

Degradation of RhB was investigated at different initial concentration of RhB values (2.0, 3.0, 4.0 mg L⁻¹) using the hybrid system based on HC and NaOCl at 0.5 mg L⁻¹ at 18.1 ± 1.3 °C. Orifice plates (plate thickness: 2 mm) were used as cavitating system under optimum conditions for pH (pH = 2.0), while the inlet pressure was fixed at 2.0 bar. The obtained results were shown in *Fig. 28*. It can be seen from the figure that, according to Parsa and Zonouzian [53], the efficiency of process was inversely proportional to the initial dye concentration. As the initial concentration increased from 2.0 to 4.0 mg

L⁻¹, the ED decreased from 76% to 61%. An increase in concentration of the contaminant in solution involves a greater amount of dye molecules, but the amount of free hydroxyl radicals remains constant.

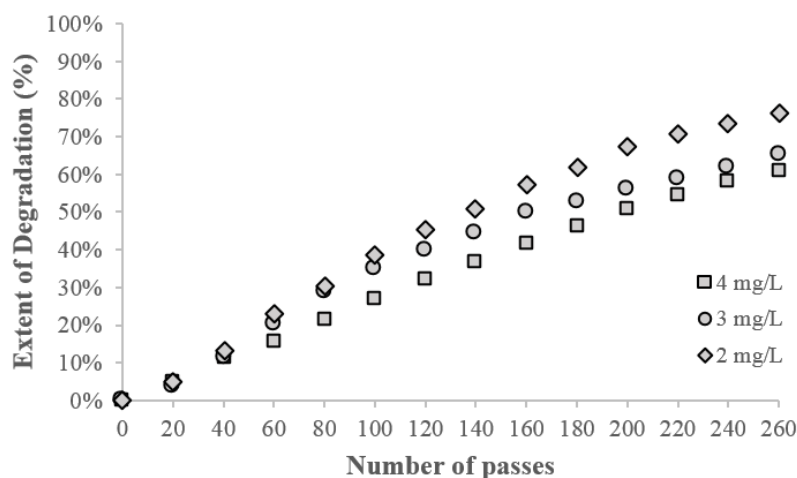


Fig. 28- Effect of initial dye concentration on RhB degradation by using orifice plate (volume 50 L; pH 2.0; initial temperature 18.1 ± 1.3 °C; pH 2.0; inlet pressure 2.0 bar; $0.5 \text{ mg NaOCl L}^{-1}$; mg RhB L^{-1}).

With increasing the initial concentration from 2.0 mg L^{-1} to 4.0 mg L^{-1} , the degradation rate constants (k) decreased from $13.3 \cdot 10^{-3} \text{ min}^{-1}$ or $20 \cdot 10^{-5} \text{ s}^{-1}$ ($R^2 = 0.9944$) to $7.8 \cdot 10^{-3} \text{ min}^{-1}$ or $13 \cdot 10^{-5} \text{ s}^{-1}$ ($R^2 = 0.9953$), respectively. This result is very similar with that reported for sonochemical degradation of RhB [65] and others HC systems. Sivakumar and Pandit [13] measured degradation rate constants of RhB using multiple hole orifice plates at $35.0\text{-}40.0$ °C in the range of $2.67\text{-}5.33 \cdot 10^{-5} \text{ s}^{-1}$. In a swirling jet-induced cavitation device, Wang et al. [66] reported a degradation rate constant k of $5.13 \cdot 10^{-3} \text{ min}^{-1}$ or $8.55 \cdot 10^{-5} \text{ s}^{-1}$ with regression coefficient $R^2 = 0.9972$ for 5.0 mg L^{-1} RhB in aqueous solution at temperature 40.0 °C and pH 5.4. Parsa and Zonouzian [53], using orifice plates in a submerged mode at temperature 40 °C, 5.8 bar and pH 5.4, showed that while the initial concentrations were increased from 2.0 mg L^{-1} to 5.0 mg L^{-1} , the degradation rate constants decreased from $9.0 \cdot 10^{-3} \text{ min}^{-1}$ to $5.7 \cdot 10^{-3} \text{ min}^{-1}$. However, from the results reported in Table 3, it can be observed that even if the ED decreased by increasing the initial dye concentration up to 4.0 mg L^{-1} , the amount of degraded RhB increased as effect of the higher concentration of RhB, resulting in an increase of the C.Y. as well. The same result was achieved by Parsa and Zonouzian [53]. Using a heterogeneous catalytic HC reactor combined with H_2O_2 , the authors observed that the C.Y. increased by increasing the initial dye concentration up to

10.0 mg L⁻¹, while decreased after this point, probably due to the limited amount of generated H₂O₂ and shortage of hydroxyl radicals.

3.8. Energy consumption analysis

Since the aim of the work is to evaluate the industrial sustainability of the cavitation processes studied for the treatment of wastewaters containing RhB, the energy consumption of different processes in degrading RhB was evaluated and compared. The parameter used for the comparison is the C.Y., which indicates the ability of the equipment in producing the desired change based on the electric energy actually used for generating cavitation. Considering HC systems, the main energy-consuming component is the pump that is used for recirculation of the aqueous solution of the pollutant through the cavitation chamber. *Table 3* shows such comparison. Concerning the HC devices alone, the energy consumption calculations shows the superiority of Ecowirl reactor compared to the orifice plate, as Ecowirl reactor enhances the extent of degradation of RhB. Moving from orifice plate to Ecowirl reactor an increase in C.Y. value from $2.07 \cdot 10^{-6}$ to $2.72 \cdot 10^{-6}$ mg J⁻¹ was calculated. Furthermore, it should be highlighted that over the experiments performed in this study, a slight higher increase in temperature of the liquid was measured using Ecowirl reactor rather than orifice plate, thus further improving the cavitation effects on RhB degradation [66]. Then, the hybrid scheme (HC + NaOCl) was analysed.

The use of NaOCl alone in a mixing process to treat dye wastewater could require lower energy as compared with the HC but it is definitely not sustainable to scale up the system [74]. However, benefits of lower energy requirements and lower chemical use can be achieved combining HC with chemical oxidation using NaOCl. At the minimum NaOCl dose tested (0.5 mg L⁻¹) and pH 4.0, the C.Y. increased of about 50% as compared to the HC alone. Using orifice plate the C.Y. increased from $2.07 \cdot 10^{-6}$ to $4.52 \cdot 10^{-6}$ mg J⁻¹, while using Ecowirl reactor C.Y. raised from $2.72 \cdot 10^{-6}$ to $4.60 \cdot 10^{-6}$ mg J⁻¹. The C.Y. can further be increased working at acid pH values or higher NaOCl concentrations. Indeed, by using Ecowirl reactor and working at pH 2.0 and 4.0 mg NaOCl L⁻¹, the C.Y. value increased up to $4.35 \cdot 10^{-5}$ mg J⁻¹. The C.Y. values of the Ecowirl reactor and the hybrid system studied were compared with those of other cavitation device reported in literature (*Table 4*). Generally, by comparing the C.Y., *Table 4* shows that HC reactors are more energy efficient as compared to the acoustic counterparts, giving higher cavitation yields. Furthermore, Ecowirl reactor is more energy efficient as compared to the other cavitating devices and the scale up of this reactor is easier. The efficient design of the Ecowirl reactor helps in reducing the treatment cost of wastewaters containing RhB.

Table 4 - Variation of cavitation yield (C.Y.) for different cavitation equipments.

Technology	Cavitation reactor	Chemicals	T (°C)	pH	p (bar)	V (L)	Flow rate (m ³ h ⁻¹)	Time (min)	[RhB] (mg L ⁻¹)	P Nominal (W)	P Abs (W)	ED (%)	[RhB] Degraded (mg L ⁻¹)	Power Density (kJ L ⁻¹)	C.Y. (mg L ⁻¹)	Reference
HC	Swirling jet-induced	H ₂ O ₂ (100 mg L ⁻¹)	50	3.0	6.0	25	3.6	180	10.0	2500	-	99.0	9.9	1080.0	9.17E-06	[43]
HC	Swirling jet-induced	No	50	3.0	6.0	25	3.6	180	10.0	2500	-	55.0	5.5	1080.0	5.09E-06	[43]
HC	Swirling jet-induced	No	40	5.4	6.0	40	-	180	5.0	3500	-	46.8	2.3	945.0	2.48E-06	[29]
HC	Heterogeneous catalytic	Catalyst Scrap iron	25	3.0	5.8	30	2.4	240	2.0	5500	-	87.0	1.7	2640.0	6.59E-07	[55]
HC	Orifice Plate	No	40	5.0	2.0	50	2.4	76	5.0	5500	-	15.0	0.7	500.0	1.50E-06	[61]
HC	Venturi	No	30	2.5	4.8	4	0.4	120	5.0	1100	-	60.0	3.0	1980.0	1.52E-06	[74]
HC	Venturi	No	30	4.7	4.8	4	0.4	120	5.0	1100	-	25.0	1.2	1980.0	6.31E-07	[74]
HC	Orifice Plate	No	30	4.7	4.8	4	0.4	120	5.0	1100	-	20.0	1.0	1980.0	5.05E-07	[74]
HC	Orifice Plate	No	20	4.0	2.0	50	6.0	130	3.0	3000	800	8.6	0.3	124.8	2.07E-06	This study [8]
HC	Orifice Plate	NaOCl (0.5 mg L ⁻¹)	20	4.0	2.0	50	6.0	130	3.0	3000	800	18.8	0.6	124.8	4.52E-06	This study [8]
HC	Orifice Plate	NaOCl (0.5 mg L ⁻¹)	20	2.0	2.0	50	6.0	130	3.0	3000	800	65.0	1.9	124.8	1.56E-05	This study [8]
HC	Ecowirl reactor	No	20	4.0	2.0	50	4.6	169	3.0	3000	800	14.7	0.4	162.2	2.72E-06	This study [8]
HC	Ecowirl reactor	NaOCl (0.5 mg L ⁻¹)	20	4.0	2.0	50	4.6	169	3.0	3000	800	24.9	0.7	162.2	4.60E-06	This study [8]
HC	Ecowirl reactor	NaOCl (4.0 mg L ⁻¹)	20	2.0	2.0	50	4.6	65	3.0	3000	800	90.5	2.7	62.4	4.35E-05	This study [8]
AC	Acoustic cavitation	No	25	5.3	-	0.3	-	120	5.0	60	-	45.0	2.2	1440.0	1.56E-06	[67]
AC	Acoustic cavitation	No	25	-	-	0.01	-	30	10.0	16.5	-	88.0	8.8	2970.0	2.96E-06	[78]

In the case of the hybrid treatment scheme based on HC and NaOCl, the optimization of operative parameters such as inlet pressures/flow rates, pH and loadings of NaOCl helps in reducing the overall treatment cost as it reduces the electrical cost and cost of chemicals. Overall, the use of Ecowirl in the hybrid treatment based on HC and NaOCl as additives at optimum loadings looks promising and economical as compared to other hydrodynamic and acoustic cavitation based process.

4. Conclusions

The present work allowed studying a swirling jet-induced reactor (Ecowirl) able to remove RhB dye from wastewater. Experimental evidences proved that Ecowirl reactor resulted in more intense cavitation as compared to multiple hole orifice plates giving better efficacy on degradation of RhB. Using only cavitation in absence of additives, the higher ED obtained can be attributed to the operative pressure measured in downstream cavitation zone of Ecowirl reactor with a value of -0.85 bar that resulted to be lower than the value downstream of the orifice plate (0.30 bar) at similar inlet operative pressure (2.0 bar), resulting in pressure drop values, ΔP_{HC} , of 2.85 and 1.7 bar, respectively. Furthermore, higher values (1.3 times more) of C.Y. in Ecowirl reactor than in hole orifice plates were observed, which means that for similar values of energy supplied to the cavitation system, a greater amount of RhB was degraded using Ecowirl reactor. A study of different geometric configurations of the cavitating device was carried out inspired by these considerations. The geometry and the fluid dynamic characteristics of the solution to treat affected the pressure distribution and the pressure recovery profile downstream of the constriction and hence the active cavitation volume, which is very important considering global effects of the HC reactor. The hybrid scheme treatment based on HC by using Ecowirl reactor (20 °C, 2.0 bar, pH 2.0 or 4.0) and NaOCl (minimal dose 0.5 mg L⁻¹) was found to be the most energy efficient and environmental friendly method to treat wastewater-containing RhB. The combined process HC and NaOCl increased the efficiency of RhB degradation as compared to HC alone or to NaOCl oxidation process implying an acceleration of the kinetic of RhB degradation and resulting in a decrease of treatment time and hence of treatment costs. Swirling jet-induced cavitation by using Ecowirl combined with NaOCl was more energy efficient if compared to other hydrodynamic and acoustic cavitation based processes. The aim of the designers should be to maximize further the energy efficiency. This can be done based on manipulation of the operative conditions and geometric parameters of the reactor, resulting in optimal ΔP_{HC} and rapid pressure increase, to give the desired effect in terms of the observed chemical change. Further studies, are needed to better understand the fluid dynamic of swirling jet induced cavitation devices.

Chapter 3

A swirling jet-induced cavitation to increase activated sludge solubilisation and aerobic sludge biodegradability

This chapter was based on:

G. Mancuso, M. Langone, G. Andreottola, A swirling jet-induced cavitation to increase activated sludge solubilisation and aerobic sludge biodegradability, *Ultrason. Sonochem.* 35 (2016) 489-501.

Chapter 3

A swirling jet-induced cavitation to increase activated sludge solubilisation and aerobic sludge biodegradability

Giuseppe Mancuso, Michela Langone, Gianni Andreottola

Department of Civil, Environmental and Mechanical Engineering, University of Trento, via Mesiano 77, 38123, Italy

Abstract

In this work, a modified swirling jet-induced hydrodynamic cavitation (HC) was used for the pre-treatment of excess sludge. In order to both improve the HC treatment efficiencies and reduce the energy consumption, the effectiveness of the HC reactor on sludge disintegration and on aerobic biodegradability was investigated at different operative conditions and parameters, such as temperature, inlet pressure, sludge total solid (TS) content and reactor geometry. The inlet pressure was related to the flow velocity and pressure drop. The best results in terms of sludge solubilisation were achieved after 2 h of HC treatment, treating a 50.0 gTS L⁻¹ and using the three heads Ecowirl system, at 35.0 °C and 4.0 bar. Chemical and respirometric tests proved that sludge solubilisation and aerobic biodegradability can be efficiently enhanced through HC pre-treatment technique. At the optimum operative conditions, the specific supplied energy was varied from 3276 to 12,780 kJ kg TS⁻¹ in the HC treatment, by increasing the treatment time from 2 to 8 h, respectively. Low endogenous decay rates (b_H) were measured on the excess sludge at low specific supplied energy, revealing that only an alteration in floc structure was responsible for the sludge solubilisation. On the contrary, higher b_H values were measured at higher specific supplied energy, indicating that the sludge solubilisation was related to a decreasing biomass viability, as consequence of dead cells and/or disrupted cells (cell lysis).

Keywords: Energy efficient, Sludge solubilisation, Swirling jet-induced cavitation Sludge disintegration, Aerobic biodegradability

1. Introduction

Activated sludge system is the most used biological process in industrial and municipal wastewater treatment plants (WWTPs). This process produces a high amount of excess sludge, which has a relevant impact on the operative costs in WWTPs. Thus, any improvements in reducing the quantity of the excess sludge are always beneficial.

Several technologies, based on destruction of bacterial cell walls and membranes were developed with the aim to reduce the sludge production by enhancing (i) the sludge biodegradability and its reuse in other biological processes, and (ii) the sludge dewaterability and consequently the performance of separation technologies.

With this purpose, several pre-treatment techniques such as biological [117,118], thermal hydrolysis [119,120], chemo-thermal [121,122], mechanical [14,28,123], chemo mechanical [124], chemical [125–127], and alkali processes [128,129] were proposed and successfully applied in WWTPs.

Among mechanical treatments, the most successful method is cavitation, that is taking a more prominent role in the field of wastewater treatment, mainly due to the ease of operation, flexibility and capability to vary the required intensities of cavitation conditions [11]. Cavitation acts by destroying bacterial cell walls and membranes resulting in a release of intracellular and extracellular matter [79]. Many of the intracellular constituents, including cytoplasm and nucleic acids, are readily biodegradable, resulting either in acceleration of both aerobic and anaerobic digestion processes in the sludge treatment line or in promoting denitrification in the wastewater treatment process. Among other benefits, cavitation process may counteract the formation of activated sludge bulking and foam, resulting in improved sludge sedimentation properties [83].

Depending on the mode of its generation, cavitation can be defined such as acoustic, hydrodynamic, optic and particle cavitation. Among these, the most used are acoustic (AC) and hydrodynamic cavitation (HC).

Over the past decades, many works were carried out on the application of the AC on activated sludge in order to increase the biogas production in the anaerobic digestion process [130], to enhance the microbial activity and the sludge dewaterability [131], to increase the soluble chemical oxygen demand (SCOD), proteins and nucleic acids concentrations [132], to improve the sludge settling [79,133,134], and to reduce the excess sludge from the activated sludge system [135].

On the contrary, HC was studied to a lesser extent than AC, but published researches showed promising outcomes in sludge pre-treatment [45], dyes removal [8], chemical compounds oxidation [136], bacteria removal [42]. Furthermore, recent studies proved its cost-effectiveness [13,14]. HC is generated by pressure variation in a flowing liquid caused by the velocity variation in the system [29,51,137]. When the static pressure at the mechanical constriction falls below the vapour pressure of the liquid, cavities are generated. At the downstream of the constriction, as the liquid jet expands, the pressure recovers and this results in the violent collapse of the cavities [29], giving rise to high pressure and temperature pulses. Thus, HC can be generated by introducing constrictions, such as orifice plate [17], Venturi [15,16] or throttling valve, in the flow.

Furthermore, the development of new HC reactor configurations attracted the attention of researchers and enterprises due to the technical feasibility of the scale-up. Recently, a high-pressure jet device, where cavitation occurs, was studied for activated sludge reduction [14]. HC was also

generated using a stator and rotor assembly, which was effectively applied for enhancement of the biogas production from activated sludge [58] and lignocellulosic biomass, like wheat straw [138].

While literature is available on anaerobic biodegradability enhancement, there is a paucity of literature on the effect of HC on the aerobic biodegradability.

In this study, a modified swirling jet-induced reactor, named Ecowirl reactor [56], was used in order to generate HC, by creating a vacuum-core vortex. The main aim of the present work was to prove the effectiveness of the Ecowirl reactor on sludge solubilisation exploring the potential for reducing the energy consumption and examining the influences of the pre-treatment on aerobic biodegradability. With this purpose, the effects of different factors such as medium temperature, inlet pressure (and consequently flow rate), solid concentration, reactor geometry, HC treatment time on sludge solubilisation, disintegration degree and microbial activity were investigated.

2. Materials and Methods

2.1. Sludge characterization

Excess activated sludge of a nitrification/denitrification process, collected at Trento municipal WWTP, Italy, was used for the experimental investigations. In order to get sludge with a high total solid (TS) concentration, sludge was collected after the dynamic thickening process. Thickened sludge was then diluted with tap water to obtain the desired TS concentration. The physical and chemical characteristics of the thickened sludge used were: pH 6.8 ± 0.2 , TS = $33.4 \pm 0.5 \text{ g L}^{-1}$, volatile solids (VS) = $27.9 \pm 0.4 \text{ g L}^{-1}$, total chemical oxygen demand (TCOD) = $38,015 \pm 321.0 \text{ mg L}^{-1}$, soluble COD (SCOD) = $318.6 \pm 5.0 \text{ mg L}^{-1}$, total Kjeldahl nitrogen (TKN) = $2856 \pm 3.0 \text{ mg L}^{-1}$, ammonia nitrogen ($\text{NH}_4 + \text{-N}$) = $33.7 \pm 1.0 \text{ mg L}^{-1}$, total phosphate (P_{TOT}) = $1062 \pm 56.0 \text{ mg L}^{-1}$.

2.2. HC system

Fig. 29 shows a schematic representation of the experimental setup for the pre-treatment using HC process. It consists of a closed loop circuit designed to treat 50.0 L of sludge from a feed tank, then taking it into a flow channel internally accommodating the HC reactor (Ecowirl reactor) and then discharging the treated sludge back to the main tank by means of a Mohno pump (3.0 kW, nominal power, Netzsch Pumps & Systems GmbH Germany).

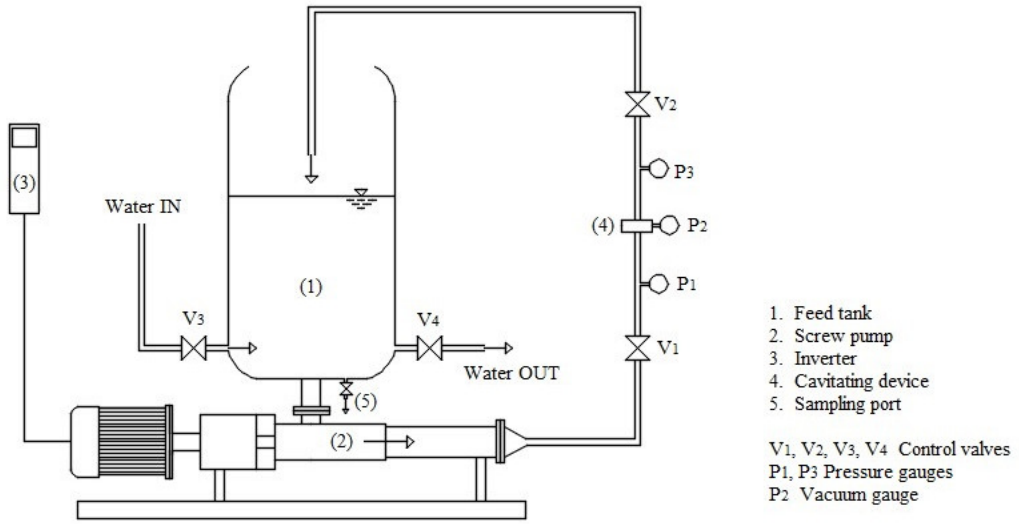


Fig. 29 - Schematic representation of the experimental setup.

A solid geometry was created using Autodesk Inventor Professional software (Fig. 30). Ecowirl reactor is a modified swirling jet reactor, in which cavitation is generated by using a multi-dimensional vortices generator, consisting of a frustum-conical pre-swirling chamber (Fig. 30 (2)) preceded by another chamber (Fig. 30 (1)) where an orifice plate with injection slots is located. Flow enters through the injection slots and a vacuum-core vortex is created. Then, the flow impacts on a plate located in a double cone chamber (Fig. 30 (3)), resulting in a fast recover of the pressure. In the present work, the sum of the regions (1) and (2) is called “Ecowirl head”. Detailed information of experimental setup and Ecowirl reactor is reported in Mancuso et al. [8]. In order to measure the pressure changes in the Ecowirl reactor, pressure gauges were located as shown in Fig. 30. The static (relative) pressure was measured.

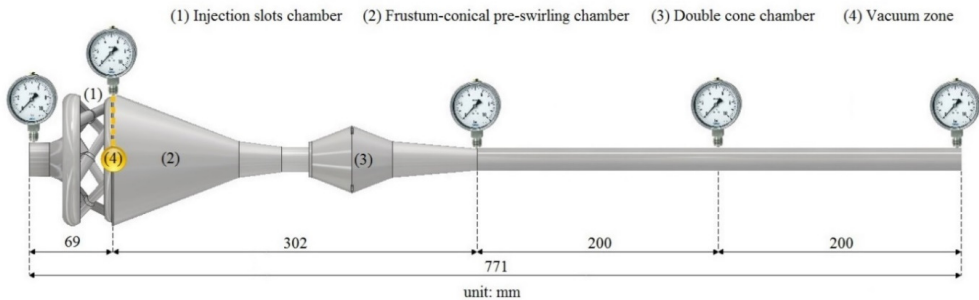


Fig. 30 - Solid geometry of Ecowirl reactor.

2.3. Methods

2.3.1. HC tests

The feed tank was filled with 50.0 L of sludge. The sludge was recirculated in the loop by using the bypass line for about 15 min in order to homogenise its content. At this stage, cavitation did not occur. In the meantime, the temperature of the sludge was adjusted at the desired temperature by using a heating and cooling system with steel coils. Temperature was kept constant throughout the experiments (with a variation of ± 3.0 °C). During the experiments, the required value of inlet pressure at cavitation system was achieved by adjusting the frequency of the pump inverter. Consequently, the flow rate and the flow velocity varied.

HC was first optimized in terms of different operative parameters. As reported in *Table 5*, effects of temperature (20.0, 25.0, 30.0 and 35.0 °C), inlet pressure (2.0, 3.0, 4.0 bar), TS content (7.0, 12.0, 23.0 and 50.0 g L⁻¹) on sludge solubilisation and disintegration degree were investigated using one Ecowirl head with the standard configuration (six injection slots, upstream diameter 10 mm - downstream diameter 8 mm). In this study, the inlet pressure, instead of flow rate and flow velocity, was taken into account because it is an easy operational parameter to set. Then the geometry of the Ecowirl reactor was studied, varying the number and the diameter of the injection slots present in the orifice plate and the number of Ecowirl heads in series (*Table 5*). Each test was conducted for 2 h. Following the optimization of HC parameters, an 8 h-experiment was carried out at 50.0 gTS L⁻¹, 4.0 bar, 35.0 °C and using 3 standard Ecowirl heads in series in order to evaluate the HC efficiencies as function of specific energy applied (SE) to the sludge.

Sludge samples were taken from the main tank through the sampling port at the initial and at the end of experiments and analysed. In 8 h-experiments sludge samples were collected at 0, 2, 4 and 8 h. pH in the main tank was continuously monitored.

2.3.2. Respirometric technique

Fig. 31 shows a schematic representation of the respirometric experimental setup used to evaluate the HC effect on aerobic degradability and microbial activity. Details are as follows: (1) a respirometric reactor that consists in a glass cylinder filled with 1.2 L of sludge; (2) a magnetic agitator to mix and homogenise the solution; (3) an air compressor; (4) an air diffusor; (5) probes to measure DO, pH and temperature of the solution; (6) a thermostatic bath to keep constant the temperature of the solution at 20.0 °C; (7) a computer used for storing and monitoring all data connected to the DO probe through a RS-232 port.

Table 5 - Operative parameters/conditions and efficiency measured at the end of each test.

Section number	Injection slots	Ecowirl heads	Injection slots D (mm)	T (°C)	P inlet (bar)	Flow rate (m ³ h ⁻¹)	A (mm ²)	v (m sec ⁻¹)	TS (g L ⁻¹)	TCOD (mg L ⁻¹)	SCOD ₀ (mg L ⁻¹)	SCOD _{low} (mg L ⁻¹)	DD PCOD (%)	DD COD NaOH (%)	DD N (%)	Absorbed power (W)
3.1	6	1	10-8	20	2.0	4.6	301.4	4.2	50.0	46,423	251	900	1.4	2.2	2.0	1042
	6	1	10-8	25	2.0	4.6	301.4	4.2	50.0	46,043	436	1053	1.4	2.1	2.2	1028
	6	1	10-8	30	2.0	4.6	301.4	4.2	50.0	36,777	737	1547	2.2	4.3	5.9	1008
	6	1	10-8	35	2.0	4.6	301.4	4.2	50.0	40,119	1039	2436	3.6	5.4	7.4	1003
3.2	6	1	10-8	25	2.0	4.6	301.4	4.2	50.0	43,043	436	1053	1.4	2.1	2.2	1028
	6	1	10-8	25	3.0	5.8	301.4	5.3	50.0	41,449	290	1415	2.7	5.1	3.0	1251
	6	1	10-8	25	4.0	6.8	301.4	6.3	50.0	33,516	96	1355	3.8	5.7	4.1	1618
	6	1	10-8	25	2.0	4.6	301.4	4.2	50.0	43,043	436	1053	1.4	2.1	2.2	1028
3.3	6	1	10-8	25	2.0	4.6	301.4	4.2	23.0	16,119	31	154	0.8	0.8	0.9	800
	6	1	10-8	25	2.0	4.6	301.4	4.2	12.0	12,236	31	71	0.3	0.8	0.9	800
3.2	6	1	10-8	25	2.0	4.6	301.4	4.2	7.0	10,666	19	36	0.2	0.6	0.7	800
	6	1	10-8	25	4.0	6.8	301.4	6.3	50.0	33,516	96	1355	3.8	5.7	4.1	1618
3.4.1	6	1	5-3	25	4.0	2.3	42.4	15.1	50.0	38,400	118	2382	5.9	8.2	6.4	889
	6	1	5-3	25	4.0	2.3	42.4	15.1	50.0	38,400	118	2382	5.9	8.2	6.4	889
3.4.1	9	1	5-3	25	4.0	2.9	63.6	12.7	50.0	38,874	123	2013	4.9	6.4	3.9	800
	12	1	5-3	25	4.0	3.3	84.8	10.8	50.0	34,607	56	1209	3.3	4.5	2.5	803
3.4.2	6	1	10-8	25	2.0	4.6	301.4	4.2	50.0	43,043	436	1053	1.4	2.1	2.2	1028
	6	2	10-8	25	2.0	3.5	301.4	3.2	50.0	38,778	130	692	1.5	2.4	3.4	1038
	6	3	10-8	25	2.0	3.0	301.4	2.8	50.0	36,527	315	1644	3.7	4.5	4.5	1500

The DO depletion in the vessel, due to the substrate utilization, was monitored over the time. First, the Oxygen Uptake Rate (OUR), expressed as $\text{mgO}_2 \text{ L}^{-1} \text{ h}^{-1}$, was determined by the slope of the plot of DO concentration versus time after stopping for few minutes the air flow inlet [139]. Then, the specific OUR (SOUR), expressed as $\text{mgO}_2 \text{ gTSS}^{-1} \text{ h}^{-1}$, was obtained dividing the OUR by the TSS concentration in the assays.

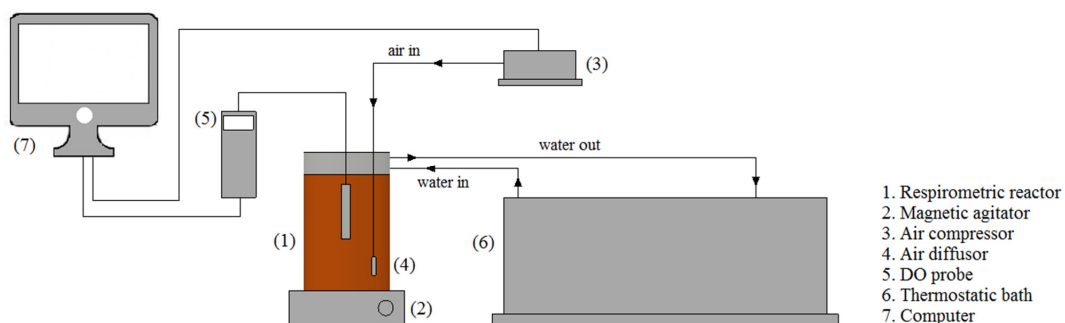


Fig. 31- Schematic representation of the respirometric experimental setup.

2.3.2.1. Aerobic biodegradability

A series of respirometric tests were carried out on filtered sludge samples from the optimized HC experiment in order to evaluate the effect due to the HC process on aerobic biodegradability as a function of the applied energy. The activated sludge from the oxidation tank of the municipal WWTP of Trento was used as inoculum. TSS content of the inoculum was $3.0 \pm 0.1 \text{ g L}^{-1}$. Samples at 0, 2, 4 and 8 h from the optimized HC experiment were analysed.

The soluble biodegradable COD (SCOD_{bio}) of the untreated and treated sludge was determined according to Andreottola et al. [139], and Wentzel et al. [140].

Low values of substrate and biomass concentrations (F/M: food to microorganism) were maintained during the test, approximately $0.05 \text{ mg COD mg}^{-1} \text{ VSS}$. For all the experiments, thiourea (20.0 mg L^{-1}) was added to inhibit the nitrification process. The recorded data of the oxygen uptake rate (OUR) were plotted as a function of time. A primary curve segment, which was characterized by a higher slope, represented substrate consumption, operated by biomass; on the contrary, the final segment, characterized by a lower slope, represented the DO consumption under endogenous conditions. The amount of exogenous oxygen consumption (ΔO_2) was determined by calculating the area under the OUR curve and subtracting the contribution of the endogenous respiration. In order to evaluate the

SCOD_{bio}, the exogenous oxygen consumption was then converted to equivalent COD using the expression based on the COD mass balance [141].

2.3.2.2. Microbial activity

A series of respirometric tests were carried out on sludge samples from the 8 h-optimized experiment in order to evaluate the effect of HC on microbial activity as a function of the applied energy. The change of sludge microbial activity was evaluated by determining the endogenous decay rate (b_H) of heterotrophic biomass, through the “single batch test” procedure [142]. For all the experiments, thiourea (20.0 mg L⁻¹) was added to inhibit the nitrification process. Samples at 0, 2, 4 and 8 h from the optimized HC experiment were analysed. Sludge samples were diluted by adding purified water in order to obtain a TSS content of 3.5 ± 0.5 g L⁻¹.

2.4. Calculations

The process efficiency was evaluated by measuring the improvement of solubilisation of sludge in terms of the SCOD-increase (Eq. 7) [143], the ratio of change in soluble chemical oxygen demand (SCOD) after cavitation to particulate chemical oxygen demand (PCOD₀ = TCOD - SCOD₀) (Eq. 8) [144], and the ratio of change in ammonia after cavitation to initial organic nitrogen content (Norg₀ = TKN₀ - NH₄⁺ - N₀) (Eq. 9):

$$\Delta\text{SCOD} (\%) = \text{SCOD}_{\text{cav}} - \text{SCOD}_0 \quad \text{Eq. 7}$$

$$\text{DD}_{\text{PCOD}} (\%) = \frac{\text{SCOD}_{\text{cav}} - \text{SCOD}_0}{\text{PCOD}_0} \times 100 = \frac{\text{SCOD}_{\text{cav}} - \text{SCOD}_0}{\text{TCOD} - \text{SCOD}_0} \times 100 \quad \text{Eq. 8}$$

$$\text{DD}_N (\%) = \frac{\text{NH}_4^+ - \text{N}_{\text{cav}} - \text{NH}_4^+ - \text{N}_0}{\text{Norg}_0} \times 100 = \frac{\text{NH}_4^+ - \text{N}_{\text{cav}} - \text{NH}_4^+ - \text{N}_0}{\text{TKN}_0 - \text{NH}_4^+ - \text{N}_0} \times 100 \quad \text{Eq. 9}$$

where SCOD_{cav} is the soluble COD of the treated sludge by using HC [mg L⁻¹] at the time t, SCOD₀ is the soluble COD of the untreated sludge [mg L⁻¹], TCOD is the total COD of the untreated sludge [mg L⁻¹], NH₄⁺ - N_{cav} is the ammonia content of the treated sludge by using HC [mg L⁻¹] at the time t, NH₄⁺ - N₀ and TKN are the ammonia and total Kjeldahl nitrogen content of the untreated sludge [mg L⁻¹]. Other index of importance in sludge disintegration includes the sludge disintegration degree calculated as the ratio of SCOD increase by cavitation to the SCOD increase by the chemical disintegration (Eq. 10) [131]:

$$DD_{\text{COD NaOH}} (\%) = \frac{\text{SCOD}_{\text{cav}} - \text{SCOD}_0}{\text{SCOD}_{\text{NaOH}} - \text{SCOD}_0} \times 100 \quad \text{Eq. 10}$$

where $\text{SCOD}_{\text{NaOH}}$ [mg L^{-1}] is the soluble COD of the reference sample obtained with a strong alkaline disintegration (NaOH digestion).

In order to compare results, the specific supplied energy (SE) was determined by using Eq. 11:

$$SE \left(\frac{\text{kJ}}{\text{kg TS}} \right) = \frac{P_{\text{abs}} \times t}{V \times \text{TS}} \quad \text{Eq. 11}$$

where P_{abs} is the pump absorbed power [W], t is the treatment time [sec], V is the volume of the treated sludge [L] and TS is the solids content [g L^{-1}].

Finally, according to Zhang et al. [143], the energy efficiency (EE), expressed as $\text{mg } \Delta\text{SCOD kJ}^{-1}$, was calculated as the mg of SCOD-increase per unit of energy supplied (Eq. 12). Higher EE values corresponded to higher removal efficiencies.

$$EE \left(\frac{\text{mg } \Delta\text{SCOD}}{\text{kJ}} \right) = \frac{V \times \Delta\text{SCOD}}{P_{\text{abs}} \times t} \times 1000 \quad \text{Eq. 12}$$

2.5. Analytical methods

At the beginning and at the end of each HC test, sludge samples were collected from the bottom of the feed tank through the sampling port (Fig. 29) and stored at 4.0 °C for subsequent analysis. TS, VS, TSS, TCOD, SCOD, TKN, $\text{NH}_4^+\text{-N}$ were calculated according to the standard methods [145]. Prior to SCOD and $\text{NH}_4^+\text{-N}$ determinations the sludge samples were centrifuged at 5000 X g and the supernatant liquid was filtered using cellulose nitrate membrane of pore size 0.45 μm by compression. The filtrates were further used in aerobic biodegradation tests. pH was monitored by using a Crison 25 portable pH-meter. All the analyses were performed in duplicate and the results were expressed as average of the values. A reference sample was defined as the soluble COD obtained by chemical sludge disintegration in 1.0 mol L^{-1} sodium hydroxide for 24 h at 20.0 °C [146].

3. Results and discussion

Objective of all the experiments was to understand the effect of different operative parameters and arrive at a set of parameters that will give the maximum disintegration degree for an activated sludge. Operative parameters, operative conditions and efficiencies measured at the end of each test are summarized in Table 5. The results were described and discussed with more details in the following

paragraphs. The experimental errors were within 2-3% of the reported value of the extent of degradation. Finally, the effect of the HC treatment on the aerobic biodegradability and microbial activity is discussed.

3.1. Effect of temperature

Heating alone up to 60 °C can increase the sludge solubilisation [147,148], however larger increases in SCOD can be obtained with AC than with heating alone [148].

Although the effect of medium temperature on sludge disintegration was studied in AC systems, the influence of temperature on sludge disintegration in HC process was not investigated. A recent study only reports the effect of temperature on HC intensity [44].

Thus, in this study, for the first time, the effect of temperature in HC systems in the range of 20.0-35.0 °C on sludge disintegration was examined. Experiments were conducted using the sludge containing 50.0 gTS L⁻¹, working with an inlet pressure of 2.0 bar. Without temperature control, the bulk solution gradually raised in temperature (data not showed). Thus, for each test, temperature was kept constant for the entire duration of the experiment by using a heating and cooling system.

From Fig. 32 it is evident that the HC efficiency in terms of sludge solubilisation was more efficient at higher temperatures. The ΔSCOD increased from 649 to 1397 mg L⁻¹ with temperatures ranged from 20.0 to 35.0 °C at 2 h. At 35.0 °C, DD_{PCOD} and DD_{COD NaOH} reached values of 3.6 and 5.4%, respectively.

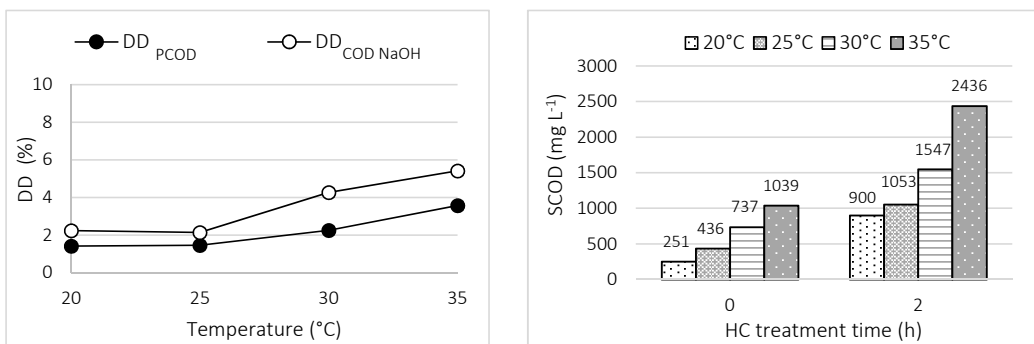


Fig. 32 - Effect of temperature on DD and SCOD (volume 50.0 L; TS content 50.0 g L⁻¹; initial pH 6.8; inlet pressure 2.0 bar; temperature 20.0-25.0-30.0-35.0 ± 3.0 °C). Ecowirl reactor standard configuration.

The effects of temperature on HC are complex, which have positive and negative effects on HC treatment efficiency. The increase of temperature implies a decrease of the surface tension, leading to an easier bubble formation [51]. However, these generated bubbles are richer in vapor content,

which cushioning their implosion, reducing the intensity of bubbles collapse [51]. Recently, Šarc et al. [44] demonstrated that the magnitude of pressure oscillations, which occur due to cavitation bubble collapses, increased for temperature of 40 °C, but then dropped significantly for higher temperatures. In this study, as a result from the obtained data, it was possible to observe the positive effects of temperature (in the range of 20.0- 35.0 °C) on sludge solubilisation in HC treatment, resulting in an increase of SCOD for increasing temperatures. Our results agree with previous studies on the effect of temperature on sludge disintegration by using AC. Indeed, Chu et al. [147], found that both ultrasonic vibration and bulk temperature rise, from 20.0 to 55.0 °C, contribute to the AC treatment efficiency. Grönroos et al. [148] observed the same effect. Huan et al. [131] showed that the temperature of sludge samples would increase with ultrasonic energy input and the rise of temperature helps to ultrasonic disintegration. Xu et al. [149] also proved that an increase in temperature involved an intensification of the sludge solubilisation in an ultrasound combined with ozone treatment.

3.2. Effect of inlet pressure: flow velocity and pressure drop

Effect of the inlet pressure on solubilisation was evaluated with the activated sludge containing 50.0 gTS L⁻¹, at 25.0 °C. The pressure measured at the inlet of the Ecowirl head was varied from 2.0 to 4.0 bar in steps of 1.0 bar. As shown in *Table 5*, increasing the inlet pressure from 2.0 to 4.0 bar, an increase in flow rate was observed from 4.6 to 6.8 m³ h⁻¹, respectively. In this study, the velocity profile along the HC device was not calculated due to the complex geometry of the Ecowirl reactor. However, the velocity of the flow through the narrowest reduced area of the orifice plate was evaluated. *Table 5* shows that being equal the geometry, increasing the flow rate an increase of flow velocity was measured.

The results shown in *Fig. 33* demonstrated that, after 2 h HC treatment, higher SCOD concentrations were measured at higher inlet pressures, and thus at higher flow velocities. The Δ SCOD increased from 617 to 1259 mg L⁻¹ with inlet pressures increased from 2.0 to 4.0 bar, respectively.

The reasons behind this are the increased turbulence level and higher local pressure oscillations due to the higher flow velocity. Recently, Šarc et al. [44] proved the importance of flow velocity, which increased with the flow rate and the inlet pressure. Authors verified that by the increase of the flow velocity the amplitude of pressure waves generally increases.

Furthermore, in this study, higher inlet pressures produced lower pressures in the vacuum zone and thus higher pressure drops (*Fig. 34*), which means higher shear forces that break down bacterial cell

walls and release the intracellular substances into aqueous phase, resulting in an increase in the sludge solubilisation. The role of the intense turbulent shear zone behind the orifice plate in enhancing cavitation activity was qualitatively established by Kumar et al. [150].

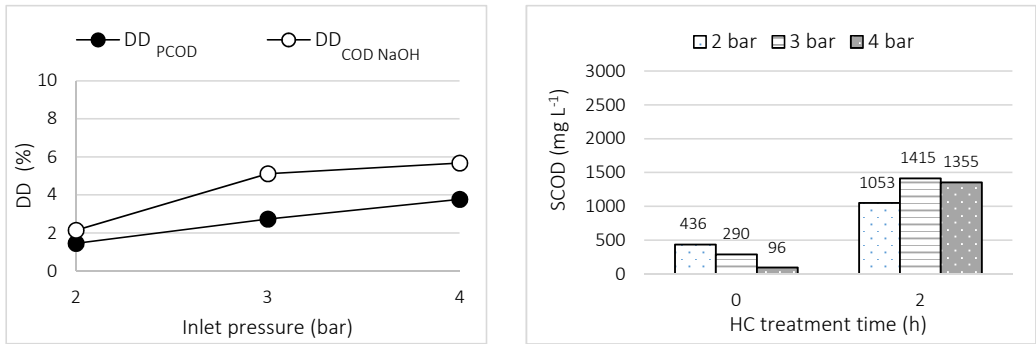


Fig. 33 - Effect of inlet pressure on DD and SCOD (volume 50.0 L; TS content 50.0 g L⁻¹; initial pH 6.8; temperature 25.0 ± 3.0 °C; inlet pressure 2.0-3.0-4.0 bar). Ecowirl reactor standard configuration.

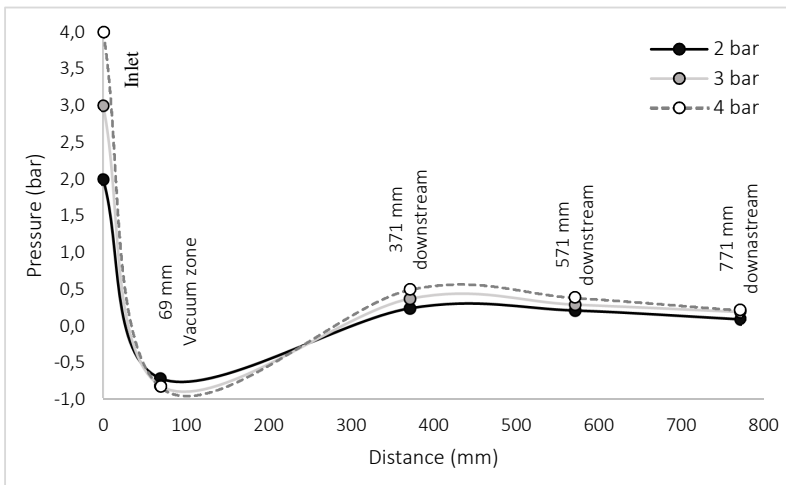


Fig. 34 - Variations in pressure in Ecowirl reactor. $\Delta P_{\text{Inlet}} - \text{Vacuum zone}$: ΔP 2 bar \approx 2.7 bar, ΔP 3 bar \approx 3.8 bar, ΔP 4 bar \approx 4.8 bar; ΔP Vacuum zone – 371 mm downstream: ΔP 2 bar \approx 1.0 bar, ΔP 3 bar \approx 1.3 bar, ΔP 4 bar \approx 1.5 bar.

As shown in the pressure profile (Fig. 34), the static (relative) pressure downstream the Ecowirl reactor decreased sharply as the flow passed the Ecowirl reactor, reaching negative values. Beyond Ecowirl reactor, static pressure started to recover but it never got to the upstream value, and a pressure drop can be measured.

The pressure measured in the vacuum zone in this study was -0.65 ± 0.13 , -0.79 ± 0.15 and -0.83 ± 0.15 bar, at 2.0, 3.0 and 4.0 bar, respectively, which was higher than the vapor pressure of the water equal to -0.96 bar at 25.0 °C. The development of cavitation for pressure higher than the vapor pressure of water was also reported theoretically by Kumar and Pandit [64] and experimentally Kim et al. [15]. The presence of dissolved gas and suspended solids improved the cavitation development due to the formation of weak spots, which might play a crucial role in creating cavitation when the pressure in the vacuum zone was higher than the vapor pressure.

The importance of the pressure drop seen in this study is in accordance with others reports on HC. Kim et al. [15] reported a very low Δ SCOD increase (20 mg L^{-1}) after 2 h of HC treatment with an activated sludge containing 18.0 g TS L^{-1} , by using a Venturi system with an inlet pressure of -0.07 bar. This Venturi system produced a pressure drop of only 0.42 bar between the inlet and the throat section. On the contrary, Lee and Han [17] reported a 23% disintegration degree (DD_{PCOD}) after 20 min of HC treatment of activated sludge ($TS = 9.8 \text{ g L}^{-1}$) working with an orifice plate and at an inlet pressure of 7.0 bar.

During our HC tests, it was necessary to progressively reduce the frequency of the pump inverter in order to keep constant the inlet pressure value, and thus the flow rate and flow velocity. This was due to a progressive alteration of the rheology of the sludge, resulting in a decrease of the viscosity of the sludge during the HC treatment, as consequence of the disruption of cell or microbial flocs [15].

3.3. Effect of solid concentration

Fig. 35 shows the effects of solid concentration on the sludge disintegration. Four sludge concentrations were tested, 7.0 , 12.0 , 23.0 and 50.0 g L^{-1} . For the sludge with the highest TS content, the higher values of Δ SCOD and DD were observed. For example, Δ SCOD for activated sludge with TS of 12.0 , 23.0 , 50.0 g L^{-1} were 2.35, 7.23 and 36.30 times higher than that for activated sludge with TS of 7.0 g L^{-1} after 2 h of HC treatment. A linear relationship between TS concentration and DD_{PCOD} was found ($DD_{\text{PCOD}} = 0.0298 \text{ TS} - 0.0111$, $R^2 = 0.989$). The increase in TS content provides more cells and aggregates and thus a higher viscosity of the sludge, due to the inter- and intra- particle interactions. Both growth and collapse of bubbles are slowed down by viscosity in HC [46]. On the other hand, the increase in TS enhances the collisions between sludge flocs and cavitation bubbles, allowing the subsequent increase in sludge disintegration. Thus, the negative effect of high viscosity of the sludge with high TS was negligible compared to the positive effect of TS concentration on the sludge disintegration.

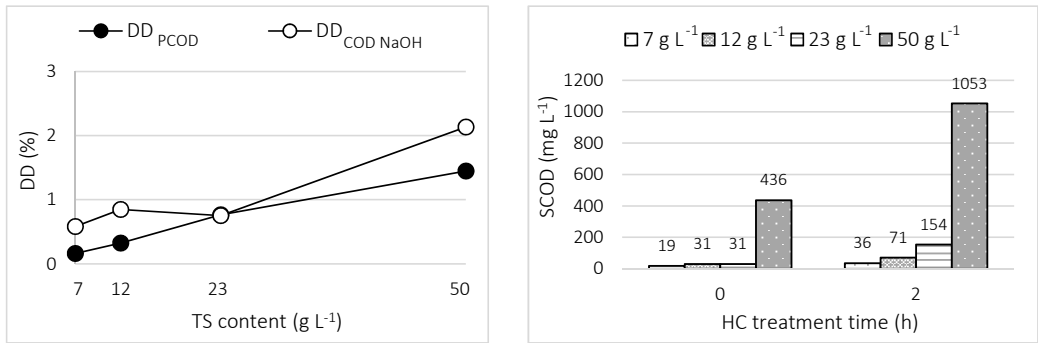


Fig. 35- Effect of TS content on DD and SCOD (volume 50.0 L; inlet pressure 2.0 bar; initial pH 6.8; temperature 25.0 °C ± 3.0 °C; TS content 7.0- 12.0- 23.0- 50.0 g L⁻¹). Ecowirl reactor standard configuration.

Kim et al. [15] discussed the effect of solid concentration (0.5, 1.5, 3.0 and 4.0%) on sludge disintegration by using a Venturi system (HC). In accordance with the present work, they observed that Δ SCOD was greater for sludge with higher solids content. They also observed that viscosity significantly decreased during the first 30 min of HC treatment, as consequence of the disruption of cell or microbial flocs. The same linear relationship was not reported in studies on AC systems, where an increase in TS content had opposite effects. The increase in TS content provides more cells to be in contact with cavitation bubbles, but can also impede the propagation of ultrasonic pressure waves and reduces the power of ultrasonic waves reached to sludge flocs. Indeed, Le et al. [151], using five synthetic mixed sludge samples (12.0, 24.0, 28.0, 32.0 and 36.0 g L⁻¹), observed a gradual increase in Δ SCOD by increasing the TS content, but the best DD was not found at the maximum TS. This is in accordance with the studies reported by Kidak et al. [152], Sahinkaya [153] and Zhang et al. [143]. On the other hand, Xu et al. [149] observed a decrease of Δ SCOD with the increase of initial sludge concentration. This result was also confirmed by Huan et al. [131], which found that sludge with low TS concentration was easier to disintegrate by AC.

3.4. Effect of geometry

3.4.1. Number and diameter of injection slots of Ecowirl reactor

Different Ecowirl heads with different number and diameter of injection slots were considered. Experiments were carried out with sludge at 50.0 g TS L⁻¹ and at 25.0 °C. The inlet pressure was set at 4.0 bar in order to reduce the possible blocking of the holes. The standard configuration (6 injection

slots, upstream diameter 10 mm - downstream diameter 8 mm) was first compared with the configuration A (6 injection slots, upstream diameter 5 mm- downstream diameter 3 mm) in order to evaluate the effect of diameter of injection slots on sludge disintegration. Then, the effect of the number of the injection slots was investigated.

Thus, the configuration A was compared with configurations B (9 injection slots, upstream diameter 5 mm- downstream diameter 3 mm) and C (12 injection slots, upstream diameter 5 mm- downstream diameter 3 mm).

The number of injection slots being equal, reducing the diameter of injection slots reduced the flow rate of the sludge in the HC system. Flow rates of the standard configuration and the configuration A were 6.8 and 2.3 m³ h⁻¹, respectively. However, the flow velocity through the reduced area of the orifice of the configuration A was higher than that calculated in the standard configuration, due to the lower flow passage area of the orifice of the configuration A (Table 5). Making a comparison between the standard configuration and the configuration A, it was possible to observe that a decrease in diameters of injection slots caused an increase in intensity of the cavitation, due to the higher flow velocity. DD_{PCOD} and DD_{COD NaOH} increased from 3.8%, and 5.7% using the standard configuration to 5.9%, and 8.2% using the Configuration A, respectively (Table 5).

The diameter of injection slots being equal, decreasing the number of injection slots the flow rate of the sludge in the HC system decreased, but the flow velocity increased (Table 5). The results are shown in Fig. 36.

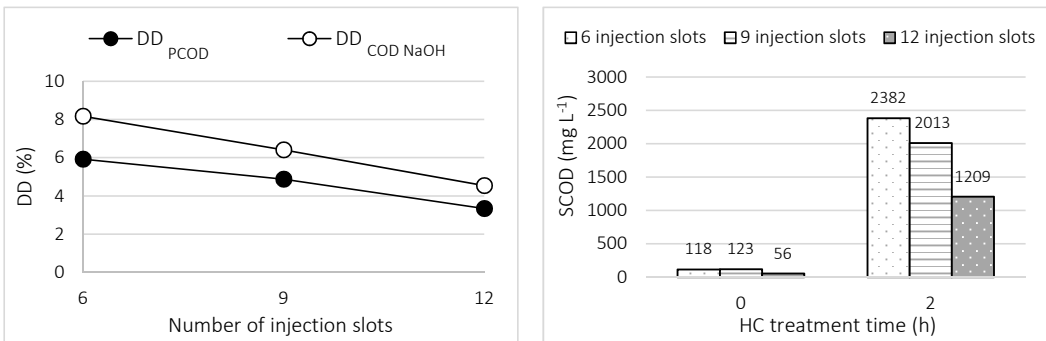


Fig. 36 - Effect of different number of injection slots on DD and SCOD (volume 50.0 L; inlet pressure 4.0 bar; initial pH 6.8; temperature 25.0 °C ± 3.0 °C; TS content 50.0 g L⁻¹). Ecowirl reactor configuration A, B, and C.

Lower number of injection slots caused high sludge disintegration degrees, due to the higher flow

velocity. According to Šarc et al. [44], all those results proved the influence of the flow velocity on the effectiveness of HC.

3.4.2. Number of Ecowirl heads

Effects of the number of Ecowirl heads in series were evaluated for the single-, two-, and three-heads systems with activated sludge containing 50.0 g TS L^{-1} , at $25.0 \text{ }^\circ\text{C}$ and 2.0 bar . Fig. 37 shows a schematic representation of Ecowirl reactor consisting of three-heads in series.



Fig. 37 - Ecowirl reactor with three-heads in series.

Increasing the number of Ecowirl heads the flow rate decreased. In addition, the calculated flow velocity through the reduced area of the orifice of the first head decreased. In spite of this observation, increasing the number of Ecowirl heads, the sludge degradation efficiency increased.

Results on sludge disintegration are reported in Fig. 38.

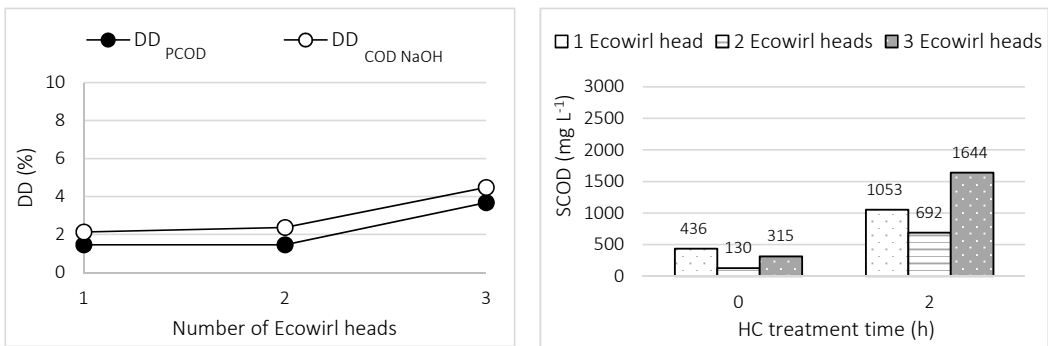


Fig. 38 - Effect of Ecowirl heads in series on DD and SCOD (volume 50.0 L ; inlet pressure 2.0 bar ; initial pH 6.8 ; temperature $25.0 \pm 3.0 \text{ }^\circ\text{C}$; TS content 50.0 g L^{-1}). Ecowirl reactor standard configuration.

After 2 h of treatment, the ΔSCOD value of the two-heads system was almost equal to that of the single-head system. On the contrary, the ΔSCOD value of the three-heads system was 2.1 time higher than that of the single-head system. Combining three Ecowirl heads in series, an increase in DD_{PCOD} and

$DD_{\text{COD NaOH}}$ from 1.4%, and 2.1% using the single-head system to 3.7%, and 4.5% using the three-heads system, respectively, was observed. The results obtained in this study are consistent with previous findings. Kim et al. [15] reported that a better HC treatment efficiency with a two-Venturi system was expected since ΔSCOD would be proportional to the volume of the cavitation zone. However, the number of the heads connected in series would be limited since there must be some energy dissipation during the course of cavitation development and collapse.

3.5. Comparison of energy efficiency

The variation of each operative condition in the HC treatment implied a variation of both the absorbed power and the COD disintegration degree, here expressed as the SCOD-increase. *Fig. 39* reports the energy efficiency (EE) vs the specific supplied energy (SE). As can be seen from the graphs, not always an increase in SE corresponds to an increase in EE. Observing the diagrams, the main findings of the investigation reported in this study can be summarized as follows:

- increasing the flow velocity by decreasing the injection slots number while keeping constant the inlet pressure, the EE increased with the increase of SE (*Fig. 39 a*);
- increasing the number of Ecowirl heads while keeping constant the inlet pressure, the EE increased with the increase of SE (*Fig. 39 b*);
- using the same geometric configuration of Ecowirl reactor and increasing the inlet pressure up to 3.0 bar, the EE increased with the SE (*Fig. 39 c*). However, no significant differences were detected, in terms of EE, working at a higher inlet pressure of 4.0 bar;
- increasing the flow velocity by decreasing the diameters of the injection slots while keeping constant the inlet pressure, the EE decreased with the increase of SE (*Fig. 39 d*). The maximum EE was obtained by using a geometry of Ecowirl reactor with the smallest diameters of the injection slots, in correspondence of which the lowest SE was applied;
- the maximum EE was obtained working at the higher temperature and the higher solid concentration tested while keeping constant the inlet pressure, in correspondence of which the lowest SE was applied (*Fig. 39 e and f*).

Thus, working at temperatures of 35.0 °C, solid concentrations of 50.0 g L⁻¹ and small diameters of injection slots of the orifice plate in the Ecowirl reactor, the highest HC treatment efficiencies was achieved with the lowest energy consumptions. In this study, the increase in the inlet pressure contributed to an increase in the EE only up to a pressure value of 3.0 bar.

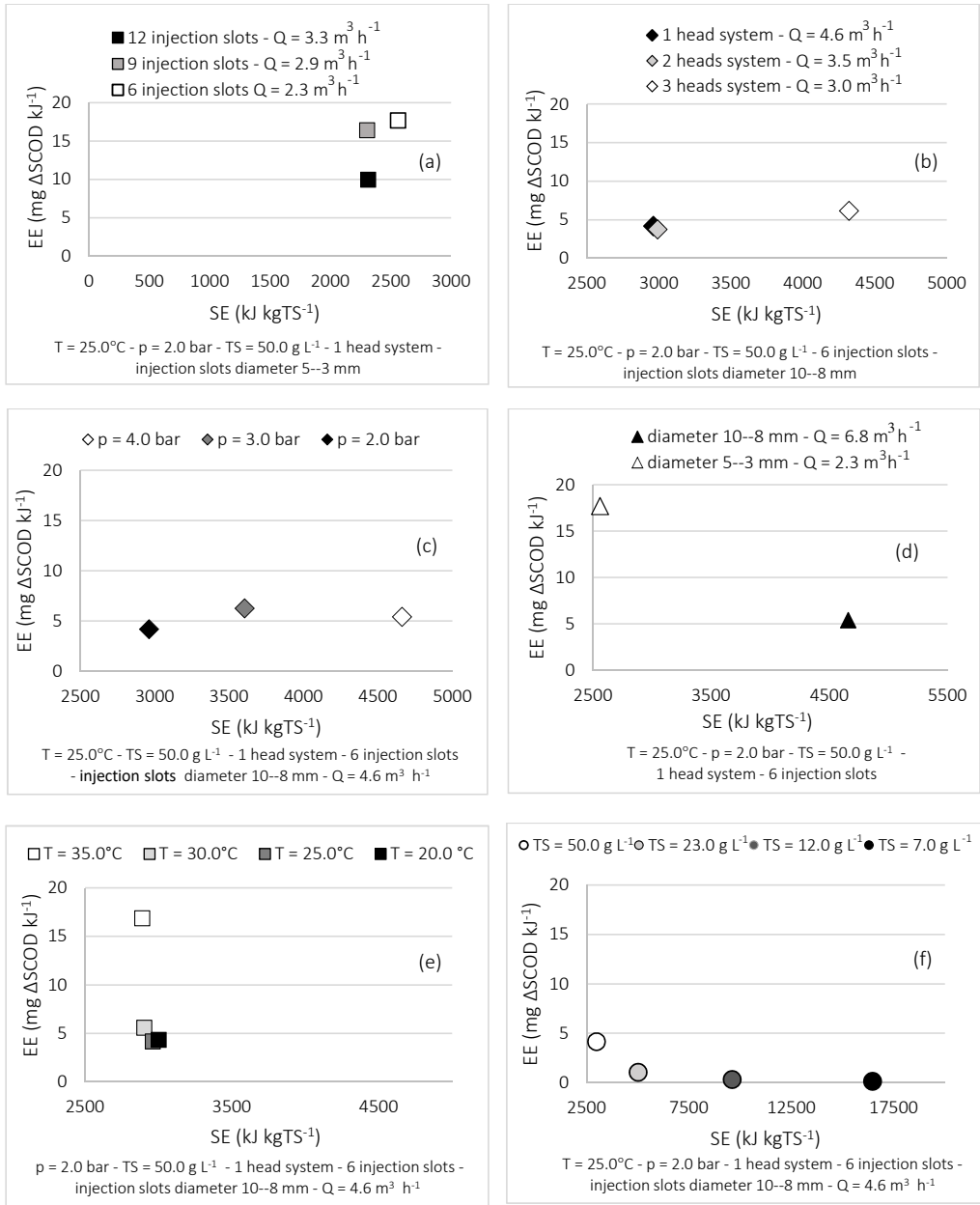


Fig. 39- Energy efficiency vs Specific supplied energy: (a) injection slots number; (b) Ecowirl heads number; (c) inlet pressure; (d) injection slots diameter; (e) temperature; (f) TS content.

3.6. Effect of supplied energy

An 8-h HC experiment was performed considering a combination of optimal parameters values as defined above, in order to evaluate the HC efficiency as function of the specific supplied energy. Thus,

a HC test was carried out with activated sludge containing 50.0 gTS L⁻¹, using the three-heads system at 35.0 °C and 4.0 bar. *Table 6* summarizes the results obtained from the HC 8 h-experiment.

Table 6 - HC 8h-optimized test.

HC time (h)	T (°C)	P inlet (bar)	Flow rate (m ³ h ⁻¹)	TS (g L ⁻¹)	TCOD (mg L ⁻¹)	SCOD (mg L ⁻¹)	SCOD _{bio} (mg L ⁻¹)	SCOD _{bio} (%)
0	35.0	4.0	4.1	50.0	46,423	244	156	64
2	35.0	4.0	4.1	50.0	44,371	1719	1293	75
4	35.0	4.0	4.1	50.0	43,200	2693	2006	68
8	35.0	4.0	4.1	50.0	41,327	4578	2236	49

HC time (h)	b _H	ΔSCOD (mg L ⁻¹)	DD _{PCOD} (%)	DD _{COD NaOH} (%)	DD _N (%)	Absorbed power (W)	SE (kJ kg TS ⁻¹)	EE (mg ΔSCOD kJ ⁻¹)
0	0.31	0	0.0	0.0	0.0	0.0	0	0.0
2	0.34	1475	6.5	4.6	6.4	1,137.5	3276*	9.0*
4	0.62	2449	10.8	7.7	8.4	2,237.5	6444	7.6
8	0.92	4334	19.2	13.6	16.4	4,437.5	12,780	6.8

n. 6 injection slots; injection slots diameter = 10–8 mm; three-heads system.
 * Calculations reported in Appendix B.

The disintegration degree and the values of SCOD before and after HC treatment are shown in *Fig. 40*. The increase in treatment time enhanced the amount of organic substance solubilized, starting from an initial mean value of SCOD of 244 mg L⁻¹ (SCOD₀) to a final value of 4578 mg L⁻¹ (SCOD_{8h}). At 4 h and 8 h of treatment, the increase of soluble chemical oxygen demand (SCOD_t – SCOD₀) was 1.7 and 2.9 time higher than the value measured after 2 h of treatment.

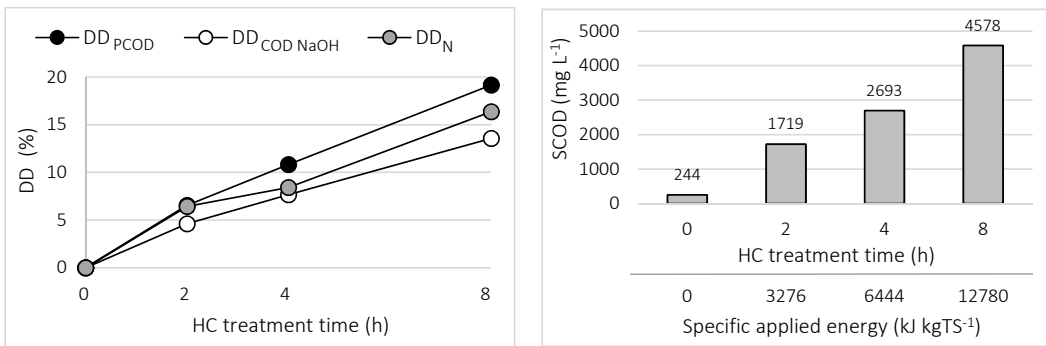


Fig. 40 - HC 8h-experiment – Effect of applied energy on DD and SCOD (volume 50.0 L; initial pH 6.8; temperature 35.0 ± 1.0 °C; TS content 50.0 g L⁻¹; inlet pressure 4.0 bar; 6 injection slots; 3 Ecowirl heads).

SCOD increased with the treatment time and, thus, with the specific supplied energy. For example, when HC time was 2, 4 and 8 h, the specific supplied energy was 3,276, 6,444 and 12,780 kJ kgTS⁻¹, while DD_{PCOD} values were 6.5, 10.8 and 19.2%, respectively.

Organic matter disintegration degree versus duration of HC treatment had a pseudo-linear trend. A similar trend also emerged by looking at DD_N . During the HC experiment, also ammonia concentrations increased. Nitrogen is mainly in proteins or amino acids. The increase in ammonia concentrations showed that proteins were made soluble and degraded, which confirms, that HC has a permanent effect on the sludge, while the SCOD indicates the level of disintegration, which is important for biodegradability evaluations. Interestingly, the Ecowirl reactor caused an increase of the pH in the bulk solution (data not showed), mainly due to the CO_2 stripping as consequence of high temperature and high turbulence. The increase in pH shifted the equilibrium towards ammonia rather than ammonium that may volatilize. However, further researches are needed to study the fate of nitrogen solubilisation, investigating the nitrogen mineralization and ammonia volatilization.

Absorbed power rating of the pump decreased with the treatment time, starting from an initial value of 1400 W at the beginning of the HC test to a final value of 1100 W after 8 h of HC treatment. This result was obtained by decreasing the frequency of the pump inverter in order to keep constant the inlet pressure value. Indeed, increasing the treatment time, a tendency of inlet pressure to increase was observed. This could be explained by a progressive alteration of the rheology of the sludge resulting in a decrease of the viscosity of the sludge during the HC treatment, as consequence of the disruption of cell or microbial flocs.

The increase in HC efficiency with the specific supplied energy found in this study agrees with other works on AC and HC. In particular, working with specific supplied energy lower than $15,000 \text{ kJ kgTS}^{-1}$, similar sludge disintegration degree were obtained by using a Venturi tube [15], a high-pressure jet device [14] and sonolysis [123,134].

Using AC, Delmas et al. [30] proved that it was possible to achieve greater efficiencies in terms of DD (about from 5% to 25%), but their acoustic cavitation system required much more energy supplied (about from 5,000 to 50,000 kJ kgTS^{-1}) than a conventional HC system. This is in accordance with the studies by Le et al. [151], where the authors measured the higher DD (30%) at $75,000 \text{ kJ kgTS}^{-1}$. Similarly, Kidak et al. [152] reached the maximum AC efficiency in terms of DD applying a specific powers of about $80,000 \text{ kJ kgTS}^{-1}$.

Though the highest specific supplied energy (SE) had the greatest SCOD increase, the energy efficiency (EE) did not improve with the power input. In order to consider both sludge characteristics and lysis efficiency, the EE was calculated during the 8-h experiment. From *Fig. 41*, it can be seen that the higher EE corresponded to the lower SE. This may be related to the fact that the HC sludge treatment might be divided into two stages of disintegration, the first stage requiring lower energy

than the second one: in the first stage of HC the structure of sludge flocs would be disintegrated and organic matter contained in the flocs can be dissolved, increasing the SCOD, while in the subsequent stage, cells can be damaged by HC cavitation, releasing intracellular organic matter, but requiring a higher energy consumption than the first stage.

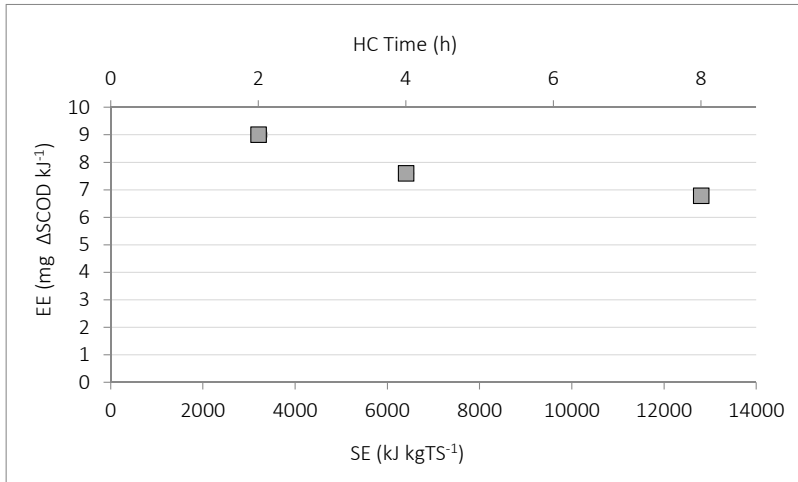


Fig. 41 - Energy efficiency vs Specific supplied energy.

3.7. Effect of HC on biodegradability of treated sludge

HC induces shear forces that break down bacterial cell walls and release the intracellular substances into aqueous phase resulting in an increase in the sludge solubilisation as well as in an enhancement of the biodegradability of the treated sludge. In this study, for the first time, respirometric tests were carried out in order to prove the increase in aerobic biodegradability due to the HC treatment. Respirometric tests were performed for HC 8 h-experiment. Fig. 42 shows four respirograms obtained from the filtrate of the samples collected at 0, 2, 4 and 8 h, where the sample at t = 0 h denotes the untreated sludge.

As can be seen from Fig. 42, HC treatment leads to an increase in the value of the area under the OUR curve, resulting in a progressive increase of the SCOD_{bio}, with the elapsed time and, thus, with the increase of the specific supplied energy. Results are summarized in Table 6. These results agree with those on SCOD (Table 6). The SCOD_{bio}/SCOD ratio was always in the range of 50-75%. Due to the increase in aerobic biodegradability, HC system might be applied to excess activated sludge in order to provide an organic carbon source for denitrification process in conventional activated sludge systems.

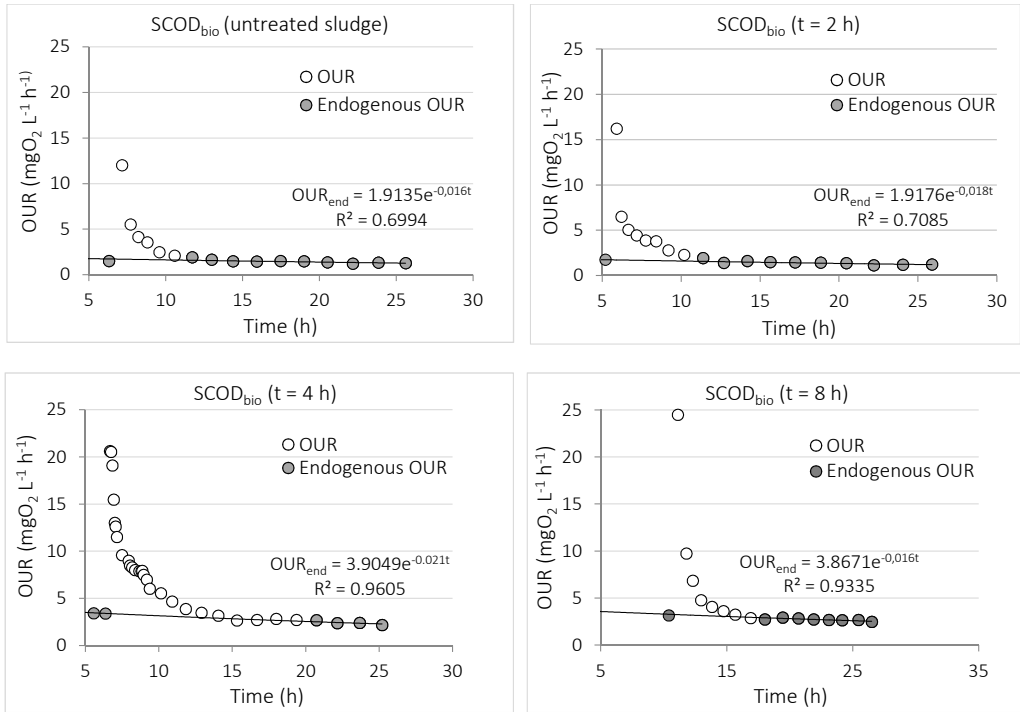


Fig. 42- Respirogram 1: filtered untreated sludge (time 0 h); Respirogram 2: filtered treated sludge after 2 h of HC; Respirogram 3: filtered treated sludge after 4 h of HC; Respirogram 4: filtered treated sludge after 8 h of HC; (volume 50.0 L; initial TS content 50.0 g L⁻¹; initial pH 6.8; inlet pressure 4.0 bar; initial temperature 35.0 ± 1.0 °C; 3 Ecowirl heads in series).

3.8. Effect of HC on microbial activity

Cell inactivation was evaluated estimating the decay rate of aerobic heterotrophic bacteria. Respirometric tests were carried out on the untreated and treated sludge collected by HC tests after 0, 2, 4 and 8 h. By plotting the OUR curve vs time, two phases could be distinguished in the graphs (Fig. 43). The phase 1 was characterized by a rapid OUR decrease that lasts for about 10 h using the untreated sludge and for more than 20 h using the HC treated sludge, due to the produced biodegradable compounds. The phase 2, that shows for 40 h a true exponential decrease of the endogenous respiration rate, directly followed it.

The decay rate was estimated as the slope of the exponential interpolation function in the phase 2 (Fig. 43). The quality of the experiments are mostly expressed in terms of R² with respect to the fitted data. Thereby it is common practice to consider acceptable R² values higher than 0.90.

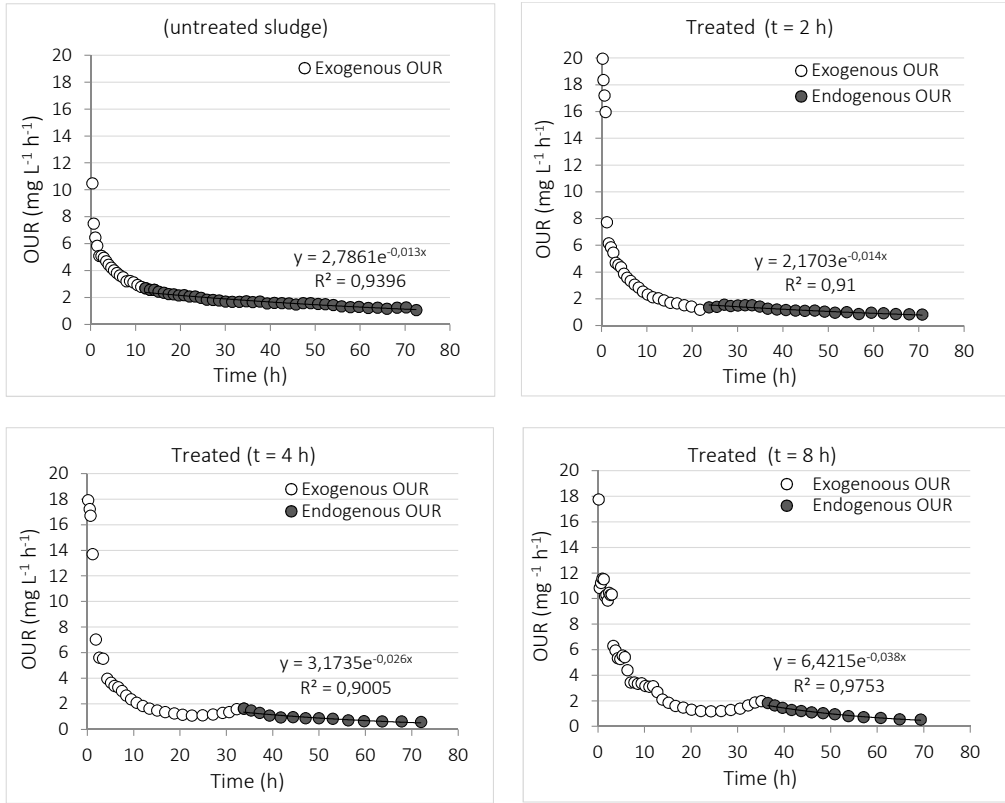


Fig. 43- OUR profiles. 1: untreated sludge (time 0 h); 2: treated sludge after 2 h of HC; 3: treated sludge after 4 h of HC; 4: treated sludge after 8 h of HC; (volume 50.0 L; initial TS content 50.0 g L^{-1} ; initial pH 6.8; inlet pressure 4.0 bar; initial temperature 35.0 ± 1.0 °C; 3 Ecowirl heads in series).

The obtained value of the untreated sludge ($b_H = 0.31\text{d}^{-1}$) was in the wide range reported in other studies for heterotrophic biomass ($0.059 - 0.500 \text{d}^{-1}$) [154]. Treating the activated sludge by HC treatment, the b_H values increased from 0.34d^{-1} to 0.91d^{-1} passing from 2 h to 8 h, respectively, thus indicating a decreasing biomass viability. Applying a specific supplied energy of $3,276 \text{kJ kgTS}^{-1}$ (2 h of HC treatment), the b_H was almost equal to that of the untreated sludge, thus showing that low specific supplied energy could only change the floc structure and may release extracellular polymeric substances (EPS), while microorganisms were not destroyed.

On the contrary, at $6,444$ and $12,780 \text{kJ kgTS}^{-1}$ (4 h and 8 h, respectively), the respirometric functions of the heterotrophic biomass were compromised, as consequence of dead cells (reduced activity) and/or disrupted cells (cell lysis). Some authors reported that in an AC system working at SE values higher than $26,000 \text{kJ kgTS}^{-1}$ [155], the disruption of microorganisms and the consequent lysis caused an increase in the concentration of soluble COD in sludge and the enhancement of biodegradability.

4. Conclusions

The present study provided interesting results about the effect of HC treatment on sludge disintegration and aerobic biodegradability. The main findings of the investigation can be summarized as follows:

- HC treatment was more efficient in terms of sludge solubilisation at higher temperatures of the HC process (up to 35.0 °C);
- Increasing the inlet pressure an acceleration in sludge disintegration was observed. Indeed, higher inlet pressures involved higher flow rate and flow velocity, increasing turbulence level and local pressure oscillations. Furthermore, higher inlet pressures involved higher pressure drops through the HC device, resulting in higher shear forces that break down bacterial cell walls and release the intracellular substances into aqueous phase;
- Comparing different sludge solid concentrations, higher values of Δ SCOD and DD were observed for the highest TS content tested, 50.0 g L⁻¹;
- In order to maximize the efficiency of HC process, different geometric configurations of the modified swirling jet induced HC reactor (Ecowirl reactor) were investigated. It was possible to observe that the geometry of the cavitating device can deeply influence the intensity of the cavitation and then the disintegration of the sludge in terms of COD and Nitrogen solubilisation. For Ecowirl reactor configurations in which the injection slots diameters were decreased, keeping constant both the injection slots number and the inlet pressure values, it was possible to observe an increase in flow rate that caused an increase in intensity of the cavitation. The same result was observed reducing the injection slots number, keeping constant both the injection slots number and the inlet pressure value. Moreover, an increase in efficiency of the HC process was also achieved combing three Ecowirl heads in series;
- A series of respirometric showed that the sludge pre-treatment by using the HC treatment process might be divided into two stages: sludge flocs were changed and disintegrated firstly, and then the exposed cells were disrupted or damaged. At the first stage, organic matter contained in the flocs was dissolved and SCOD increased. At the second stage, some cells were damaged/disrupted by HC cavitation, requiring a higher energy consumption than the first stage in order to damage the cell membrane and completely disrupt it. The intracellular organic matter was released, which resulted in a further increase of SCOD and a decrease of microbial activity.

Among possible applications, the HC experiments conducted in this study indicate that the excess activated sludge can be available as carbon source for biological processes in WWTP, such as denitrification process. Alternatively, HC could be applied as a pre-treatment for anaerobic digestion, in order to increase the biogas production. However, further studies on the anaerobic biodegradability are needed. The HC treatment could be applied either at high SE as a side-stream treatment or at low SE as an in-line treatment in biological tanks.

Moreover, although the effectiveness of Ecowirl reactor was already experimentally proved in this study, authors are developing a mathematical model in order to both understand the fluid dynamics inside the modified swirling jet induced HC reactor and optimize the geometry of this device with the main goal of enhancing the HC efficiencies, resulting in a decrease of the energy consumption.

Chapter 4

Experimental and numerical investigation on performance of a swirling jet-induced reactor

Chapter 4

Experimental and numerical investigation on performance of a swirling jet-induced reactor

Giuseppe Mancuso ^a, Michela Langone ^a, Jana Jablonská ^b, Gianni Andreottola ^a, Milada Kozubková ^b

^a *Department of Civil, Environmental and Mechanical Engineering, University of Trento, via Mesiano 77, 38123, Italy*

^b *Department of Hydrodynamics and Hydraulic Equipment, VŠB - Technical University of Ostrava, 17. Listopadu 2172/15, 70800, Ostrava, Czech Republic*

Abstract

In this work, a three-dimensional Computational Fluid Dynamic (CFD) analysis of a swirling jet-induced reactor was implemented in order to gain a better understanding of the fluid dynamics into the hydrodynamic cavitation (HC) reactor and to investigate the effect of reactor geometry on flow velocity and flow pressure distributions. Firstly, using the swirling jet-induced reactor, experimental tests were performed at 0.25 bar and 2.0 bar, in order to have flow cavitating and non-cavitating conditions, respectively and to collect inlet flow rate and outlet flow pressure to use as boundary conditions in the mathematical model. Secondly, a two-phase mathematical model was defined. For the non-cavitating flow, the results of the numerical computations were in good agreement with the experimental data, showing a rotating flow around the swirling jet-induced reactor central axis and at the exit of the double cone. The highest flow velocities and flow pressure drops were observed in reactor geometry with the smallest injection slots diameters. In cavitating flow, a similar flow behaviour in the swirling jet-induced reactor was observed. However, a discrepancy between the cavitating model and the experimental data did not allowed modelling the HC process, maybe caused by a lack of grid density in the meshed fluid domain and/or an inclusion of some incorrect information in the cavitating model. Furthermore, cavitation noise that is generated during flow through the swirling jet-induced reactor was measured at different values of the inlet flow pressure, allowing getting the onset of cavitation and supercavitation into the swirling jet-induced reactor.

Keywords: Hydrodynamic cavitation, Swirling jet-induced cavitation, ANSYS, Computational Fluid Dynamics, Modelling

1. Introduction

In the past, many studies were carried out with the main aim of preventing the generation of cavitation in hydraulic machinery such as pumps, turbines or valves [1,5,6]. HC is specific multiphase flow of gases and liquid. If the pressure of mixture is equal to the saturated pressure, the vapour cavitation occurs. In case of pressure lower than atmospheric pressure, the air can be observed due

to the release from the liquid. The mixture is then considered as the mixture of liquid, vapour and air [156]. The prevention of HC is an important concern in order to avoid severe damage due to the negative effects of cavitation such as erosions, vibrations and noises, [1,5]. On the contrary, in recent years there is an increasing interest in using HC process in various important applications, especially in the field of environmental protection, [8,9,58,157]. In order to cope with a decrease in available water resources worldwide, an increasing demand of drinkable water by population and the more restrictive environmental legislations on water quality, cavitation has come to be increasingly applied as innovative technique in the field of wastewaters treatment, [158]. Due to its elevated oxidative capability, linked to its ability of generating highly reactive free radicals and thermal hot spots [34,48], cavitation process was used to treat the increasing presence of bio-refractory, toxic or carcinogenic molecules and pathogens in wastewater streams.

Recently, a novel swirling jet-induced reactor, named Ecowirl (patented by Econovation GmbH, Germany and commercialized and optimized by Officine Parisi S.R.L., Italy), was successfully used by our research group in order to degrade a toxic and carcinogenic dye (Rhodamine B, RhB) from waste aqueous solutions [8], and to increase the activated sludge solubilisation and the aerobic sludge biodegradability in wastewater treatment plants [9,158]. Based on our experimental results, it was observed that in the studied swirling jet-induced reactor some parameters and operative conditions such as fluid temperature, type of fluid, geometry of the cavitating device, flow rate, flow velocity and flow pressure can deeply influence the intensity of cavitation and the way in which it is generated, [8,9]. Although the effectiveness of the swirling jet-induced reactor was experimentally proved, some difficulties such as proper measurements of flow velocity and flow pressure into the complex geometry of the reactor as well as the need of a better understanding of the fluid dynamics into the reactor in turbulent and cavitating conditions have highlighted the fact that a three-dimensional computational fluid dynamic CFD analysis was necessary.

Many researchers focused on the mathematical modelling of different HC devices such as orifice plates, nozzles, Venturi, swirling jet or rotor-stator systems. Numerical investigations were conducted to predict cavitation and to determine whether computational methods can be used as a reliable tool to evaluate the performance characteristics of cavitating devices. However, the definition of a mathematical problem can be difficult because it can include very complex geometries of HC devices in addition to turbulent flows and cavitating conditions.

Palau-Salvador et al. [84] performed numerical predictions of cavitation flows based on CFD for simple geometries, such as orifices, nozzles and Venturi systems, using the commercial CFD code FLUENT 6.1.

Navickas and Chen [85] studied cavitating Venturi internal flow characteristics by means of the FLOW-3D three-dimensional fluid flow program. Their results indicated that numerical methods are effective in obtaining relative magnitudes of significant parameters affecting the performance of the cavitating device. In order to optimize a multi-hole injector nozzle, He et al. [86] modelled the three-dimensional nature of the nozzle flow investigating on the effect of the geometry and dynamics factors on the spray characteristics in turbulent and cavitating conditions. Müller et Kleiser [87] developed a numerical method for the vortex breakdown in a compressible swirling jet non-cavitating flow. Ashrafizadeh and Ghassemi [88] performed an experimental and numerical investigation on the performance of small-sized cavitating Venturi. Badve et al. [63] made a mathematical model describing the shear rate and pressure variation in a complex flow field created in a rotor-stator type HC reactor.

In this work, numerical modelling simulations were implemented by means of a CFD software (ANSYS 16.2) with the main purpose to gain a better understanding of the fluid dynamics into the swirling jet-induced reactor studied by our research group and, further, to optimize this new technology in terms of design and operative conditions.

2. Materials and Methods

In order to widen the knowledge of the HC process into the studied swirling jet-induced reactor and validate the mathematical model with experimental data, a series of tests was performed as reported in following sub-sections.

2.1. Experimental setup

Fig. 44 shows a schematic representation of the experimental setup used in the present work. It was a closed hydraulic loop and it consisted of (1) a feed tank filled with tap water, (2) a mono screw pump (3.0 kW, Netzsch Pumps & Systems GmbH Germany), (3) an inverter (Bonfiglioli Vectron- Active) to adjust the number of pump revolutions; (4) a flow-meter (G2 Stainless Steel Industrial Flowmeters, Great Plains Industries, Inc.); (5) a cavitating device (Ecowirl reactor); (6) a frequency-meter (PCE-VT 2700); three pressure transducers (Afriso) to measure the inlet (P1), the outlet (P2) and the vacuum (P3) pressure, respectively.

Fig. 45 shows a schematic representation of geometry of the studied swirling jet-induced reactor, in which HC is generated by using a multi-dimensional vortices generator, consisting of a frustum-conical pre-swirling chamber (2) preceded by another chamber (1) where are located six injection slots (*Fig.*

45, cross section A-A) through which the flow enters generating a vacuum-core vortex (4) and a double cone chamber (3) where a triangular plate (Fig. 45, cross section B-B) is placed and in which the flow impacts generating cavitation [8,9].

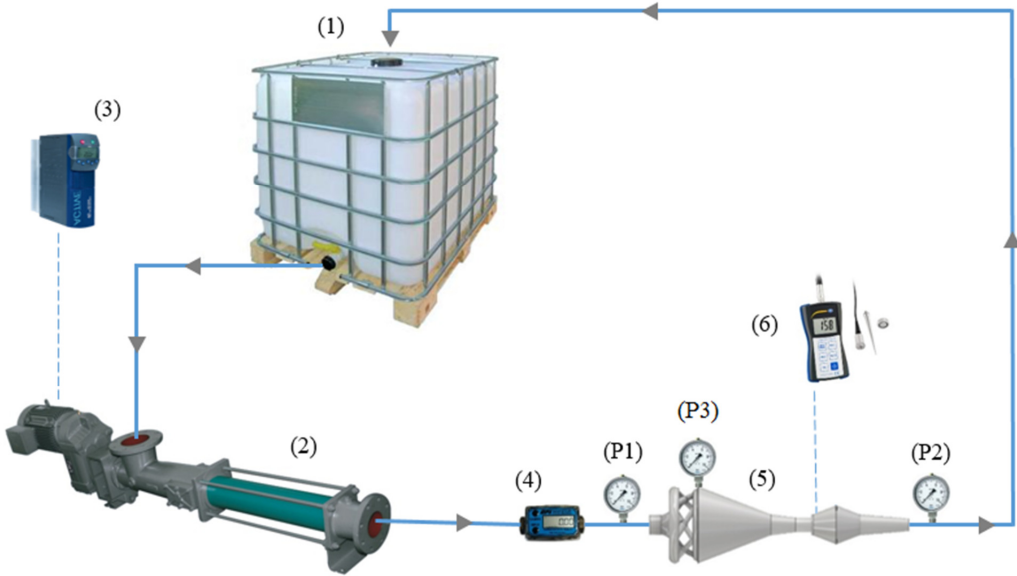


Fig. 44- Schematic representation of the experimental setup: (1) Feed water tank; (2) Mono screw pump; (3) Inverter; (4) Flow-meter; (5) Cavitating device (Ecowirl reactor); (6) Frequency-meter; (P1), (P2), (P3) Upstream, downstream and vacuum pressure transducers.

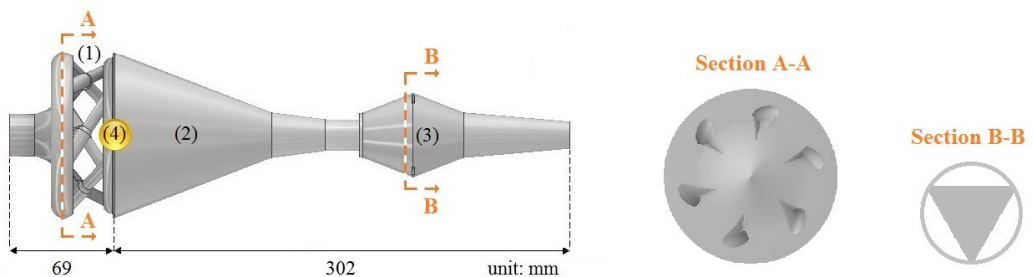


Fig. 45- Schematic representation of geometry of the studied swirling jet reactor.

2.2. Experimental tests

A feed tank of volume of 1,000 L was filled with tap water at environment temperature. Water flow was pumped through the swirling jet-induced reactor by using the mono screw pump. The inverter was used to control the pump flow rate (on the range of 0.5 - 6.0 m³ h⁻¹) and the inlet pressure (about 0.25- 10.0 bar) of the water flow by adjusting the frequency. The methods included flow rate, flow

pressure and cavitation noise measurements. The flow-meter allowed measuring the water flow rate prior to the swirling jet-induced reactor. Upstream, downstream and vacuum-core vortex pressures were measured by using pressure transducers. Cavitation noise measurements were made by using the frequency-meter. Then the water was discharged again back into the feed tank.

Fluid dynamics into the swirling jet-induced reactor was analysed in non-cavitating and cavitating flows. Based on results of our previous experimental tests [8,9] and on negative pressures measurements in the swirling jet-induced reactor vacuum zone (*Fig. 44 (P3)*, *Fig. 45 (4)* and *Table 7*), the presence of HC at inlet pressure higher than 2 bar was assumed.

Table 7 - Parameters and operative conditions for different Ecowirl injection slots diameters.

Upstream diameter	Configuration	Φ Upstream	Φ Upstream	Presence	Inlet	Vacuum	Outlet	Flow
		injection slots	injection slots					
		(mm)	(mm)		(bar)	(bar)	(bar)	(m ³ h ⁻¹)
	EW1	10	8	No	0.25	0.00	0.00	1.38
				Yes	2.00	-0.55	0.45	4.57
				Yes	3.00	-0.65	0.68	5.59
				Yes	4.00	-0.78	0.88	6.57
	EW2	5	3	No	0.25	0.00	0.00	0.21
				Yes	2.00	-0.60	0.00	1.67
				Yes	3.00	-0.80	0.10	2.02
				Yes	4.00	-0.85	0.1	2.33

2.3. Reactor geometrical configurations

In this study, two different geometric configurations of the swirling jet-induced reactor were taken into account by varying the diameters of the six injection slots (*Fig. 45 (1)* and section A-A). In the studied swirling jet-induced reactor, injection slots were characterized by different upstream and downstream diameters: configurations EW1 (10 mm upstream- 8 mm downstream) and EW2 (5 mm upstream- 3 mm downstream) were used, respectively (*Table 7*).

Firstly, the comparison between the two reactor configurations, EW1 and EW2, was carried out considering a non-cavitating flow at the same inlet flow pressure of 0.25 bar. Then, an inlet flow pressures of 2 bar was used in order to generate HC in the flow. Reducing the injection slots diameters while keeping constant the inlet flow pressure, from configuration EW1 to configuration EW2, a decrease in both flow rate and outlet flow pressure was measured. Detailed information of operative conditions and parameters is reported in *Table 7*.

2.4. Cavitation noise measurements

Cavitation noise measurements were performed by means of a frequency-meter (PCE-VT 2700)

placed on the external surface at the entrance of the HC reactor double cone, *Fig. 44*. In this region, it is mainly expected to take place cavitation process, resulting in subsequent noise generation. As the sound probe also received signals from pump's motor, it was necessary to reject the signal from motor's site. Tests were carried out using the two different swirling jet-induced reactor configurations, EW1 and EW2, in cavitating flows at inlet pressure of 2.0, 3.0 and 4.0 bar. Fast Fourier Transform (FFT) analysis was performed on the collected data in order to identify main noise frequencies [156,159].

2.5. Numerical simulations

A numerical approach was employed in order to investigate the fluid dynamics in the swirling jet-induced reactor in non-cavitating and cavitating flows as well as the effect of the reactor geometry on the flow velocity and flow pressure distributions into the reactor.

Based on experimental investigations, CFD simulations were performed by means of ANSYS FLUENT 16.2 software. First, only water phase was considered in the model. Then, since the flow through the swirling jet-induced reactor is a multiphase fluid, the mixture multiphase approach was employed. The primary phase was defined as liquid water, while the other phases can be vapour and air.

ANSYS software incorporates a 3D pressure-based solver and calculates the equations in transient-state conditions. The flow pressure distribution in the swirling jet-induced reactor is governed by Reynolds equation, which is derived from Navier-Stokes continuity and momentum equations.

Fluid flow is based on mass and momentum transfer described by continuity equation and Navier-Stokes equations, which are valid for all types of flows. The general mass conservation equation for compressible as well as incompressible flow is given as:

$$\frac{\partial \rho}{\partial t} + \Delta(\rho \cdot \vec{v}) = 0 \quad \text{Eq. 17}$$

where ρ is the fluid density, \vec{v} the fluid velocity vector and t the time.

The momentum equation is:

$$\frac{\partial \rho}{\partial t} (\rho \cdot \vec{v}) + \nabla(\rho \cdot \vec{v} \cdot \vec{v}) = \nabla P + \nabla(\vec{\tau}) + \rho \cdot \vec{g} + \vec{F} \quad \text{Eq. 18}$$

where t is the time, ρ the fluid density, \vec{v} the fluid velocity vector, P the static pressure, τ the stress tensor (given in *Eq. 19* below), \vec{g} the gravity acceleration vector and \vec{F} the external body force vector.

The stress tensor is written as:

$$\bar{\tau} = \mu \left[(\nabla \cdot \vec{v} + \nabla \cdot \vec{v}^T) - \frac{2}{3} \nabla \times \vec{v} \cdot \mathbf{I} \right] \quad \text{Eq. 19}$$

where, μ is the fluid viscosity, \mathbf{I} the unit tensor and the second term on right hand side is effect of volume dilation.

The flow in the swirling jet-induced reactor was classified as turbulent flow. In this case, the Reynolds equations were derived from Navier Stokes equations using Reynolds time averaging method. The k- ϵ RNG (Re-Normalisation Group) model was chosen as turbulence model to simulate time averaging flow characteristics for turbulent flow conditions. It is a two equations model that gives a general description of turbulence by means of two transport equations. In this model, variable k (turbulent kinetic energy) represents the energy in turbulence, while variable ϵ (turbulent dissipation) is the rate of dissipation of the turbulent kinetic energy. The gravity can be taken into account too. The above-defined system of fluid flow with cavitation is extended by mass transfer equation for each phase, i.e. vapour phase or air phase. The system of equations is supplemented by boundary conditions (mass flow rate of water and gases, pressure, turbulent quantities). For other investigation the LES turbulent model of high quality will be used, which can model the big eddy turbulent vortices.

2.5.1. Reactor model and boundary conditions

The swirling jet-induced reactor geometry was made by means of Autodesk Inventor Professional 2017 software, *Fig. 46*.

Fluid domain was meshed in ANSYS-FLUENT (*Fig. 47*) by means of a simple grid system, which mainly consisted of tetrahedral cells except for the region near the body surface, for which prismatic cells were used for resolving the boundary layer.

The Navier Stokes equations were solved using 3D double precision pressure based on transient state analysis. As the Reynolds number was high ($Re = 30,305$ at 20°C and $4.57 \text{ m}^3 \text{ h}^{-1}$, reactor configuration reactor EW1), turbulent flow conditions were assumed. Elements size were varied from 0.2 to 0.4 mm, giving a total number of elements 1,172,616. The heights of the cells near the wall of the swirling jet-induced reactor were set to values depending on dimensionless y plus parameter (wall distance) varied between 8 and 50.

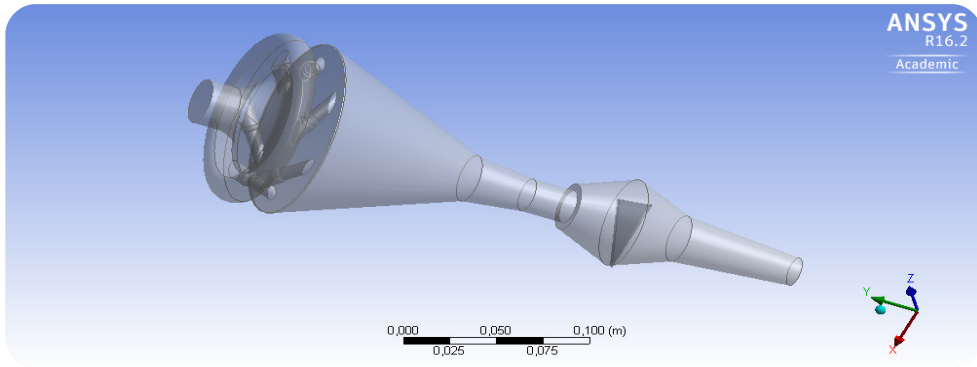


Fig. 46- Swirling jet-induced reactor fluid geometry.

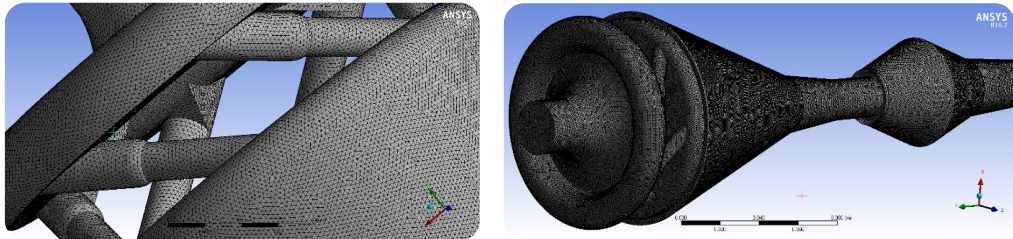


Fig. 47- Swirling jet-induced reactor fluid domain.

As boundary conditions, the flow rate [kg sec^{-1}] was imposed at inlet of the HC system and the relative static pressure [bar] was given at outlet. These parameters were known from the experimental investigation. In order to validate the model, the inlet flow pressure provided by numerical simulations were compared to experimental results.

Next, the dissolved air was taken into consideration. The mass flow of the air was set to the value, which allows obtaining pressure at inlet close to the experimentally measured one.

In this study, due to the high volume of water used in experimental tests as well as to the short treatment time, temperature effects were neglected.

After choosing the turbulence model and defining boundary conditions, calculations with smaller time step ($\Delta t = 10^{-5}$ sec) with data saving from monitor points were carried out.

3. Results

A three-dimensional analysis was firstly used to analyse the fluid dynamics into the swirling jet-induced reactor in the non-cavitating case, for which a very low inlet flow pressure was set. The effects

of reactor geometry on flow velocity and flow pressure distributions were investigated. Then, the three-dimensional model was used to investigate the effect of reactor geometry on flow velocity and flow pressure distributions in cavitating conditions at higher inlet flow pressures. Based on experimental observations, results of numerical simulations on flow velocity and flow pressure distributions allowed identifying the areas where it is supposed that HC mainly occurs. Finally, cavitation noise measurements were carried out in order to investigate on the intensity of cavitation.

3.1. Non-cavitating model

3.1.1. Fluid dynamics

CFD simulations were performed for each of the two different reactor configurations EW1 and EW2 (*Table 7*) at the same inlet flow pressure of 0.25 bar (relative value). Based on experimental tests, this value of flow inlet pressure was chosen in order to have a non-cavitating flow. First, only water phase was considered in the mathematical model to get quickly the basic information about pressure distribution. As boundary conditions of the mathematical model, flow rate at inlet and relative static pressure at outlet were included. In order to validate the model, CFD results were compared to the experimental data, taking into account the relative static pressure at inlet. Due to a discrepancy between flow pressures provided by the model and flow pressures experimentally measured (*Table 8*), it was necessary to take into account the dissolved air in the model (two-phase model).

Table 8 - Comparison between experiments and numerical simulations in non-cavitating flow.

Non-cavitating flow	Configuration	Φ Upstream injection slots (mm)	Φ Upstream injection slots (mm)	Inlet pressure (bar)	Vacuum pressure (bar)	Outlet pressure (bar)	Flow rate (m ³ h ⁻¹)
Experiment				0.25	0.00	0.00	1.38
Computation with air	EW1	10	8	0.25	0.00	0.00	1.37
Computation without air				0.13	0.00	0.00	0.85
Experiment				0.25	0.00	0.00	0.21
Computation with air	EW2	5	3	0.25	0.00	0.00	0.20
Computation without air				0.14	0.00	0.00	0.13

The mass flow of the dissolved air was set to $7.0533E^{-05}$ kg sec⁻¹, which allowed obtaining flow pressures close to the experimentally measured one. With this arrangement, the numerical results obtained showed very good agreements with experimental data, showing a discrepancy at the concerned parameters and operative conditions less than 2%. These results were valid for both reactor configurations EW1 and EW2.

Results of numerical simulations on the fluid dynamics into the swirling jet-induced reactor in the

non-cavitating flow showed the same flow behaviour, regardless of the geometrical configuration investigated (EW1 or EW2).

Fig. 48 shows the velocity vectors coloured by velocity magnitude [m sec^{-1}], obtained using the swirling jet-induced reactor configuration EW1. In the frustum-conical pre-swirling chamber, a rotating flow around the swirling jet-induced reactor central axis was observed. It is interesting to note that although the rotating flow impacts on the triangular plate placed perpendicularly to the flow direction in the double cone chamber, the flow continues to be rotating at the exit of the double cone chamber. It might be supposed that the establishment of some small vortex into the fluid after the triangle plate promotes the intensification of the turbulence.

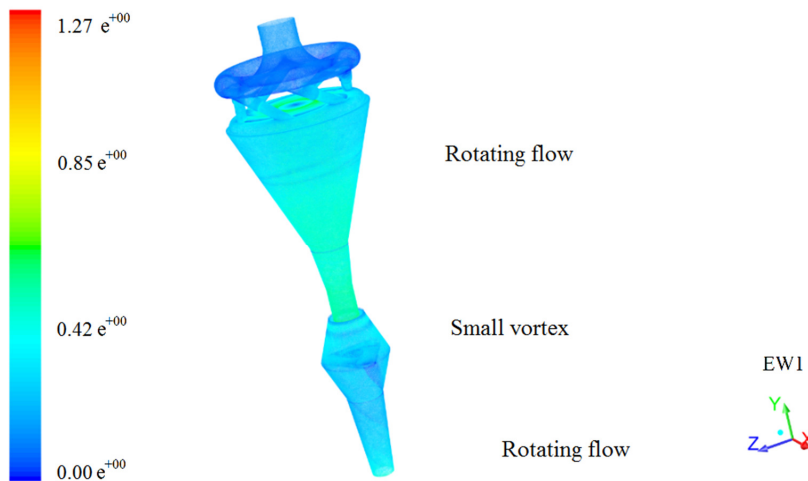


Fig. 48- Swirling jet-induced reactor fluid dynamics: velocity vectors coloured by velocity magnitude [m sec^{-1}], inlet flow pressure 0.25 bar (configuration EW1).

3.1.2. Flow velocity and flow pressure distributions

Results refer to a non-cavitating flow in order to gain a better understanding of the influence of reactor geometry on flow pressure and flow velocity distributions.

Numerical simulations were performed by using reactor configurations EW1 and EW2, respectively.

Fig. 49 shows the results in terms of contours of velocity magnitude [m sec^{-1}] and relative static flow pressure [bar]. Results on flow velocity distributions (*Fig. 49, a and e*) are shown in an axial cross section of the swirling jet-induced reactor, while results on flow pressure distributions are shown both in an axial cross section (*Fig. 49, b and f*) and on the reactor walls (*Fig. 49, c and g*), respectively.

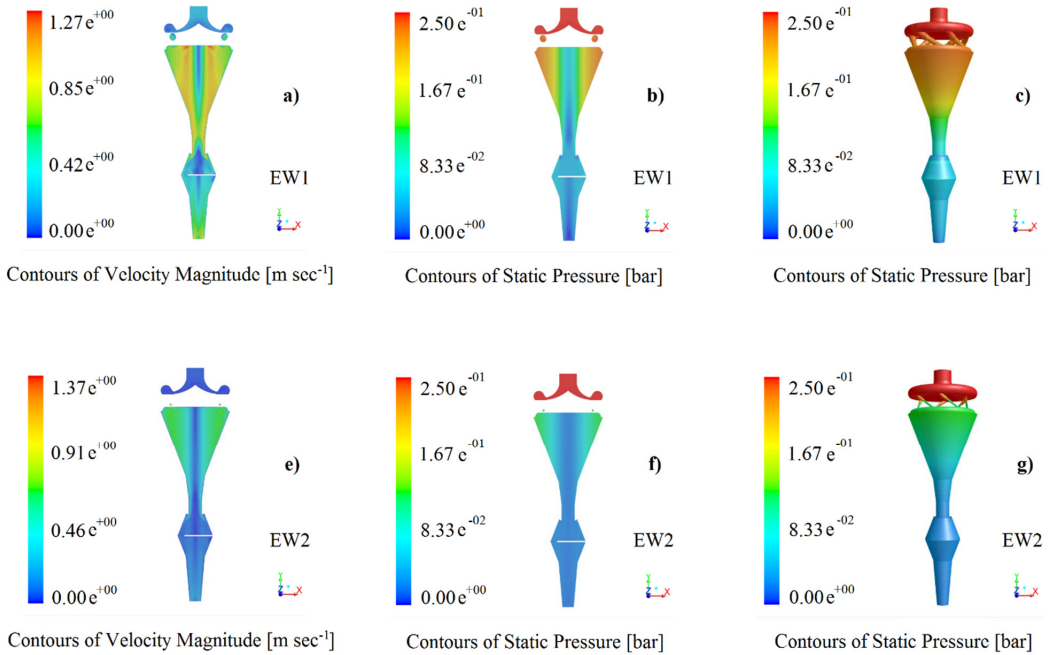


Fig. 49- Contours of velocity magnitude [m sec^{-1}], and static pressure [bar] for configurations EW1 (a, b, c) and EW2 (e, f, g), at inlet flow pressure 0.25 bar. The flow velocity magnitude and the flow static pressure range from blue to red corresponding to low and high flow velocities and flow static pressures, respectively.

As shown in *Fig. 49* and according to the Bernoulli principle, due to the presence of injection slots, in both configurations EW1 and EW2, an increase in flow velocity was observed at the expense of the flow pressure both in the axial cross section and on the reactor walls.

In the frustum-conical pre-swirling chamber, the axial flow velocity was very low in EW1 and EW2 (*Fig. 49, a and e*), whereas flow velocity increased away from the reactor central axis (*Fig. 49, a and e*). In this reactor region, the lowest flow pressures were observed in the zone closest to the central axis. These findings are in accordance with very low flow pressures experimentally measured at the central axis (this study, *Fig. 45 vacuum-core vortex (4)* and *Table 7*).

Moreover, in both configurations EW1 and EW2, an increase in flow velocity and thus a decrease in flow pressure at the entrance of the double cone chamber were observed. The highest flow velocities and the lowest flow pressures in the reactor were observed at the entrance of the double cone chamber.

However, the absence of negative flow pressures in the central axis of the frustum-conical pre-swirling

chamber and a very low-pressure drop between the inlet and the outlet of the injection slots chamber, in both numerical results and experimental measurements, confirmed that HC did not yet occur at the concerned flow inlet pressure of 0.25 bar.

Comparing the two different configurations EW1 and EW2 at the same inlet flow pressure of 0.25 bar, the highest flow velocities and flow pressure drops were observed in reactor geometry with the smallest injection slots diameters, EW2 (*Fig. 49 e, f and g*).

3.2. Cavitating model

Our previous experimental tests proved that a variation in inlet flow pressure and thus in flow rate and flow velocity in the swirling jet-induced reactor can influence the intensity of cavitation [8,9], as implies different pressure drops into the reactor (defined as the difference between the inlet flow pressure upstream to the injection slots chamber and the outlet flow pressure downstream to injection slots chamber), Moreover, increasing the inlet flow pressure, negative flow pressures downstream to the injection slots chamber and generation of cavitating bubbles were experimentally observed [8,9]. Experimental results also proved that the intensity of cavitation can be deeply influenced by the HC reactor geometry [8,9].

Therefore, in order to enhance cavitation effects and then to obtain higher pressure drops in the studied HC reactor, the quantitative understanding of fluid dynamics into the swirling jet-induced reactor is very crucial.

3.2.1. Fluid dynamics

Studying the fluid dynamics into the swirling jet-induced reactor, the inlet flow pressure was increased to 2.0 bar in order to have a cavitating flow into the swirling jet-induced reactor. CFD simulations were performed for each of the two different reactor configurations EW1 and EW2 (*Table 7*) at the same inlet relative pressure of 2.0 bar.

At 2.0 bar inlet flow pressure, the presence of HC was experimentally proved by our previous tests performed to degrade the Rhodamine B in polluted aqueous solutions using reactor configuration EW1 [8] and to solubilize sludge in wastewater streams using both reactor configurations EW1 and EW2 [9]: HC effects were measured in terms of Rhodamine B degradation and sludge solubilisation, respectively. Furthermore, inlet flow pressure of 2.0 bar allowed measuring negative pressures downstream to the injection slots chamber and pressure drops of about 2.55-2.85 bar [8] between the inlet and the outlet of the injection slots chamber (*Table 7*).

Investigating the flow dynamics by using the two configurations EW1 and EW2, the same qualitative flow behaviour between results of numerical simulations at inlet flow pressure of 0.25 bar, *Fig. 48* (non-cavitating flow) and at inlet flow pressure of 2.0 bar, *Fig. 50* (cavitating flow) was observed (see section 3.1.1).

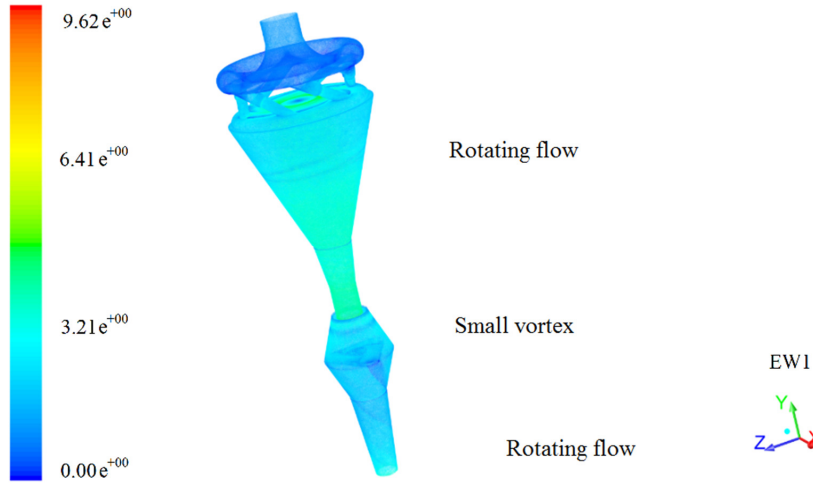


Fig. 50- Swirling jet-induced reactor fluid dynamics: velocity vectors coloured by velocity magnitude [m sec^{-1}], inlet flow pressure 2 bar (configuration EW1).

However, in order to validate the model, CFD results were compared to the experimental data, taking into account the relative static pressure at inlet. As better discussed in the following paragraph on flow velocity and flow pressure distributions, results of numerical simulations did not successfully fit the measured data from the experiments, not achieving cavitating conditions into the swirling jet-induced reactor. In this case, no value of mass flow of dissolved air allowed coping with the discrepancy between flow pressures provided by the model and flow pressures experimentally measured.

3.2.2. Flow velocity and flow pressure distributions

Numerical simulations confirmed that due to the higher inlet flow pressure, higher flow velocities in configurations EW1 and EW2 were obtained at 2.0 bars, *Fig. 51*, as compared with those found at 0.25 bars.

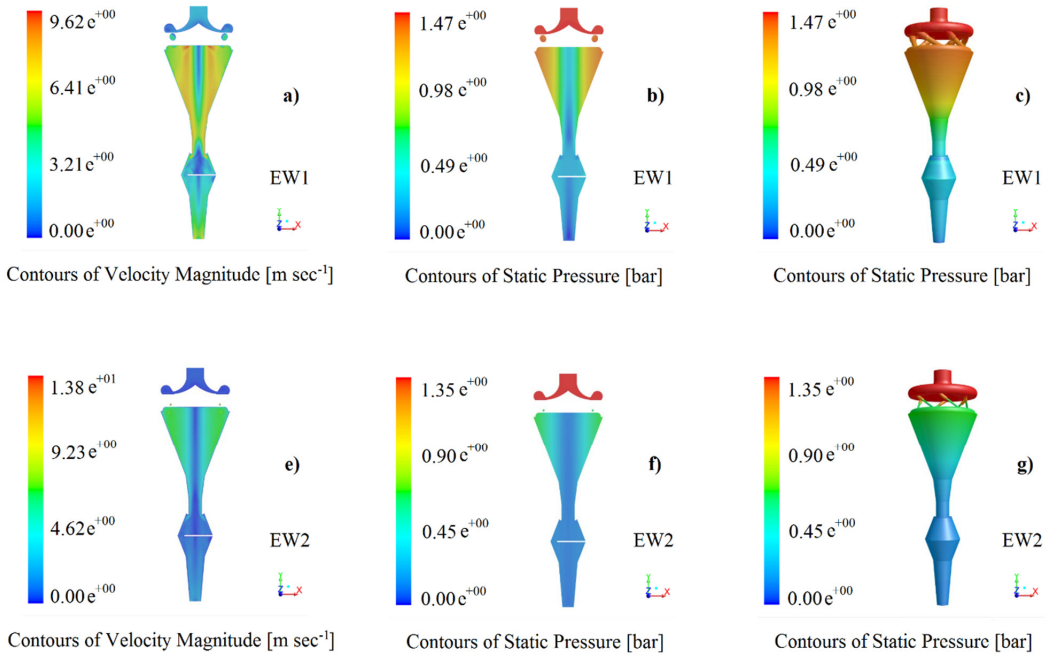


Fig. 51- Contours of velocity magnitude [m sec^{-1}] and static pressure [bar] for configurations EW1 (a, b, c) and EW2 (e, f, g), at inlet flow pressure of 2.0 bar. The flow velocity magnitude and the flow static pressure range from blue to red corresponding to low and high flow velocities and flow static pressures, respectively.

Again, results on flow velocity distributions (Fig. 51, a and e) showed that, in the frustum-conical pre-swirling chamber, the axial flow velocity was very low, whereas flow velocity increased away from the reactor central axis. In this reactor region, the lowest flow pressures were observed in the zone closest to the central axis. These findings are in accordance with very low flow pressures experimentally measured at the central axis (this study, Fig. 45 vacuum-core vortex (4) and Table 7) and with the supposed vacuum-core vortex as defined in previous experimental studies on the swirling jet-induced reactor, [8,9]. Moreover, an increase in flow velocity and thus a decrease in flow pressure at the entrance of the double cone chamber were further observed. Based on these numerical results, it could be supposed that increasing the inlet flow pressure, HC could be mainly observed at the entrance of the double cone chamber.

Comparing the two configurations EW1 and EW2, higher flow velocities and then higher-pressure drops into the HC reactor were observed using the configuration EW2. This result could suggest that increasing the inlet flow pressure until the onset of cavitation, its intensity could be higher in

configuration EW2 than in configuration EW1. This result would be in agreement with previous investigations on the effect geometry of the studied swirling jet-induced reactor on cavitation intensity, where configuration EW2 was more efficient, in terms of COD solubilisation, if compared to configuration EW1 [9].

Numerical simulations did not successfully fit the measured data from the experiments. Results of numerical simulations provided lower values of inlet flow pressure in both configurations EW1 and EW2: 1.47 bar and 1.35 bar, respectively, rather than 2.0 bar. Consequently, flow pressure drops in both configurations EW1 and EW2 were lower if compared to experimental measured data. Furthermore, fixing an inlet pressure of 2.0 bar, results of numerical simulations should have shown negative values of flow pressure in the vacuum-core vortex zone as measured in experimental HC tests, but, as shown in *Fig. 51*, only flow pressures higher than atmospheric pressure were observed. In this case, no value of mass flow of dissolved air allowed obtaining comparable flow pressures between the model and experimental measurements.

These discrepancies between results of numerical simulations and experimental data showed that the model suffers from several assumptions, maybe caused by a lack of grid density in the meshed fluid domain and/or an inclusion of some incorrect information in the two-phase cavitating model. Thus, further studies are needed to better define the cavitating model of the studied swirling jet-induced reactor.

3.2.3. Cavitation noise measurements

Cavitation noise generated by the flow in swirling jet-induced reactor was measured by means of the frequency-meter at 2.0, 3.0, and 4.0 bars. After the numerical simulations, the frequency-meter was installed at the entrance of the double cone chamber where the cavitation intensity was supposed to be higher.

After collecting the data, the FFT analysis was performed to identify main noise frequencies rejecting the signal from motor's site. *Fig. 52* and *Fig. 53* show the results for the two geometric configurations (EW1 and EW2, *Table 7*) at inlet flow pressure of 2.0, 3.0 and 4.0 bar, respectively.

As shown in *Fig. 52* and *Fig. 53*, by using both configurations EW1 and EW2, it was possible to observe two main frequency picks at 3,000 and 5,000 Hz. According to Jablonská and Kozubková [156], it could be explained by the presence of two different cavitation processes: vapour cavitation (5,000 Hz) and air cavitation (3,000 Hz). While in configuration EW1, the highest frequency pick was observed for the frequency of 5,000 Hz, in configuration EW2 the highest frequency pick was observed for the

frequency of 3,000 Hz. This means that in EW1 configuration (higher diameters of injection slots) cavitation was mainly vapour type. On the contrary, in configuration EW2 the dissolved air started to play a more significant role in HC process.

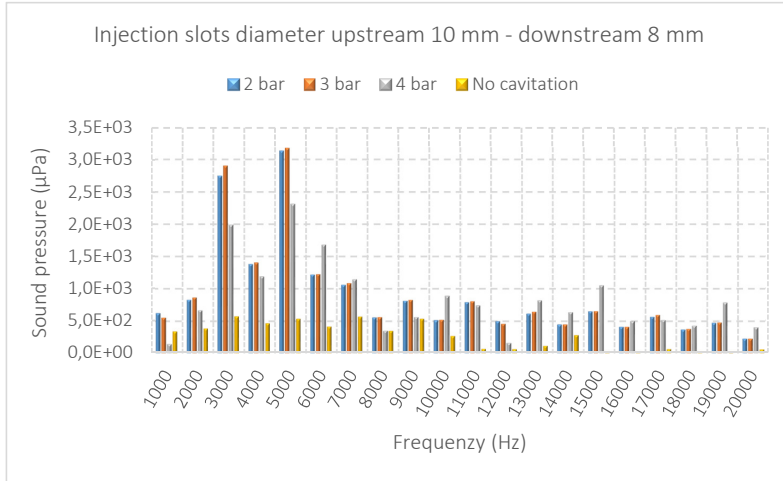


Fig. 52 - FFT analysis of cavitation noise measurements, HC reactor configuration EW1.

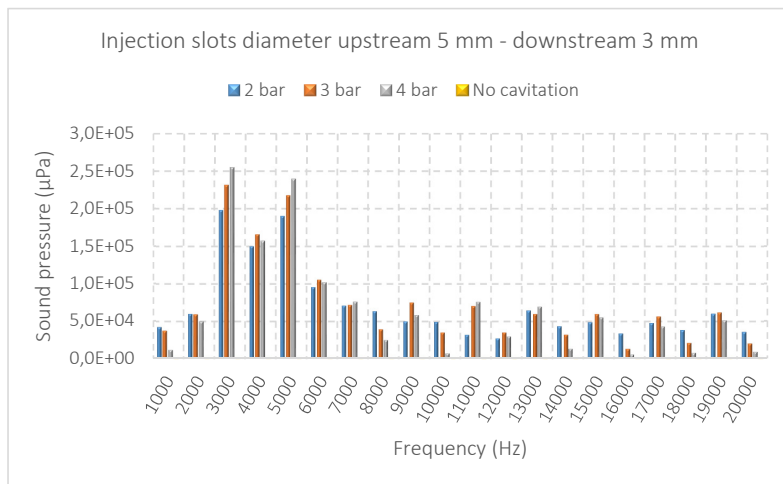


Fig. 53 - FFT analysis of cavitation noise measurements, HC reactor configuration EW2.

Furthermore, making a comparison between configurations EW1 and EW2 (Fig. 52 and Fig. 53), it was possible to observe that a decrease in diameters of injection slots caused an increase in sound pressure, indicating a higher cavitation intensity. These results are in agreement with the previous

study by Mancuso et al. [9] on wastewater treatment processes by using the swirling jet-induced reactor, in which authors observed higher treatment efficiencies, in terms of COD solubilisation, reducing the injection slots diameters.

It is interesting to note that in the configuration EW1 at both 3,000 and 5,000 Hz (*Fig. 52*), the sound pressure increased with an increase in the inlet flow pressure until an optimum value of 3.0 bar. At 4.0 bar flow pressure, the sound pressure was observed to drop marginally. These results can be attributed to the onset of air cavitation that enhances phenomena of bubbles coalescence reducing the cavitation noise and then the cavitation intensity. These findings are in agreement with the previous study by Mancuso et al. [8] on the effect of inlet flow pressure on Rhodamine B degradation, in which HC reactor configuration EW1 was used.

On the contrary, in configuration EW2, an increase in inlet flow pressure implied an increase in sound pressure, indicating that the onset of air cavitation did not yet occur for the inlet flow pressures taken into account. These findings are in agreement with the previous study by Mancuso et al. [9] on the effect of inlet flow pressure on sludge solubilisation, in which HC reactor configuration EW2 was used at 4.0 bars, showing a higher sludge solubilisation degree as compared with the configuration EW1 at 4.0 bars.

For higher frequencies of 7,000 Hz, in both configuration EW1 and EW2, it was possible to observe a data trend characteristic of pulsating flow due to the presence of both cavitation and turbulence [160] as well as to the regime of the mono screw pump.

4. Conclusions

In this study, a three-dimensional CFD analysis of a swirling jet-induced reactor in cavitating flow and non-cavitating flow conditions was implemented. Operating with an inlet pressure of 0.25 bars, non-cavitating conditions were obtained. For the non-cavitating flow, the results of the numerical computations were in good agreement with the experimental data. The modelled fluid dynamics into the swirling jet-induced reactor reflected the same flow velocity and flow pressure distributions observed during the experimental tests. Results of numerical simulations allowed identifying some reactor areas in which the highest flow velocities and then the lowest flow pressures were observed. A rotating flow around the swirling jet-induced reactor central axis and at the exit of the double cone was observed. Numerical simulations confirmed that different reactor geometric configurations can influence flow velocity and flow pressure distributions.

A variation in inlet flow pressure and thus in flow rate and in flow velocity in the swirling jet-induced

reactor implies a pressure drop into the reactor that could result in the onset of cavitation. Fixing an inlet pressure of 2.0 bar, numerical simulations were also carried out in cavitating flow conditions. The modelled fluid dynamics into the swirling jet-induced reactor reflected the same flow behaviour observed for non-cavitating flow, but a discrepancy between the cavitating model and the experimental data did not allow modelling the HC process into swirling jet-induced reactor. In flow cavitating conditions, numerical results showed different values of flow velocity and flow pressure if compared to the experimental data, probably caused by a lack of grid density in the meshed fluid domain and/or an inclusion of some incorrect information in the cavitating model. Further studies could be intended: i) to focus on making a more accurate meshed fluid domain of the swirling jet-induced reactor in order to get even more accurate results by numerical simulations, ii) to optimize the mathematical model in terms of governing equations in cavitating conditions and considering the vapour phase in model definition in order to use the mathematical model as a reliable tool, iii) to use Large Eddy Simulation (LES) as numerical technique to simulate three-dimensional turbulence into the cavitating model.

Moreover, cavitation noise measurements can be used as a helpful method to get the onset of vapour cavitation and air cavitation into the swirling jet-induced reactor.

Summary and outlook

Summary and outlook

Hydrodynamic cavitation (HC) appears to be very effective for intensification of chemical and mechanical processing in many applications in the field of environment protection, and in particular in the specific area of sludge and wastewater treatment.

In the last years, many efforts were made by many researchers worldwide in order to develop new geometrical configurations of cavitating devices with the main purpose of getting higher pollutant removal efficiencies with the lowest energy consumption.

In this thesis, a modified swirling jet-induced reactor was used (i) to treat a toxic and carcinogenic pollutant dye (Rhodamine B, RhB) in waste dye aqueous solutions and (ii) to improve the activated sludge solubilisation and aerobic sludge biodegradability in biological wastewater processes.

Treating pollutes aqueous solutions by Rhodamine B, higher extents of degradation were obtained using the modified swirling jet-induced reactor rather than a multi hole orifice plate system at similar operative conditions. Using HC alone, an increase in the extent of degradation from 8.6% to 14.7% was observed moving from orifice plates to swirling jet-induced reactor. An intensification in degradation rate of RhB by using the swirling jet-induced cavitation in presence of NaOCl as additive was observed, reaching an extent of degradation of 83.4% in 37 min.

Using the swirling jet-induced cavitation as pre-treatment technique of excess sludge, the best results in terms of sludge solubilisation were achieved after 2 h of HC treatment, treating a 50.0 gTS L⁻¹ and using the three heads Ecowirl system, at 35.0 °C and 4.0 bar. Chemical and respirometric tests proved that sludge solubilisation and aerobic biodegradability can be efficiently enhanced through HC pre-treatment technique.

Although the effectiveness of the swirling jet-induced reactor was already experimentally proved, the geometrical configuration of the cavitating device can be further optimized with the main goal of enhancing the treatment efficiencies and reducing the energy consumption. With this purpose, numerical simulations can be used as a useful tool to both model new optimized reactor geometries and predict new results in terms of cavitation intensities.

List of Figures

List of Figures

<i>Fig. 1-</i> Increase in the number of peer-reviewed publications listed in the databases of Web of Science with “innovative wastewater” and “hydrodynamic cavitation wastewater” as keys words.	8
<i>Fig. 2-</i> Phase diagram of water (adapted from Brennen [27])......	10
<i>Fig. 3-</i> Growth, implosion and collapse of bubbles in cavitation process. 1-3: static pressure < vapour pressure → vapour bubble grows at low pressure; 4: static pressure = vapour pressure → no further growth of bubble; 5-15: static pressure > vapour pressure → implosion and collapse; 9-15: → micro-jets (adapted from Cavitation- Easily explained!, IET Institute for Energy Technology, https://www.youtube.com/watch?v=U-uUYCFDTrc).	11
<i>Fig. 4-</i> Effect of a constriction on flow velocity and pressure in a Venturi system: a) contours of flow velocity magnitude; b) contours of flow pressure magnitude; c) high-speed camera frames. .	13
<i>Fig. 5-</i> Attached cavitation on: a) hydrofoil and b) bluff body. The flow is from left to right (reproduced from Brennen [27])......	16
<i>Fig. 6 -</i> a) Formation, b) separation and c) collapse of a cavitation cloud on the suction surface of a hydrofoil. The flow is from left to right (reproduced from Brennen [27]).	17
<i>Fig. 7-</i> Schematic representation of “developed HC” (a) where highly dynamical vapour cloud shedding associated with high pressure pulsations is expected and “supercavitation” (b), which is characterised by a single quasi steady large cavitation pocket (reproduced from Dular et al. [20]).	17
<i>Fig. 8 -</i> Travelling bubble cavitation in convected cavitation (reproduced from Brennen [27]).	18
<i>Fig. 9-</i> Vortex cavitation in a) hydrofoil, b) propeller and c) turbine (reproduced from Brennen [27]).	19
<i>Fig. 10-</i> Mechanism of degradation of organic pollutants.	19
<i>Fig. 11-</i> Overview of the effective parameters in HC (reproduced from Braeutigam et al. [50])......	20
<i>Fig. 12-</i> HC Cavitation reactor classification (adapted from Ozonek [51]).	21
<i>Fig. 13-</i> Schematic representation of the experimental setup of a continuous HC reactor (closed loop), (adapted from [8,9,13,20])......	33
<i>Fig. 14 -</i> Schematic representation of the experimental setup of a pulsating HC reactor (closed loop) (reported by [20]).	34
<i>Fig. 15-</i> Schematic representation of opened loops.	35

<i>Fig. 16-</i> HC devices: a) hole orifice plates; b) Venturi systems; c) rotor-stator systems.	36
<i>Fig. 17-</i> Main fields of application of HC in a wastewater treatment plant.	36
<i>Fig. 18-</i> Schematic representation of the experimental setup.	44
<i>Fig. 19-</i> (a) Orifice plate; (b) Ecowirl reactor.	45
<i>Fig. 20-</i> Schematic representation of the operation of Ecowirl reactor.	46
<i>Fig. 21-</i> Geometry of double cone type C in the Ecowirl reactor.	47
<i>Fig. 22-</i> Comparison between different HC devices alone (volume 50 L; initial RhB concentration 3.0 mg L ⁻¹ ; pH 4.0; inlet pressure 2.0 bar; initial temperature 20.0 ± 1.0 °C).	49
<i>Fig. 23 -</i> Synergetic effect between HC and NaOCl on degradation of RhB (volume 50 L; initial RhB concentration 3.0 mg L ⁻¹ ; pH 4.0; inlet pressure 2.0 bar; initial temperature 20.0 ± 1.0 °C). ...	52
<i>Fig. 24-</i> Effect of HC using Ecowirl in presence of NaOCl on degradation of RhB (volume 50 L; initial RhB concentration 3.0 mg L ⁻¹ ; pH 4.0; inlet pressure 2.0 bar; initial temperature 19.0 ± 1.0 °C; mg NaOCl L ⁻¹).	53
<i>Fig. 25-</i> Effect of inlet pressure on degradation of RhB by using (a) orifice plate and (b) Ecowirl reactor (volume 50 L; initial dye concentration 3.0 mg L ⁻¹ ; pH 4.0; initial temperature 19.0 ± 0.5 °C; 0.5 mg NaOCl L ⁻¹ ; inlet pressure).	54
<i>Fig. 26-</i> Effect of the geometry of the double cone chamber of Ecowirl reactor on degradation of RhB (volume 50 L; initial RhB concentration 3.0 mg L ⁻¹ ; pH 4.0; inlet pressure 2.0 bar; initial temperature 19.0 ± 2.5 °C; 0.5 mg NaOCl L ⁻¹ ; double cone).	57
<i>Fig. 27 -</i> (a) Effect of pH on degradation of RhB by using orifice plate, (b) Degradation kinetics (volume 50 L; initial RhB concentration 3.0 mg L ⁻¹ ; initial temperature 18.2 ± 2.6 °C; inlet pressure 2.0 bar; 0.5 mg NaOCl L ⁻¹ ; pH).	58
<i>Fig. 28-</i> Effect of initial dye concentration on RhB degradation by using orifice plate (volume 50 L; pH 2.0; initial temperature 18.1 ± 1.3 °C; pH 2.0; inlet pressure 2.0 bar; 0.5 mg NaOCl L ⁻¹ ; mg RhB L ⁻¹).	60
<i>Fig. 29-</i> Schematic representation of the experimental setup.	70
<i>Fig. 30 -</i> Solid geometry of Ecowirl reactor.	70
<i>Fig. 31 -</i> Schematic representation of the respirometric experimental setup.	73
<i>Fig. 32 -</i> Effect of temperature on DD and SCOD (volume 50.0 L; TS content 50.0 g L ⁻¹ ; initial pH 6.8; inlet pressure 2.0 bar; temperature 20.0-25.0-30.0-35.0 ± 3.0 °C). Ecowirl reactor standard configuration.	76
<i>Fig. 33 -</i> Effect of inlet pressure on DD and SCOD (volume 50.0 L; TS content 50.0 g L ⁻¹ ; initial pH 6.8;	

temperature 25.0 ± 3.0 °C; inlet pressure 2.0-3.0-4.0 bar). Ecowirl reactor standard configuration.....	78
<i>Fig. 34</i> - Variations in pressure in Ecowirl reactor. ΔP_{Inlet} – Vacuum zone: ΔP 2 bar ≈ 2.7 bar, ΔP 3 bar ≈ 3.8 bar, ΔP 4 bar ≈ 4.8 bar; ΔP Vacuum zone – 371 mm downstream: ΔP 2 bar ≈ 1.0 bar, ΔP 3 bar ≈ 1.3 bar, ΔP 4 bar ≈ 1.5 bar.....	78
<i>Fig. 35</i> - Effect of TS content on DD and SCOD (volume 50.0 L; inlet pressure 2.0 bar; initial pH 6.8; temperature 25.0 °C ± 3.0 °C; TS content 7.0- 12.0- 23.0- 50.0 g L ⁻¹). Ecowirl reactor standard configuration.....	80
<i>Fig. 36</i> - Effect of different number of injection slots on DD and SCOD (volume 50.0 L; inlet pressure 4.0 bar; initial pH 6.8; temperature 25.0 °C ± 3.0 °C; TS content 50.0 g L ⁻¹). Ecowirl reactor configuration A, B, and C.....	81
<i>Fig. 37</i> - Ecowirl reactor with three-heads in series.....	82
<i>Fig. 38</i> - Effect of Ecowirl heads in series on DD and SCOD (volume 50.0 L; inlet pressure 2.0 bar; initial pH 6.8; temperature 25.0 ± 3.0 °C; TS content 50.0 g L ⁻¹). Ecowirl reactor standard configuration.....	82
<i>Fig. 39</i> - Energy efficiency vs Specific supplied energy: (a) injection slots number; (b) Ecowirl heads number; (c) inlet pressure; (d) injection slots diameter; (e) temperature; (f) TS content.....	84
<i>Fig. 40</i> - HC 8h-experiment – Effect of applied energy on DD and SCOD (volume 50.0 L; initial pH 6.8; temperature 35.0 ± 1.0 °C; TS content 50.0 g L ⁻¹ ; inlet pressure 4.0 bar; 6 injection slots; 3 Ecowirl heads).....	85
<i>Fig. 41</i> - Energy efficiency vs Specific supplied energy.....	87
<i>Fig. 42</i> - Respirogram 1: filtered untreated sludge (time 0 h); Respirogram 2: filtered treated sludge after 2 h of HC; Respirogram 3: filtered treated sludge after 4 h of HC; Respirogram 4: filtered treated sludge after 8 h of HC; (volume 50.0 L; initial TS content 50.0 g L ⁻¹ ; initial pH 6.8; inlet pressure 4.0 bar; initial temperature 35.0 ± 1.0 °C; 3 Ecowirl heads in series).....	88
<i>Fig. 43</i> - OUR profiles. 1: untreated sludge (time 0 h); 2: treated sludge after 2 h of HC; 3: treated sludge after 4 h of HC; 4: treated sludge after 8 h of HC; (volume 50.0 L; initial TS content 50.0 g L ⁻¹ ; initial pH 6.8; inlet pressure 4.0 bar; initial temperature 35.0 ± 1.0 °C; 3 Ecowirl heads in series).....	89
<i>Fig. 44</i> - Schematic representation of the experimental setup: (1) Feed water tank; (2) Mono screw pump; (3) Inverter; (4) Flow-meter; (5) Cavitating device (Ecowirl reactor); (6) Frequency-meter; (P1), (P2), (P3) Upstream, downstream and vacuum pressure transducers.....	98

<i>Fig. 45-</i> Schematic representation of geometry of the studied swirling jet reactor.	98
<i>Fig. 46-</i> Swirling jet-induced reactor fluid geometry.	102
<i>Fig. 47-</i> Swirling jet-induced reactor fluid domain.	102
<i>Fig. 48-</i> Swirling jet-induced reactor fluid dynamics: velocity vectors coloured by velocity magnitude [m sec ⁻¹], inlet flow pressure 0.25 bar (configuration EW1).	104
<i>Fig. 49-</i> Contours of velocity magnitude [m sec ⁻¹], and static pressure [bar] for configurations EW1 (a, b, c) and EW2 (e, f, g), at inlet flow pressure 0.25 bar. The flow velocity magnitude and the flow static pressure range from blue to red corresponding to low and high flow velocities and flow static pressures, respectively.....	105
<i>Fig. 50-</i> Swirling jet-induced reactor fluid dynamics: velocity vectors coloured by velocity magnitude [m sec ⁻¹], inlet flow pressure 2 bar (configuration EW1).....	107
<i>Fig. 51-</i> Contours of velocity magnitude [m sec ⁻¹] and static pressure [bar] for configurations EW1 (a, b, c) and EW2 (e, f, g), at inlet flow pressure of 2.0 bar. The flow velocity magnitude and the flow static pressure range from blue to red corresponding to low and high flow velocities and flow static pressures, respectively.....	108
<i>Fig. 52 -</i> FFT analysis of cavitation noise measurements, HC reactor configuration EW1.....	110
<i>Fig. 53 -</i> FFT analysis of cavitation noise measurements, HC reactor configuration EW2.....	110

List of Tables

List of Tables

<i>Table 1</i> - Parameters and operative conditions for the two different cavitating devices used.	47
<i>Table 2</i> - Flow characteristics for the two different cavitating devices used.....	48
<i>Table 3</i> - Operative parameters and efficiency measured at the end of each test.	51
<i>Table 4</i> - Variation of cavitation yield (C.Y.) for different cavitation equipments.....	62
<i>Table 5</i> - Operative parameters/conditions and efficiency measured at the end of each test.	72
<i>Table 6</i> - HC 8h-optimized test.....	85
<i>Table 7</i> - Parameters and operative conditions for different Ecowirl injection slots diameters.....	99
<i>Table 8</i> - Comparison between experiments and numerical simulations in non-cavitating flow.....	103

References

References

- [1] M. Čudina, Detection of cavitation phenomenon in a centrifugal pump using audible sound, *Mech. Syst. Signal Process.* 17 (2003) 1335–1347.
- [2] P.J. McNulty, I.S. Pearsall, Cavitation inception in pumps, *J. Fluids Eng.* 104 (1982) 99–104.
- [3] G.D. Neil, R.L. Reuben, P.M. Sandford, E.R. Brown, J.A. Steel, Detection of incipient cavitation in pumps using acoustic emission, *J. Process Mech. Eng.* 211 (1997) 267–277.
- [4] A.J. Stepanoff, Cavitation in Centrifugal Pumps With Liquids Other Than Water, *J. Eng. Power.* 83 (1961) 79–89.
- [5] X. Escaler, E. Egusquiza, M. Farhat, F. Avellan, M. Coussirat, Detection of cavitation in hydraulic turbines, *Mech. Syst. Signal Process.* 20 (2006) 983–1007.
- [6] K. Ogawa, T. Kimura, Hydrodynamic characteristics of a butterfly valve–Prediction of pressure loss characteristics, *ISA Trans.* 34 (1995) 319–326.
- [7] W.M.J. Batten, A.S. Bahaj, A.F. Molland, J.R. Chaplin, The prediction of the hydrodynamic performance of marine current turbines, *Renew. Energy.* 33 (2008) 1085–1096.
- [8] G. Mancuso, M. Langone, M. Laezza, G. Andreottola, Decolourization of Rhodamine B: A swirling jet-induced cavitation combined with NaOCl, *Ultrason. Sonochem.* 32 (2016) 18–30.
- [9] G. Mancuso, M. Langone, G. Andreottola, A swirling jet-induced cavitation to increase activated sludge solubilisation and aerobic sludge biodegradability, *Ultrason. Sonochem.* 35 (2016) 489–501.
- [10] N.T. Le, C. Julcour-lebigue, H. Delmas, An executive review of sludge pretreatment by sonication, *JES.* 37 (2015) 139–153.
- [11] P.R. Gogate, A.M. Kabadi, A review of applications of cavitation in biochemical engineering / biotechnology, *Biochem. Eng. J.* 44 (2009) 60–72.
- [12] P.R. Gogate, Cavitation: an auxiliary technique in wastewater treatment schemes, *Adv. Environ. Res.* 6 (2002) 335–358.
- [13] M. Sivakumar, A.B. Pandit, Wastewater treatment: a novel energy efficient hydrodynamic cavitation technique., *Ultrason. Sonochem.* 9 (2002) 123–31.
- [14] T. Suenaga, M. Nishimura, H. Yoshino, H. Kato, M. Nonokuchi, T. Fujii, et al., High-pressure jet device for activated sludge reduction: Feasibility of sludge solubilization, *Biochem. Eng. J.* 100 (2015) 1–8.

- [15] H.J. Kim, D.X. Nguyen, J.H. Bae, The performance of the sludge pretreatment system with venturi tubes, *Water Sci. Technol.* 57 (2008) 131–137.
- [16] K. Hirooka, R. Asano, A. Yokoyama, M. Okazaki, A. Sakamoto, Y. Nakai, Reduction in excess sludge production in a dairy wastewater treatment plant via nozzle-cavitation treatment: case study of an on-farm wastewater treatment plant., *Bioresour. Technol.* 100 (2009) 3161–6.
- [17] I. Lee, J.I. Han, The effects of waste-activated sludge pretreatment using hydrodynamic cavitation for methane production, *Ultrason. Sonochem.* 20 (2013) 1450–1455.
- [18] M. Petkovšek, M. Mlakar, M. Levstek, M. Strazar, B. Širok, M. Dular, A novel rotation generator of hydrodynamic cavitation for waste-activated sludge disintegration, *Ultrason. Sonochem.* 26 (2015) 408–414.
- [19] P.N. Patil, P.R. Gogate, L. Csoka, A. Dregelyi-kiss, M. Horvath, Intensification of biogas production using pretreatment based on hydrodynamic cavitation, *Ultrason. Sonochem.* 30 (2016) 79–86.
- [20] M. Dular, T. Griessler-bulc, I. Gutierrez-Aguirre, E. Heath, T. Kosjek, Use of hydrodynamic cavitation in (waste) water treatment, *Ultrason. Sonochem.* 29 (2016) 577–588.
- [21] Y.T. Didenko, W.B. McNamara III, K.S. Suslick, Hot Spot Conditions during Cavitation in Water, *J. Am. Chem. Soc.* 121 (1999) 5817–5818.
- [22] D.V. Pinjari, A.B. Pandit, Cavitation milling of natural cellulose to nanofibrils, *Ultrason. Sonochem.* 17 (2010) 845–852.
- [23] Y.T. Shah, A.B. Pandit, V.S. Moholkar, *Cavitation Reaction Engineering*, Luss Dan, 1999.
- [24] B.T.J. Mason, J.P. Lorimer, *Applied sonochemistry: The uses of power ultrasound in chemistry and processing*, Wiley-VCH Verlag GmbH, Weinheim. 208 (2004).
- [25] T.J. Mason, J.P. Lorimer, *Sonochemistry , theory, applications and uses of ultrasound in chemistry*, in: E.H. Publishers (Ed.), Chichester, 1989: pp. 1150–1151.
- [26] R.T. Knapp, J.W. Daily, F.G. Hammit, *Cavitation*, in: McGraw-Hill, New York, 1970.
- [27] C.E. Brennen, *Cavitation and bubble dynamics*, Oxford University, 1995.
- [28] S. Pilli, P. Bhunia, S. Yan, R.J. Leblanc, R.D. Tyagi, R.Y. Surampalli, Ultrasonic pretreatment of sludge : A review, *Ultrason. Sonochem.* 18 (2011) 1–18.
- [29] P.R. Gogate, A.B. Pandit, Engineering design methods for cavitation reactors II: Hydrodynamic cavitation, *AIChE J.* 46 (2000) 1641–1649.
- [30] H. Delmas, N.T. Le, L. Barthe, C. Julcour-lebigue, Optimization of hydrostatic pressure at varied sonication conditions – power density , intensity , very low frequency – for isothermal

- ultrasonic sludge treatment, *Ultrason. Sonochem.* 25 (2015) 51–59.
- [31] F. Avellan, M. Farhat, Shock pressure generated by cavitation vortex collapse, in: *Proc. Third International Symp. Cavitation Noise Eros. Fluid Syst., FED-vol 88, ASME Winter Annual Meeting San Francisco, CA, 1989*: pp. 119–125.
- [32] I. Akhatov, O. Lindau, A. Topolnikov, R. Mettin, N. Vakhitova, W. Lauterborn, Collapse and rebound of a laser-induced cavitation bubble, *Phys. Fluids*. 13 (2001) 2805–2819.
- [33] J.-P. Franc, J.-M. Michel, *Fundamentals of Cavitation*, 2005.
- [34] P. Riesz, D. Berdahl, C.L. Christman, Free radical generation by ultrasound in aqueous and nonaqueous solutions, *Environ. Health Perspect.* VOL. 64 (1985) 233–252.
- [35] Y.G. Adewuyi, Critical Review sonochemistry in environmental remediation . 1 . Combinative and hybrid sonophotochemical oxidation processes for the treatment of pollutants in water, 39 (2005) 3409–3420.
- [36] M. Farhat, A. Chakravarty, E. Field, Luminescence from hydrodynamic cavitation, *Math. Phys. Eng. Sci.* 467 (2011) 591–606.
- [37] D.. Sunartio, M.. Ashokkumar, F. Grieser, Study of the coalescence of acoustic bubbles as a function of frequency, power, and water-soluble additives, *J. Am. Chem. Soc.* 129 (2007) 6031–6036.
- [38] H.. Zhao, J.-X.. Wang, Q.-A.. Wang, J.-F.. Chen, J. Yun, Controlled liquid antisolvent precipitation of hydrophobic pharmaceutical nanoparticles in a microchannel reactor, *Ind. Eng. Chem. Res.* 46 (2007) 8229–8235.
- [39] J.M. Jiju, *Application of advanced oxidation processes for the degradation of organic water pollutants*, Mahtama Gandhi University, 2000.
- [40] V.S.. Moholkar, B. Pandit, A., Bubble behavior in hydrodynamic cavitation: Effect of turbulence, *AIChE J.* 43 (1997) 1641–1648.
- [41] Y.. Yan, R.B. Thorpe, Flow regime transitions due to cavitation in the flow through an orifice, *Int. J. Multiph. Flow.* 16 (1990) 1023–1045.
- [42] K.K. Jyoti, A.B. Pandit, Water disinfection by acoustic and hydrodynamic cavitation, *Biochem. Eng. J.* 7 (2001) 201–212.
- [43] V.K. Saharan, M.P. Badve, A.B. Pandit, Degradation of Reactive Red 120 dye using hydrodynamic cavitation, *Chem. Eng. J.* 178 (2011) 100–107.
- [44] A. Šarc, T. Stepišnik-Perdih, M. Petkovšek, M. Dular, The issue of cavitation number value in studies of water treatment by hydrodynamic cavitation, *Ultrason. Sonochem.* 34 (2017) 51–59.

- [45] M. Petkovšek, M. Zupanc, M. Dular, T. Kosjek, E. Heath, B. Kompare, et al., Rotation generator of hydrodynamic cavitation for water treatment, *Sep. Purif. Technol.* 118 (2013) 415–423.
- [46] F. Jean-Pierre, M. Jean-Marie, *Fundamentals of Cavitation*, 2004.
- [47] J. Choi, C. Hsiao, G. Chahine, S. Ceccio, Growth, oscillation and collapse of vortex cavitation bubbles, *J. Fluid Mech.* 624 (2009) 255–279.
- [48] P.R. Gogate, A.B. Pandit, A review of imperative technologies for wastewater treatment I: Oxidation technologies at ambient conditions, *Adv. Environ. Res.* 8 (2004) 501–551.
- [49] H. Kimoto, Y. Sumita, Heat transfer characteristics of a circular cylinder in a conduit under cavitation, *Trans. JSME.* 49 (1986) 2312–2313.
- [50] P. Braeutigam, M. Franke, Z.L. Wu, B. Ondruschka, Role of different parameters in the optimization of hydrodynamic cavitation, *Chem. Eng. Technol.* 33 (2010) 932–940.
- [51] J. Ozonek, *Application of Hydrodynamic Cavitation in Environmental Engineering*, 2012.
- [52] H.J. Kim, D.X. Nguyen, J.H. Bae, The performance of the sludge pretreatment system with venturi tubes, *Water Sci. Technol.* 57 (2008) 131–137.
- [53] J. Basiri Parsa, S.A. Ebrahimzadeh Zonouzian, Optimization of a heterogeneous catalytic hydrodynamic cavitation reactor performance in decolorization of Rhodamine B: Application of scrap iron sheets, *Ultrason. Sonochem.* 20 (2013) 1442–1449.
- [54] J. Ozonek, K. Lenik, Effect of different design features of the reactor on hydrodynamic cavitation process, 52 (2011) 112–117.
- [55] J. Wang, X. Wang, P. Guo, J. Yu, Degradation of reactive brilliant red K-2BP in aqueous solution using swirling jet-induced cavitation combined with H₂O₂, *Ultrason. Sonochem.* 18 (2011) 494–500.
- [56] M. Langone, R. Ferrentino, G. Trombino, W.D.E. Puisseau, G. Andreottola, E.C. Rada, et al., Application of a Novel Hydrodynamic Cavitation System in Wastewater Treatment Plants, 77 (2013).
- [57] P.N. Patil, P.R. Gogate, L. Csoka, A. Dregelyi-Kiss, M. Horvath, Intensification of biogas production using pretreatment based on hydrodynamic cavitation, *Ultrason. Sonochem.* 30 (2016) 79–86.
- [58] M. Petkovšek, M. Mlakar, M. Levstek, M. Stražar, B. Širok, M. Dular, A novel rotation generator of hydrodynamic cavitation for waste-activated sludge disintegration, *Ultrason. Sonochem.* 26 (2015) 408–414.
- [59] A.L. Prajapat, P.R. Gogate, Intensified depolymerization of aqueous polyacrylamide solution

using combined processes based on hydrodynamic cavitation , ozone , ultraviolet light and hydrogen peroxide, *Ultrason. Sonochem.* 31 (2016) 371–382.

- [60] M.M. Gore, V.K. Saharan, D. V. Pinjari, P. V. Chavan, A.B. Pandit, Degradation of reactive orange 4 dye using hydrodynamic cavitation based hybrid techniques, *Ultrason. Sonochem.* 21 (2014) 1075–1082.
- [61] R.K. Joshi, P.R. Gogate, Degradation of dichlorvos using hydrodynamic cavitation based treatment strategies, *Ultrason. Sonochem.* 19 (2012) 532–539.
- [62] X.. Wang, Y. Zhang, Degradation of alachlor in aqueous solution by using hydrodynamic cavitation, *J. Hazard. Mater.* 161 (2009) 202–207.
- [63] M.P. Badve, T. Alpar, A.B. Pandit, P.R. Gogate, L. Csoka, Modeling the shear rate and pressure drop in a hydrodynamic cavitation reactor with experimental validation based on KI decomposition studies, *Ultrason. Sonochem.* 22 (2015) 272–277.
- [64] P.S. Kumar, A.B. Pandit, Modeling Hydrodynamic Cavitation, *Chem. Eng. Technol.* 22 (1999) 1017–1027.
- [65] S. Merouani, O. Hamdaoui, F. Saoudi, M. Chiha, Sonochemical degradation of Rhodamine B in aqueous phase: Effects of additives, *Chem. Eng. J.* 158 (2010) 550–557.
- [66] X. Wang, J. Wang, P. Guo, W. Guo, G. Li, Chemical effect of swirling jet-induced cavitation: Degradation of rhodamine B in aqueous solution, *Ultrason. Sonochem.* 15 (2008) 357–363.
- [67] K.P. Mishra, P.R. Gogate, Intensification of degradation of Rhodamine B using hydrodynamic cavitation in the presence of additives, *Sep. Purif. Technol.* 75 (2010) 385–391.
- [68] K. Grübel, J. Suschka, Hybrid alkali-hydrodynamic disintegration of waste-activated sludge before two-stage anaerobic digestion process, *Environ. Sci. Pollut. Res.* 22 (2015) 7258–7270.
- [69] I. Lee, J. Han, The effects of waste-activated sludge pretreatment using hydrodynamic cavitation for methane production, *Ultrason. Sonochem.* 20 (2013) 1450–1455.
- [70] X. Wang, J. Wang, P. Guo, W. Guo, C. Wang, Degradation of rhodamine B in aqueous solution by using swirling jet-induced cavitation combined with H₂O₂, *J. Hazard. Mater.* 169 (2009) 486–491.
- [71] L.F.R. Montgomery, G. Bochmann, Pretreatment of feedstock for enhanced biogas production, *IEA Bioenergy.* (2014) 1–20.
- [72] P.R. Gogate, A.B. Pandit, Hydrodynamic cavitation reactors: a state of the art Review, *Chem. Eng.* 17 (2001) 1–85.
- [73] K.S. Kumar, V.S. Moholkar, Conceptual design of a novel hydrodynamic cavitation reactor, *Chem.*

Eng. Sci. 62 (2007) 2698–2711.

- [74] P.R. Gogate, G.S. Bhosale, Comparison of effectiveness of acoustic and hydrodynamic cavitation in combined treatment schemes for degradation of dye wastewaters, *Chem. Eng. Process. Process Intensif.* 71 (2013) 59–69.
- [75] J. Wang, Y. Guo, P. Guo, J. Yu, W. Guo, X. Wang, Degradation of reactive brilliant red K-2BP in water using a combination of swirling jet-induced cavitation and Fenton process, *Sep. Purif. Technol.* 130 (2014) 1–6.
- [76] M. Zupanc, T. Kosjek, M. Petkovšek, M. Dular, B. Kompare, B. Širok, et al., Removal of pharmaceuticals from wastewater by biological processes, hydrodynamic cavitation and UV treatment., *Ultrason. Sonochem.* 20 (2013) 1104–12.
- [77] M. Zupanc, T. Kosjek, M. Petkovšek, M. Dular, B. Kompare, B. Sirok, et al., Shear-induced hydrodynamic cavitation as a tool for pharmaceutical micropollutants removal from urban wastewater., *Ultrason. Sonochem.* (2013) 18–19.
- [78] P.R. Gogate, I.Z. Shirgaonkar, M. Sivakumar, P. Senthilkumar, N.P. Vichare, A.B. Pandit, Cavitation reactors: Efficiency assessment using a model reaction, *AIChE J.* 47 (2001) 2526–2538.
- [79] X. Feng, H. Lei, J. Deng, Q. Yu, H. Li, Physical and chemical characteristics of waste activated sludge treated ultrasonically, *Chem. Eng. Process. Process Intensif.* 48 (2009) 187–194.
- [80] G. Zhang, P. Zhang, J. Yang, H. Liu, Energy-efficient sludge sonication: Power and sludge characteristics, *Bioresour. Technol.* 99 (2008) 9029–9031.
- [81] P.R. Gogate, I.Z. Shirgaonkar, M. Sivakumar, P. Senthilkumar, N.P. Vichare, A.B. Pandit, Cavitation reactors : Efficiency assessment using a model reaction, 47 (2001).
- [82] S. Manickam, M. Ashokkumar, *Cavitation: A Novel Energy-Efficient Technique for the Generation of Nanomaterials*, 2014.
- [83] J.B. Bien, E.S. Kempa, J.D. Bien, Influence of ultrasonic field on structure and parameters of sewage sludge for dewatering process, *Water Sci. Technol.* 36 (1997) 287–291.
- [84] G. Palau-Salvador, P. González-Altozano, J. Arviza-Valverde, Numerical modeling of cavitating flows for simple geometries using FLUENT V6 . 1, *Spanish J. Agric. Res.* 5 (2007) 460–469.
- [85] J. Navickas, L. Chen, Cavitating venturi performance characteristics, *ASME Fluids Eng. Div.* 177 (1993) 153–159.
- [86] Q. Wang, Z. Jiang, Effect of nozzle geometrical and dynamic factors on cavitating and turbulent flow in a diesel multi-hole injector nozzle, *Int. J. Therm. Sci.* 70 (2013) 132–143.
- [87] S.B. Müller, L. Kleiser, Large-Eddy Simulation of Vortex Breakdown in Compressible Swirling Jet

Flow, in: Conf. Turbulence Interact., 2006.

- [88] S.M. Ashrafizadeh, H. Ghassemi, Experimental and numerical investigation on the performance of small-sized cavitating venturis, *Flow Meas. Instrum.* 42 (2015) 6–15.
- [89] R. Jain, M. Bhargava, N. Sharma, Electrochemical Studies on a Pharmaceutical Azo Dye: Tartrazine, *Ind. Eng. Chem. Res.* 42 (2) (2003) 243–247.
- [90] T. Puzyn, A. Mostrag-Szlichtyng, *Organic Pollutants Ten Years After the Stockholm Convention-Environmental and Analytical Update*, 2012.
- [91] P. Peralta-Zamora, E. Esposito, R. Pelegrini, R. Groto, J. Reyes, N. Durán, Effluent Treatment of Pulp and Paper, and Textile Industries using Immobilised Horseradish Peroxidase, *Environ. Technol.* 19 (1998).
- [92] D.T. Sponza, Toxicity studies in a chemical dye production industry in Turkey, *J. Hazard. Mater.* 138 (2006) 438–447.
- [93] A. Gottlieb, C. Shaw, A. Smith, A. Wheatley, S. Forsythe, The toxicity of textile reactive azo dyes after hydrolysis and decolourisation, *J. Biotechnol.* 101 (2003) 49–56.
- [94] D. Tan, B. Bai, D. Jiang, L. Shi, S. Cheng, D. Tao, et al., Rhodamine B induces long nucleoplasmic bridges and other nuclear anomalies in *Allium cepa* root tip cells, *Environ. Sci. Pollut. Res.* 21 (2014) 3363–3370.
- [95] A. Pandey, P. Singh, L. Iyengar, Bacterial decolorization and degradation of azo dyes, *Int. Biodeterior. Biodegrad.* 59 (2007) 73–84.
- [96] T. Robinson, G. McMullan, R. Marchant, P. Nigam, Remediation of dyes in textile effluent: A critical review on current treatment technologies with a proposed alternative, *Bioresour. Technol.* 77 (2001) 247–255.
- [97] T.L. Fry, M.R. Dunbar, A review of biomarkers used for wildlife damage and disease management, *USDA Natl. Wildl. Res. Cent.-Staff Publ.* (2007) 216–222.
- [98] P. Fisher, Review of Using Rhodamine B as a Marker for Wildlife Studies, *Wildl. Soc. Bull.* 27 (1999) 318–329.
- [99] S.D. Richardson, C.S. Willson, K. a Rusch, Use of Rhodamine water tracer in the marshland upwelling system., *Ground Water.* 42 (2004) 678–688.
- [100] R. Jain, M. Mathur, S. Sikarwar, A. Mittal, Removal of the hazardous dye rhodamine B through photocatalytic and adsorption treatments, *J. Environ. Manage.* 85 (2007) 956–964.
- [101] J. Rochat, P. Demenge, J.C. Rerat, Toxicologic study of a fluorescent tracer: rhodamine B, *Toxicol. Eur. Res.* 1 (1978) 6–23.

- [102] G. Crini, Non-conventional low-cost adsorbents for dye removal: A review, *Bioresour. Technol.* 97 (2006) 1061–1085.
- [103] C. Visvanathan, R. Ben Aim, K. Parameshwaran, Membrane Separation Bioreactors for Wastewater Treatment, *Crit. Rev. Environ. Sci. Technol.* 30 (2000) 1–48.
- [104] G.Z. Kyzas, J. Fu, K. a. Matis, The change from past to future for adsorbent materials in treatment of dyeing wastewaters, *Materials (Basel)*. 6 (2013) 5131–5158.
- [105] R. Andreozzi, Advanced oxidation processes (AOP) for water purification and recovery, *Catal. Today*. 53 (1999) 51–59.
- [106] M. V. Bagal, P.R. Gogate, Degradation of diclofenac sodium using combined processes based on hydrodynamic cavitation and heterogeneous photocatalysis, *Ultrason. Sonochem.* 21 (2014) 1035–1043.
- [107] K.P. Mishra, P.R. Gogate, Intensification of degradation of aqueous solutions of rhodamine B using sonochemical reactors at operating capacity of 7 L, *J. Environ. Manage.* 92 (2011) 1972–1977.
- [108] P.R. Gogate, M. Sivakumar, A.B. Pandit, Destruction of Rhodamine B using novel sonochemical reactor with capacity of 7.5 l, *Sep. Purif. Technol.* 34 (2004) 13–24.
- [109] P.R. Gogate, Hydrodynamic Cavitation for Food and Water Processing, *Food Bioprocess Technol.* 4 (2010) 996–1011.
- [110] A.G. Chakinala, P.R. Gogate, A.E. Burgess, D.H. Bremner, Treatment of industrial wastewater effluents using hydrodynamic cavitation and the advanced Fenton process, *Ultrason. Sonochem.* 15 (2008) 49–54.
- [111] M. Badve, P. Gogate, A. Pandit, L. Csoka, Hydrodynamic cavitation as a novel approach for wastewater treatment in wood finishing industry, *Sep. Purif. Technol.* 106 (2013) 15–21.
- [112] T. Joyce Tiong, G.J. Price, Ultrasound promoted reaction of Rhodamine B with sodium hypochlorite using sonochemical and dental ultrasonic instruments, *Ultrason. Sonochem.* 19 (2012) 358–364.
- [113] Q. Zeng, J. Fu, Y. Shi, H. Zhu, Degradation of C.I. disperse Blue 56 by ultraviolet radiation/sodium hypochlorite, *Ozone Sci. Eng.* 31 (2009) 37–44.
- [114] M. V. Bagal, P.R. Gogate, Wastewater treatment using hybrid treatment schemes based on cavitation and Fenton chemistry: A review, *Ultrason. Sonochem.* 21 (2014) 1–14.
- [115] K. Ramamurthi, K. Nandakumar, Characteristics of flow through small sharp- edged cylindrical orifices, *Flow Meas. Instrum.* 10 (1999) 133–143.

- [116] M.H. Priya, Giridhar Madras, Kinetics of TiO₂-Catalyzed Ultrasonic Degradation of Rhodamine Dyes, *Ind. Eng. Chem.* 45 (2006) 913–921.
- [117] S. Kavitha, C. Jayashree, S. Adish Kumar, I.T. Yeom, J. Rajesh Banu, The enhancement of anaerobic biodegradability of waste activated sludge by surfactant mediated biological pretreatment, *Bioresour. Technol.* 168 (2014) 159–166.
- [118] S. Kavitha, S. Adish Kumar, K.N. Yogalakshmi, S. Kaliappan, J. Rajesh Banu, Effect of enzyme secreting bacterial pretreatment on enhancement of aerobic digestion potential of waste activated sludge interceded through EDTA, *Bioresour. Technol.* 150 (2013) 210–219.
- [119] Y. Xue, H. Liu, S. Chen, N. Dichtl, X. Dai, N. Li, Effects of thermal hydrolysis on organic matter solubilization and anaerobic digestion of high-solid sludge, *Chem. Eng. J.* 264 (2014) 174–180.
- [120] R. Cano, A. Nielfa, M. Fdz-Polanco, Thermal hydrolysis integration in the anaerobic digestion process of different solid wastes: Energy and economic feasibility study, *Bioresour. Technol.* 168 (2014) 14–22.
- [121] E. Neyens, J. Baeyens, C. Creemers, Alkaline thermal sludge hydrolysis., *J. Hazard. Mater.* 97 (2003) 295–314.
- [122] A.G. Vlyssides, P.K. Karlis, Thermal-alkaline solubilization of waste activated sludge as a pre-treatment stage for anaerobic digestion, *Bioresour. Technol.* 91 (2004) 201–206.
- [123] G. Lehne, A. Muller, J. Schwedes, Mechanical disintegration of sewage sludge, *Water Sci. Technol.* 43 (2001) 19–26.
- [124] J.I.N. Yiyang, L.I. Huan, M.R. Bux, W. Zhiyu, N.I.E. Yongfeng, Combined alkaline and ultrasonic pretreatment of sludge before aerobic digestion, *J. Environ. Sci.* 21 (2009) 279–284.
- [125] L. Shao, X. Wang, H. Xu, P. He, Enhanced anaerobic digestion and sludge dewaterability by alkaline pretreatment and its mechanism, *J. Environ. Sci. (China)*. 24 (2012) 1731–1738.
- [126] C. Li, H. Li, Y. Zhang, Alkaline treatment of high-solids sludge and its application to anaerobic digestion, *Water Sci. Technol.* 71 (2015) 67–74.
- [127] A. Scheminski, R. Krull, D.C. Hempel, Oxidative treatment of digested sewage sludge with ozone, *Water Sci. Technol.* 42 (2000) 152–158.
- [128] H. Li, C. Li, W. Liu, S. Zou, Optimized alkaline pretreatment of sludge before anaerobic digestion, *Bioresour. Technol.* 123 (2012) 189–194.
- [129] H. City, T. City, Enhancement of anaerobic digestion of waste activated sludge by alkaline solubilization, *Bioresour. Technol.* 62 (1997) 85–90.
- [130] C. Bougrier, H. Carrère, J.P. Delgenès, Solubilisation of waste-activated sludge by ultrasonic

- treatment, *Chem. Eng. J.* 106 (2005) 163–169.
- [131] L. Huan, J. Yiyang, R.B. Mahar, W. Zhiyu, N. Yongfeng, Effects of ultrasonic disintegration on sludge microbial activity and dewaterability, *J. Hazard. Mater.* 161 (2009) 1421–1426.
- [132] P. Zhang, G. Zhang, W. Wang, Ultrasonic treatment of biological sludge: Floc disintegration, cell lysis and inactivation, *Bioresour. Technol.* 98 (2007) 207.
- [133] C. Liu, B. Xiao, A. Dauta, G. Peng, S. Liu, Z. Hu, Bioresource Technology Effect of low power ultrasonic radiation on anaerobic biodegradability of sewage sludge, *Bioresour. Technol.* 100 (2009) 6217–6222.
- [134] V. Naddeo, V. Belgiorno, M. Landi, T. Zarra, R.M.A. Napoli, Effect of sonolysis on waste activated sludge solubilisation and anaerobic biodegradability, *DES.* 249 (2009) 762–767.
- [135] G. Zhang, P. Zhang, J. Yang, Y. Chen, Ultrasonic reduction of excess sludge from the activated sludge system, *J. Hazard. Mater.* 145 (2007) 515–519.
- [136] S.. Raut-Jadhav, D.. Saini, S.. Sonawane, A. Pandit, Effect of process intensifying parameters on the hydrodynamic cavitation based degradation of commercial pesticide (methomyl) in the aqueous solution, *Ultrason. Sonochem.* 28 (2016) 283–293.
- [137] C.E. Brennen, *Cavitation and bubbles dynamics*, 1995.
- [138] P.N. Patil, P.R. Gogate, L. Csoka, A. Dregelyi-kiss, M. Horvath, Intensification of Biogas production using pretreatment based on hydrodynamic cavitation, *Ultrason. Sonochem.* (2015).
- [139] G. Andreottola, P. Foladori, M. Ferrari, G. Ziglio, *Respirometria applicata alla depurazione delle acque: Principi e metodi. II Ed.*, (2002).
- [140] M.C. Wentzel, A. Mbewe, M.T. Lakay, G.A. Ekama, Batch test for characterisation of the carbonaceous materials in municipal wastewaters, *Water SA.* 25 (1999) 327–335.
- [141] G.A. Ekama, P.L. Dold, G.R. Marais, Procedures for determining influent COD fractions and the maximum specific growth rate of heterotrophs in activated sludge systems, *Water Sci. Technol.* 18 (1986) 91–114.
- [142] P. Vanrolleghem, H. Spanjers, B. Petersen, P. Ginestetf, I. Takacs, Estimating (combinations of) Activated Sludge Model No. 1 parameters and components by respirometry, *Water Sci. Technol.* 39 (1999) 195–214.
- [143] G. Zhang, P. Zhang, J. Yang, H. Liu, Energy-efficient sludge sonication: power and sludge characteristics, *Bioresour. Technol.* 99 (2008) 9029–9031.
- [144] C. Bougrier, C. Albasi, J.P. Delgenès, H. Carrère, Effect of ultrasonic, thermal and ozone pre-treatments on waste activated sludge solubilisation and anaerobic biodegradability, *Chem. Eng.*

Process. Process Intensif. 45 (2006) 711–718.

- [145] American Public Health Association (APHA). Standard Methods for the Examination of Water and Wastewater, twentyfirst ed. Washington DC, USA, 2005.
- [146] M.R. Salsabil, A. Prorot, M. Casellas, C. Dagot, Pre-treatment of activated sludge: Effect of sonication on aerobic and anaerobic digestibility, Chem. Eng. J. 148 (2009) 327–335.
- [147] C.P. Chu, B.V. Chang, G.S. Liao, D.S. Jean, D.J. Lee, Observations on changes in ultrasonically treated waste-activated sludge, Water Res. 35 (2001) 1038–1046.
- [148] A. Grönroos, Kyllönen H., Korpijärvi K., Pirkonen P., Paavola T., Jokela J., et al., Ultrasound assisted method to increase soluble chemical oxygen demand (SCOD) of sewage sludge for digestion, Ultrason. Sonochem. 12 (2005) 115–120.
- [149] G. Xu, S. Chen, J. Shi, S. Wang, G. Zhu, Combination treatment of ultrasound and ozone for improving solubilization and anaerobic biodegradability of waste activated sludge, J. Hazard. Mater. 180 (2010) 340–346.
- [150] P.S. Kumar, M.S. Kumar, A.B. Pandit, Experimental quantification of chemical effects of hydrodynamic cavitation, Chem. Eng. Sci. 55 (2000) 1633–1639.
- [151] N.T. Le, C. Julcour-lebigue, H. Delmas, Ultrasonic sludge pretreatment under pressure, Ultrason. Sonochem. 20 (2013) 1203–1210.
- [152] R. Kidak, A. Wilhelm, H. Delmas, Effect of process parameters on the energy requirement in ultrasonical treatment of waste sludge, Chem. Eng. Process. Process Intensificatio. 48 (2009) 1346–1352.
- [153] S. Sahinkaya, Disintegration of municipal waste activated sludge by simultaneous combination of acid and ultrasonic pretreatment, Process Saf. Environ. Prot. 93 (2013) 201–205.
- [154] M. Friedrich, I. Takács, A new interpretation of endogenous respiration profiles for the evaluation of the endogenous decay rate of heterotrophic biomass in activated sludge, Water Res. 47 (2013) 5639–5646.
- [155] G. Andreottola, P. Foladori, M. Vian, An integrated approach for the evaluation of bacteria damage and biodegradability increase in sonication of excess sludge, in: Proc. IWA Spec. Conf. Sustain. Sludge Manag. State Art, Challenges Perspect. Moscow, Russ. 29–31 May, 2006.
- [156] J. Jablonská, M. Kozublová, Identification methods of cavitation, in: 23rd Int. Conf. Hydraul. Pneum. Prague, Czech Repub., 2016.
- [157] M. Dular, T. Griessler-bulc, I. Gutierrez, E. Heath, T. Kosjek, A.K. Klemenčič, et al., Use of hydrodynamic cavitation in (waste)water treatment, Ultrason. Sonochem. (2015).

- [158] W.D.E. Puiseau, G. Andreottola, E.C. Rada, M. Ragazzi, Application of a Novel Hydrodynamic Cavitation System in Wastewater Treatment Plants, (2013).
- [159] V.H. Arakeri, R.N. Iyer, A new technique in cavitation noise research, in: *Int. Symp. Cavitation*, Vol. 1, Ed. by H. Murai, Sendai, Japan, 1986: pp. 299–304.
- [160] J.P. Nasa, L. Wind, P.S.P. View, M. Rayleigh, J. Panda, Experiments on the instabilities in swirling and non-swirling free jets, *Phys. Fluids*. 6 (1994) 263–276.

Appendix A

Appendix A

Cavitation yield for HC (Ecowirl) at optimum pressure (2.0 bar) and pH (pH = 4.0) alone and combined with NaOCl

Following conditions were used for the operation of HC alone:

- Reaction volume - 50 L
- Initial dye concentration - 3.0 mg L⁻¹
- Absorbed Power rating of pump - 0.8 kW (800 W)
- Treatment time - 169 min

In HC alone, 14.7% decolourization of RhB was observed at operative conditions. The cavitation yield for HC reactors can be calculated as follows:

C.Y. = RhB degraded / Power density

$$\text{RhB degraded} = (14.7 \cdot 3 \text{ mg L}^{-1}) / 100 = 0.441 \text{ mg L}^{-1}$$

$$\text{Power density} = (P_{\text{abs}} \cdot t) / V = (800 \text{ W} \cdot 169 \text{ min} \cdot 60 \text{ sec min}^{-1}) / 50 \text{ L} = 162,240 \text{ J L}^{-1}$$

$$\text{C.Y.} = 0.441 \text{ mg L}^{-1} / 162,240 \text{ J L}^{-1} = 2.72 \cdot 10^{-6} \text{ mg J}^{-1}$$

Following conditions were used for the operation of HC and NaOCl (0.5 mg L⁻¹):

- Reaction volume - 50 L
- Initial dye concentration - 3.0 mg L⁻¹
- Absorbed Power rating of pump - 0.8 kW (800 W)
- Treatment time - 169 min

In HC combined with 0.5 mg NaOCl L⁻¹, 24.9% decolourization of RhB was observed at operative conditions. The cavitation yield for HC reactors can be calculated as follows:

C.Y. = RhB degraded / Power density

$$\text{RhB degraded} = (24.9 \cdot 3 \text{ mg L}^{-1}) / 100 = 0.747 \text{ mg L}^{-1}$$

$$\text{Power density} = (P_{\text{abs}} \cdot t) / V = (800 \text{ W} \cdot 169 \text{ min} \cdot 60 \text{ sec min}^{-1}) / 50 \text{ L} = 162,240 \text{ J L}^{-1}$$

$$\text{C.Y.} = 0.747 \text{ mg L}^{-1} / 162,240 \text{ J L}^{-1} = 4.60 \cdot 10^{-6} \text{ mg J}^{-1}$$

Appendix B

Appendix B

- *SCOD-increase:*

$$\Delta\text{SCOD (\%)} = \text{SCOD}_{\text{cav}} - \text{SCOD}_0 \quad \text{Eq. 7}$$

$$\text{SCOD}_0 = 251.0 \text{ mg L}^{-1}$$

$$\text{SCOD}_{\text{cav}} = 900.0 \text{ mg L}^{-1}$$

$$\Delta\text{SCOD (\%)} = 900.0 - 251.0 = 649 \text{ mg L}^{-1}$$

- *Disintegration degree (DD_{PCOD}):*

- Reaction volume - 50.0 L
- TS content - 50.0 mg L⁻¹
- Inlet pressure - 2.0 bar
- Temperature - 20.0°C

$$DD_{\text{PCOD}} (\%) = (\text{SCOD}_{\text{cav}} - \text{SCOD}_0) \times 100 / \text{PCOD}_0 = (\text{SCOD}_{\text{cav}} - \text{SCOD}_0) \times 100 / (\text{TCOD} - \text{SCOD}_0) \quad \text{Eq. 8}$$

- SCOD₀ - 251.0 mg L⁻¹
- SCOD_{cav} - 900.0 mg L⁻¹
- TCOD - 46,423 mg L⁻¹

$$DD_{\text{PCOD}} (\%) = (900.0 \text{ mg L}^{-1} - 251.0 \text{ mg L}^{-1}) \times 100 / (46,423 \text{ mg L}^{-1} - 251.0 \text{ mg L}^{-1}) = 1.4\%$$

- *Disintegration degree (DD_{N}):*

$$DD_{\text{N}} (\%) = (\text{NH}_4^+\text{-N}_{\text{cav}} - \text{NH}_4^+\text{-N}_{\text{o}}) \times 100 / (\text{TKN}_0 - \text{NH}_4^+\text{-N}_{\text{o}}) \quad \text{Eq. 9}$$

- NH₄⁺-N_o - 26.8 mg L⁻¹
- NH₄⁺-N_{cav} - 86.0 mg L⁻¹
- TKN₀ - 3,009 mg L⁻¹

$$DD_{\text{N}} (\%) = (86.0 - 26.8) \times 100 / (3,009 - 26.8) = 2.0\%$$

- *Disintegration degree ($DD_{\text{COD NaOH}}$):*

$$DD_{\text{COD NaOH}} (\%) = (\text{SCOD}_{\text{cav}} - \text{SCOD}_0) \times 100 / (\text{SCOD}_{\text{NaOH}} - \text{SCOD}_0) \quad \text{Eq. 10}$$

- SCOD₀ - 251.0 mg L⁻¹
- SCOD_{cav} - 900.0 mg L⁻¹
- SCOD_{NaOH} - 29,350.0 mg L⁻¹

$$DD_{\text{COD NaOH}} (\%) = (900.0 \text{ mg L}^{-1} - 251.0 \text{ mg L}^{-1}) \times 100 / (29,350 \text{ mg L}^{-1} - 251.0 \text{ mg L}^{-1}) = 2.2\%$$

▪ *Specific supplied energy (SE):*

- Inlet pressure - 4.0 bar
- Temperature - 35.0°C

$$SE \text{ (kJ kgTS}^{-1}\text{)} = (P_{\text{abs}} \times t) / (V \times \text{TS})$$

Eq. 11

- TS content - 50.0 g L⁻¹
- Absorbed Power rating of pump - 1,137.5 W
- Reaction volume - 50.0 L
- Treatment time - 120 min (7,200 sec)

$$SE \text{ (kJ kgTS}^{-1}\text{)} = (1,137.5 \times 7,200) / (50.0 \times 50.0) = 3,276 \text{ kJ kgTS}^{-1}$$

▪ *Energy efficiency (EE):*

- Inlet pressure - 4.0 bar
- Temperature - 35.0°C

$$EE \text{ (mg } \Delta\text{SCOD kJ}^{-1}\text{)} = (V \times \Delta\text{SCOD}) \times 1000 / (P_{\text{abs}} \times t)$$

Eq. 12

- Reaction volume - 50.0 L
- ΔSCOD - 1,475 mg L⁻¹
- Absorbed Power rating of pump - 1,137.5 W
- Treatment time - 120 min (7,200 sec)

$$EE \text{ (mg } \Delta\text{SCOD kJ}^{-1}\text{)} = (50 \times 1,475) \times 1000 / (1,137.5 \times 7,200) = 9.0 \text{ mg } \Delta\text{SCOD kJ}^{-1}$$

Acknowledgements

Acknowledgements

I would like to express my sincere gratitude to my supervisor *Prof. Gianni Andreottola* for constantly supporting me throughout my PhD, for sharing his extensive knowledge, enthusiasm and wisdom with me and for simply giving me the opportunity to become a PhD.

I would also like to thank my colleague *Michela Langone* for suggesting me always the best and for helping me in this undertaking.

Many thanks to *Andrea and Francesco Parisi*, I am extremely grateful for your constant assistance throughout my experimental activity, for your professionalism and for your generosity and goodness.

Many thanks to *Prof. Kozubková* for welcoming me within her research group and for making me discover the fantastic world of Computational Fluid Dynamics.

Thanks to my *PhD* and *laboratory colleagues*. A special thanks to my friend *Marco* for hardly working to my project and for being constantly by my side during his Master's thesis.

I would like to show my gratitude to my *father*, my *mother* and my sister *Martina*. Thank you for always just wanting the best for me. I can never thank you enough for making me feel the main priority in your lives. What I have done, I have done to make you proud.

Thanks to my *grandparents* for being always present in my life and for teaching me how to live a fully and good life.

A special and full of love thanks to my girlfriend *Floriana* for her understanding, for her constantly encouragement and for helping me survive all the stress from this three years and not letting me give up.

Huge thanks to my best friend *Riccardo* for getting me in this trouble life. Thank you for daily teaching me the meaning of a true friendship. It does not matter where we are in this world or in our lives, I know you will always pick up.

Thanks to my friend *Pietro* for making joyful days both in Trento and in Sicily.

Big thanks to my Samba's friends... *Saimon, Ali, Piripiska, Burim, Giancarlo brulerino e Rachelina*, the fox *Roberto* and the cat *Vincenzo, Sonny, Matteo, Francesco "vai via", Federico, Balà balà balà, Lu'u, Hannan, Bruno, Gonarina, Pablito, Duc, Mark, Jenny, Marta*... Thanks for making me happy and for making me feel member of a big family.

Thanks to all my *old friends* and people who have been close to me during these three years.

Publications and relevant works

Publications & relevant works

- Paper published in Journal Elsevier- Ultrasonics Sonochemistry
G. Mancuso, M. Langone, M. Laezza, G. Andreottola, *Decolourization of Rhodamine B: A swirling jet-induced cavitation combined with NaOCl*, Ultrason. Sonochem. 32 (2016) 18–30.
- Paper published in Journal Elsevier- Ultrasonics Sonochemistry
G. Mancuso, M. Langone, G. Andreottola, *A swirling jet-induced cavitation to increase activated sludge solubilisation and aerobic sludge biodegradability*, Ultrason. Sonochem. 35 (2016) 489-501.
- Paper published in Journal Elsevier- Journal of Environmental Management
P.P. Falciglia, R. Maddalena, G. Mancuso, V. Messina, F.G.A. Vagliasindi, *Lab-scale investigation on remediation of diesel-contaminated aquifer using microwave energy*, J. Environ. Manage. 167 (2016) 196–205.
- Paper published in Journal Elsevier- Separation and Purification Technology
P.P. Falciglia, G. Mancuso, P. Scandura, F.G.A. Vagliasindi, *Effective decontamination of low dielectric hydrocarbon-polluted soils using microwave heating : Experimental investigation and modelling for in situ treatment*, Sep. Purif. Technol. 156 (2015) 480–488.
- Paper published in SIDISA 2016- International Symposium on Sanitary and Environmental Engineering- Rome 19-23 June 2016
P.P. Falciglia, G. Mancuso, R. Maddalena, V. Messina, P. Roccaro, F.G.A. Vagliasindi, *Lab-scale investigation on microwave heating for in situ remediation of hydrocarbon-contaminated aquifers*, Proceedings of SIDISA (2016), International Symposium on Sanitary and Environmental Engineering, Rome, Italy, 19-23 June 2016. ISBN 978-88-496-391-1.
- Paper published in IDA- Ingegneria dell’Ambiente
P.P. Falciglia, G. Mancuso, R. Maddalena, V. Messina, P. Roccaro, F.G.A. Vagliasindi, *Bonifica di acquiferi contaminati da idrocarburi mediante trattamenti a microonde*, Ing. Dell’ambiente. 3 (2016) 214–226.

- Presentation of Poster

G. Mancuso, M. Langone, R. Ferrentino, G. Andreottola, *Disintegration of waste-activated sludge using a novel hydrodynamic cavitation system.*

2nd IWA Specialist Conference on Eco Technologies for Sewage Treatment Plants 2014 - "EcoSTP2014", Verona, Italy, 23 – 27 June 2014.

- Presentation of Poster

G. Mancuso, P.P. Falciglia, P. Scandura, F. G. A. Vagliasindi, *Development and application of a mathematical model for thermal desorption treatments of diesel fuel polluted soils by microwave heating stabilisation.*

RemTech 2014 – 8th Remediation Technologies and Requalification of Territory Exhibition, Ferrara, Italy, 17- 19 September 2014

In the past decades, hydrodynamic cavitation (HC) process was the subject of study by many researchers worldwide. This phenomenon was widely studied in order to understand the reason of its negative effects on hydraulic machinery such as pumps, turbines, valves, etc. Many efforts were made in order to better understand mechanisms of HC process with the main aim of preventing its generation and trying to avoid severe physical damage such as erosions, vibrations and noises.

In recent years, in order to cope with a decrease in available water resources worldwide, an increasing demand of water by population in developing/developed countries and more restrictive environmental legislations on water quality, HC was increasingly used as a novel energy-efficient technique in the field of wastewaters treatment.

The main purpose of this thesis is to investigate on the effectiveness of a modified swirling-jet device called Ecowirl reactor, patented by Econovation GmbH, Germany and produced and commercialized by Officine Parisi s.r.l., Italy. Experimental studies were carried out in order to evaluate the effects of different operative conditions and parameters such as reactor geometry, flow rate, flow velocity, pressure, medium pH, medium concentration and medium temperature on (i) the degradation of a toxic and carcinogenic pollutant dye (Rhodamine B, RhB) in waste dye aqueous solutions and on (ii) the improvement of activated sludge solubilisation and aerobic sludge biodegradability in the field of biological wastewater treatments.

In order to better understand the fluid dynamics into Ecowirl reactor, it was modelled. The model based on previous experimental data was implemented in a Computational Fluid Dynamics software (ANSYS, 16.2).

Giuseppe Mancuso is a Civil and Environmental Engineer. He was born in Piazza Armerina, Italy on 17 September 1985. He received the Beng Degree in Civil and Environmental Engineering from the University of Catania on 18 October 2010 and the Meng Degree in Civil and Environmental Engineering from the University of Catania on 24 July 2013, respectively.

In 2014, the National Chemical Council rewarded his Master's thesis as the best national thesis. His research included the decontamination of hydrocarbon-polluted soils using microwave heating and the application of stabilization/solidification technique to radioactive polluted soils, respectively.

In 2014, he became a PhD student at the Department of Civil, Environmental and Mechanical Engineering of University of Trento. His current research interests include wastewater treatment, polluted soils remediation and Computational Fluid Dynamics.